ABSTRACT

LEE, JAE JUN. Quantifying the Benefits of Improved Rolling of Chip Seals. (Under the direction of Dr. Y. Richard Kim).

This dissertation presents an improvement in the rolling protocol for chip seals based on an evaluation of aggregate retention performance and aggregate embedment depth. The flip-over test (FOT), Vialit test, modified sand circle test, digital image processing technique, and the third-scale Model Mobile Loading Simulator (MMLS3) are employed to evaluate the effects of the various rolling parameters and to measure chip seal performance. The samples used to evaluate the chip seal rolling protocol were obtained directly from field construction. In order to determine the optimal rolling protocol, the effects of roller type, number of coverages, coverage distribution on the sublayers of a multiple chip seal (i.e., the split seal and triple seal), and rolling pattern are evaluated using the results of aggregate retention performance tests, the modified sand circle method, and the digital image process. It is found that two types of roller, the pneumatic tire roller and the combination roller, are recommended as the optimal rollers for the chip seal. In addition, it is found that the optimal number of coverages for the chip seal, as determined from measurements of the aggregate, is three coverages. Moreover, the performance of the triple seal without coverage at the bottom layer does not affect the aggregate retention performance, although the split seal does require coverage at the bottom layer. Finally, it is found that the rolling pattern is strongly related to a delayed rolling time between the aggregate spreader and the initial rolling time. Therefore, it was recommended that two pneumatic tire rollers applied initial one coverage with optimal delayed rolling time (between 2 min. and 4 min.) to entire lane width, and then the combination roller applied two additional coverages. Further, it is confirmed that the delayed rolling time is related to the aggregate moisture condition and the ambient temperature.

Quantifying the Benefits of Improved Rolling of Chip Seals

by
Jaejun Lee

A dissertation submitted to the Graduate Faculty of
North Carolina State University
in partial fulfillment of the
requirements for the Degree of
Doctor of Philosophy

Civil Engineering

Raleigh, North Carolina

2008

APPROVED BY:

_____	_____
Dr. Y. Richard Kim Chair of Advisory Committee	Dr. Akhtarhusein A. Tayebali
_____	_____
Dr. Richard L. Lemaster	Dr. Roy H. Borden

DEDICATION

To

My Family,

하늘나라에 계시는 아버지께 이 논문을 바칩니다.

BIOGRAPHY

Jae Jun Lee was born in Chonbuk, Korea on May 5, 1972, the son of Yoonhyoung Lee and Myoungsuk Choi. He received his Bachelor's degree in Civil Engineering in 1997 from Chonbuk National University, Jeonju, Korea and Master's degree in Civil Engineering in 1999 from Hanyang University, Seoul, Korea. During that time, he studied in structural materials (concrete). In May 1999, he was lucky to get married with Shin, Huieun, his lovely wife, with God's blessing before his graduate study in abroad. In January of 2001, he began graduate studies at the City College of the City University of New York to pursue his second Master degree in Civil Engineering with a concentration in Structure Engineering. While he was studying there, he studied the concrete behavior at the early time with ultrasonic method. After graduated the CCNY, he enrolled to University of North Carolina State University, joined the Ph.D. program in transportation engineering at the department of Civil Engineering with the aid of his advisor, Dr. Kim, in 2004. While he has been serving as a research assistant, he was able to complete his course work and conduct heavy-duty experimental and analytical research.

ACKNOWLEDGEMENTS

First of all, my genuine thanks and deep appreciation go to my advisor, Professor Y. Richard Kim, for his unfailing support and guidance during my doctoral program. He has been a continuous source of knowledge and encouragement. I was truly happy working with him and hope to continue doing so.

I do not know how to thank all my parents (mother: Myung-sook Choi, father-in-law: Moon-soon Shin, mother-in-law: Sook-hee Lee) enough for their unconditional love and support that allow me to finish my study in the United States. I thank my lovely wife Huieun Shin for her being sweet, patient, and kind all the times. Her encouragement made me feel energized whenever I was exhausted with school's life. I will take care of you and support you until the end of my life. I love you.

I thank sisters and brothers-in-law who have always supported me to finish my study in the United States.

Also, I wish to thank the members of my dissertation committee members: Dr. Borden, Dr. Tayebali, and Dr. Lemaster, for their help and the time. They generously gave their time and expertise to better my work. I thank them for their contribution and their good natured support. I would like to acknowledge our alumni: Dr. Sug-joon Lee, Dr. Ju-Sang Lee and Dr. Sang-yum Lee help me to study asphalt at NC State. I express my deep gratitude to my fellow members: Chulmin Baek, Taeyoung Yoon, Shane Underwood, Andrew LaCroix, and Andrew Jerome.

Also, I express gratitude to the NCDOT for supporting the project and providing the resources to construct the field sections.

TABLE OF CONTENTS

LIST OF TABLES

LIST OF FIGURES

1. INTRODUCTION

1.1 Research Needs and Significance

Chip seals have served as one of the most common preventive maintenance treatments for road surfaces in the United States over the past 75 years because they provide economical benefits to extend pavement life. The chip seal system includes design methods and means of construction to establish and successfully provide low and high volume loads (Gransberg et al. 2005).

The most common failures of the chip seal are bleeding or flushing and aggregate loss from the top layer. Generally, a significant amount of aggregate loss occurs soon after construction with the initial trafficking, and typically is caused by improper construction, inadequate chip seal design, and poor material selection (Transit New Zealand 2005). Therefore, the aggregate loss in the early life of the chip seal can be reduced by improving the construction procedures.

In general, chip seal construction procedures consist of three steps: spraying emulsion, spreading a layer of aggregate, and rolling the layer of aggregate. In order to ensure the best chip seal performance, these steps should be continuous without any interruption. That is, having an adequate initial rolling using a sufficient number of rollers is an important factor in extending the service life of the chip seal (South Africa 1986).

One of the areas in the chip seal construction procedure that needs to be improved is the rolling process. The purpose of rolling is to achieve the desired aggregate embedment depth (which is the principal criterion in the chip seal design) by redistributing the aggregate and seating it in the binder (Benson et al. 1953). Another function of compaction is to achieve the bonding that results from proper embedment into the binder and from the most efficient orientation of the aggregates. Researchers have studied chip seal construction systems by roller type (Hudson et al. 1986), by rolling time (Gransberg et al. 2004), by roller pass (Hudson and Petrie 1990), and by roller weight (Petrie 1990) to improve the chip seal's quality and performance (Gransberg et al. 2005).

To improve the current chip seal rolling practice, it is necessary to have an accurate picture of the current practice and to quantify the benefits of changes in the compaction protocol. In order to investigate the benefits of the rolling protocol, the performance of aggregate retention, adhesion, and embedment of depth must be measured. The flip-over test (FOT) and the third-scale Model Mobile Loading Simulator (MMLS3) are employed to evaluate aggregate retention performance. Adhesion performance, according to different compaction operations, is estimated by the Vialit test. The embedment depth of the chip seal, one of the most critical factors, is measured using the modified sand circle method. This research uses these tests and procedures to determine the optimal rolling protocol for the chip seal based on an evaluation of the various performance characteristics.

1.2 Research Objectives

The primary objectives of the research are:

1. to determine the optimal roller type;
2. to determine the optimal number of coverages;
3. to determine the optimal coverage distributions of the multilayer seal among the sublayers; and
4. to determine the optimal rolling pattern in order to conduct proper rolling the entire aggregate before the emulsion breaks.

1.3 Dissertation Organization

This dissertation is composed of eight chapters. Chapter 1 presents the research needs and objectives. Chapter 2 summarizes the literature review of chip seal aggregate retention performance test methods and the effects of various roller types and rolling patterns. Chapter 3 describes the physical characteristics of selected materials and experimental test methods employed in this study. Chapter 3 also explains that one of the

critical procedures in this research is fabricating the field samples so that they correspond to the actual construction sequence. Chapter 3 also presents the test protocols for the FOT, Vialit test, and MMLS3 test used in this study to evaluate aggregate retention performance. In Chapter 4, a determination of the optimal roller type is described by an evaluation of the aggregate retention performance results. Chapter 5 explains the determination of the optimal number of coverages for chip seal construction using samples obtained from actual field construction. Chapter 6 reports the results of coverage distribution of the multiple chip seals (split and triple seals) from the three different aggregate retention test methods. Chapter 7 discusses the results from the investigation of the effects of various rolling patterns and delayed rolling time on the aggregate loss performance. Conclusions from this research and future research recommendations are given in Chapter 8.

2. LITERATURE REVIEW

2.1 General

The chip seal has a history of more than seventy years and is widely used by state Departments of Transportation (DOTs) in the United States and other countries for pavement preventive maintenance. The chip seal, also known as surface treatment, seal coat, or surface dressing, offers significant advantages, primarily as an economical and efficient means to provide skid resistance and fast construction. Crucial factors, such as traffic volume, the condition of the existing pavement, and a proper rolling operation, influence the performance and the service life of a chip seal. One of the principal factors is the rolling process that constitutes an important step in achieving a high quality chip seal. The roller presses the aggregate into the thin emulsion film to provide a uniform mosaic of aggregate. If the aggregate is not properly embedded into the emulsion film, chip seal failure may occur soon after construction due to traffic loading.

2.2 Adhesion between Aggregate and Emulsion

The adhesion of the emulsion to the aggregate in a chip seal system is strongly associated with the performance and service life of the chip seal.

2.2.1 Factors Affecting the Adhesion

Various factors influence the adhesion between the emulsion and the aggregate; such factors are strongly associated with the performance of the chip seal. Aggregate properties that influence bonding include surface texture, surface area, porosity,

absorption and mineralogy. The breaking and curing characteristics of the emulsion also affect the development of the bond.

Mathews (1958) explains factors that affect the adhesion, such as wetting the aggregate and the strength of the adhesive bond under both dry and wet conditions. Wetting the aggregate refers to covering the aggregate with the binder in the emulsion. The viscosity of the binder controls the maximum covered area on the aggregate surface. In a chip seal, the dustiness of the aggregate prevents adequate adhesion between the aggregate and the binder because of the inability of the binder to penetrate through the dusty layer. Thus, the aggregate should be wet and spread immediately after the emulsion is sprayed in the chip seal construction.

Emmanuel (1999) studied the phenomenon of breaking the mechanism in the emulsion using an abrasion cohesion test method. He found it possible to quantitatively evaluate the rate of cohesion recovery of aggregates in a chip seal.

Khalid (2000) researched the correlation between aggregate retention found from the Mini Fretting Test (MFT) and rheological properties determined by the Dynamic Shear Rheometer (DSR). Based on his research, this relationship assists in setting a corresponding minimum $G^*/\sin\delta$ value for a specified temperature, frequency and conditioning period; in turn, this information can be used to create performance-related binder specifications for a chip seal. Khalid found that the long-term chip seal performance could be predicted by the development of a chip seal's strength during its early life.

2.2.2 Emulsion Setting Behavior

Breaking the emulsion refers to the bitumen of an emulsion separating from water. The breaking mechanism of a CRS-2 is illustrated in Figure 2-1. As described in Figure 2-1, the first step in the emulsion breaking process is initiated by the absorption of an emulsifier into a foreign substance, such as aggregate or a pavement surface. Thus, breaking occurs when the emulsion is sprayed on the pavement surface and the aggregate is spread on the emulsion in the chip seal construction (AEMA 2004, John et al. 2003).

Curing the emulsion is often confused with breaking the emulsion. Curing is simply the evaporation of water from the emulsion. Evaporation can occur considerably quickly under favorable weather conditions. Therefore, the required curing time can be reduced to achieve proper strength (AEMA 2004). Because strong energy differences exist between the aggregate surface and the emulsified binder, a mechanical force is necessary to push the water away from the interface between the aggregate and the binder (Senadheera et al. 2006).

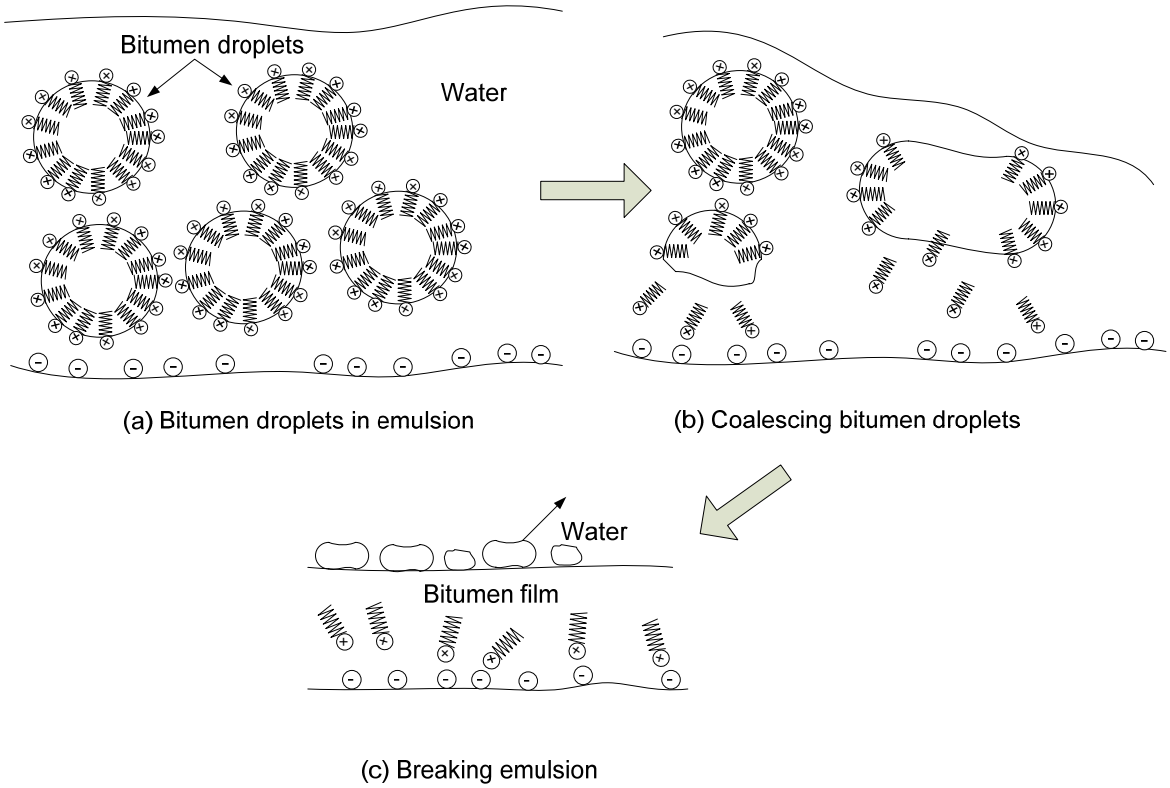

Figure 2-1 Emulsifier ions forming micelles in a stable system (Transit New Zealand 1993)

2.3 *Construction Factors of the Chip Seal*

The chip seal construction process, as shown in Figure 2-2, consists of three steps: spraying emulsion, spreading a layer of aggregate, and rolling the layer of aggregate. The rolling is one of the most important steps during construction to ensure the best chip seal performance. The main purpose of rolling is to seat the aggregate into the emulsion film, which generates an improved adhesion between the aggregate and the emulsion in the chip seal system. Also, the reorientation of the aggregate by the roller is a critical aspect of the roller operation. The rolling process determines the reorientation of the aggregate so that the flatter side contacts the existing pavement.

Figure 2-2 Chip seal construction procedure

This reorientation enables the greatest surface area possible for contact between the aggregate and emulsion. Generally, compaction is started by a roller; however, the final process is finished by applied traffic. The effectiveness of the compaction varies according to various factors, such as the rolling pattern, roller types and the number of passes.

2.3.1 Roller Types

In chip seal construction, a roller is employed to embed the aggregates into the emulsion film and to ensure an initial bond with the binder film without crushing the aggregate. Several different types of rollers are currently used in chip seal construction, including the pneumatic tire roller, steel wheel roller, vibratory steel wheel roller, rubber-coated vibrating drum roller, and combination roller. The combination roller is composed of a rubber-coated steel drum and a pneumatic tire. The pneumatic tire roller and the steel wheel roller are commonly employed for rolling aggregate in chip seal construction in the United States. In the United Kingdom (John et al. 2003), rubber-covered steel-drummed vibratory rollers are considered to be the optimal roller for establishing a uniform mosaic of aggregate and improving the initial adhesion between the aggregate and the binder. New Zealand (Transit New Zealand 2005) uses three types of rollers: the pneumatic tire roller, the rubber-coated vibrating drum roller, and the combination roller.

2.3.1.1 Pneumatic tire roller

The pneumatic tire roller, as shown in Figure 2-3, consists of nine pneumatic tire wheels to roll a layer of aggregate. This roller uses a set of smooth (i.e., having no tread) tires on each axle, typically four on one axle and five on the other. The tires on the front axle are aligned with the gaps that are between the tires on the rear axle to provide a uniform rolling coverage over the width of the roller. This roller is widely employed in chip seal work in the United States to achieve proper embedment and reorientation of the aggregate into the emulsion film. The NCDOT (2000) emphasizes that a uniform tire

pressure is required, as specified by the manufacturer, to successfully embed the aggregate in the asphalt mat using a pneumatic tire roller. The most common roller speed is recommended to be less than 5 mph, as specified in most state standard specification and construction manual. Bullard et al. (1992) note problems at a speed greater than 5 mph whereby aggregate is "picked up" on the tires. This problem can lead to the dangerous condition of loose aggregate flying in real traffic. Nonetheless, other states, such as California and Oklahoma, allow a slightly higher speed of 6 mph and 7 mph, respectively. Transit New Zealand (2005) reports that a pneumatic tire with a tread pattern roller enhances travel safety in wet weather; this finding is contrary to the results obtained from smooth tire rollers used for general chip seal work by NCDOT.

Figure 2-3 Pneumatic tire roller

2.3.1.2 Steel wheel roller

A steel wheel roller has a smooth surface steel drum, as shown in Figure 2-4 and is currently used in chip seal construction to roll the aggregate. The steel wheel roller produces a smooth pavement, which improves the travel experience. However, the use of the steel wheel roller requires caution because it can crush the aggregate, especially on high spots (Jackson et al. 1989). Also, the steel wheel roller is not recommended when the underlying pavement has irregularities, such as rutting, because the steel wheel drum creates a bridge over the rutting and fails to embed the aggregate into the emulsion film (Gransberg et al. 2005).

Figure 2-4 Steel wheel roller

2.3.1.3 Rubber-coated steel drum roller

Outside the United States, the rubber-coated steel roller is currently considered to be the best roller to achieve a uniform aggregate mosaic without crushing the aggregate.

Also, this roller provides high contact pressure necessary for the appropriate embedment depth of the aggregate into the emulsion film, because the rubber-coated steel wheel drum is more effective in reorienting the aggregate particles (Austroads; Transit New Zealand 2005; John et al. 2003). The rubber-coated steel wheel drum is practically applying with the pneumatic tire roller in New Brunswick in Canada (Miller 1987).

2.3.1.4 Combination roller

Figure 2-5 shows the combination roller that combines the use of a steel wheel drum on the front axle with four rubber tire wheels on the rear axle. The combination roller is currently used in hot mix asphalt (HMA) pavement construction sites. It provides the positive effects of both the pneumatic tire and the steel wheel drum (Gransberg et al. 2005).

Figure 2-5 Combination roller, showing two axles

Transit New Zealand (2005) is currently using a combination roller that combines a rubber-coated steel drum on the front axle with a single row of pneumatic tires on the

rear axle. Again, this arrangement provides the advantages of both the pneumatic tire roller and the rubber-coated roller in the embedment and reorientation of the aggregates.

2.3.2 Number of Coverages

To achieve an adequate embedment of the aggregate into the emulsion film and proper reorientation of the aggregates, the required number of coverages and appropriate speed is important to the rolling process. An insufficient number of coverages may cause aggregate loss at an early stage by traffic loading. However, neither North Carolina's standard specifications nor most construction manuals require a specific number of rolling passes. Only 7 out of 39 states have a required number (three or four passes) in their specifications. Transit New Zealand (1993) has a minimum of five roller passes at 5 mph to provide adequate embedment of the aggregates.

Hudson et al. (1986) have researched the effects of the pneumatic tire roller passes in new chip seal construction. Measurements were taken after the chips were spread but before rolling, then after sequences of roller passes, and finally after traffic had been opened for one and two days. Measurements that were taken include those from sand circles, photogrammetry, and the visual examination of enlarged photographs. Hudson et al. found that significant improvements were generally observed from the sand circle measurements and photogrammetry for the first three roller passes. However, it was difficult to measure a change in texture after 6 roller passes.

2.3.3 Rolling Pattern

The determination of an optimal rolling pattern used for chip seal construction depends on the number and types of rollers, because the roller must cover the entire width of the spread aggregate before the emulsion breaks. That is, the roller should cover the full width of the aggregate spreader. In order to roll the entire surface width effectively before the breaking of the emulsion, it is crucial to establish a proper rolling pattern, which is associated with the number of rollers that are used. Adequate coverage using two

pneumatic tire rollers can be achieved with no more than three passes. This number of passes is commonly the minimum that is required. (Stevenson et al. 2000). A recommended performance guideline (AEMA 2004) suggests a minimum of three rollers for an average chip seal construction using one rolling pattern. The rolling pattern is that two rollers should be kept close to the chip spreader at all times so that the first pass of the roller covers the aggregate before the emulsion breaks, while the third roller does the back-rolling.

The Alaska DOT has its own rolling pattern with a minimum of three rollers to complete the rolling before the breaking of the binder. The pattern is designed so that the first two rollers move side by side, rolling the outer edges. The third roller follows closely behind, rolling the center of the lane.

The rollers should be employed in a staggered pattern for proper rolling, as specified in the Arizona guide (2003) and the Texas manual (2004). The Texas DOT (2004) recommends a rolling system for a 12-foot wide asphalt surface that uses three or four pneumatic tire rollers with three passes: one forward, one in reverse, and a final pass that extends into the next section of pavement, as shown in Figure 2-6. The lead roller is usually on the inside, and each of the others offset approximately one-third the roller width. The schematic diagram in Figure 2-6 illustrates this echelon pattern.

Gransberg et al. (2004) discuss a rolling pattern that uses a minimum of three rollers and four rollers. These two patterns are shown in Figure 2-7. One is a staggered pattern that uses three rollers. The other is a diagonal pattern that uses four rollers. As shown in Figure 2-7, two different areas receive different roller passes. One receives only three passes; another receives six passes due to the overlap between the two rolling patterns. Although the number of rollers increases by only one (i.e., from three to four), the area that experiences six uniform passes is dramatically increased as the rolling pattern changes. According to this case study, therefore, the best rolling pattern should be determined for a specific number of rollers.

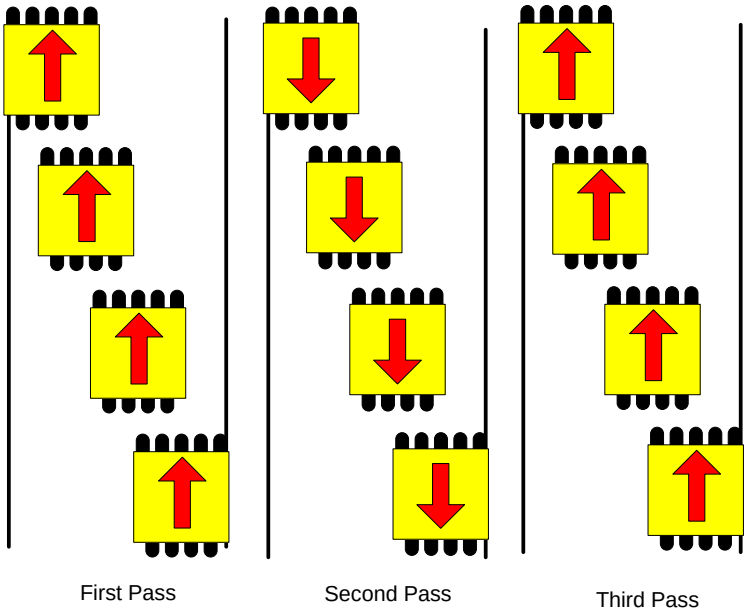

Figure 2-6 Illustration of echelon rolling pattern (Texas DOT 2004)

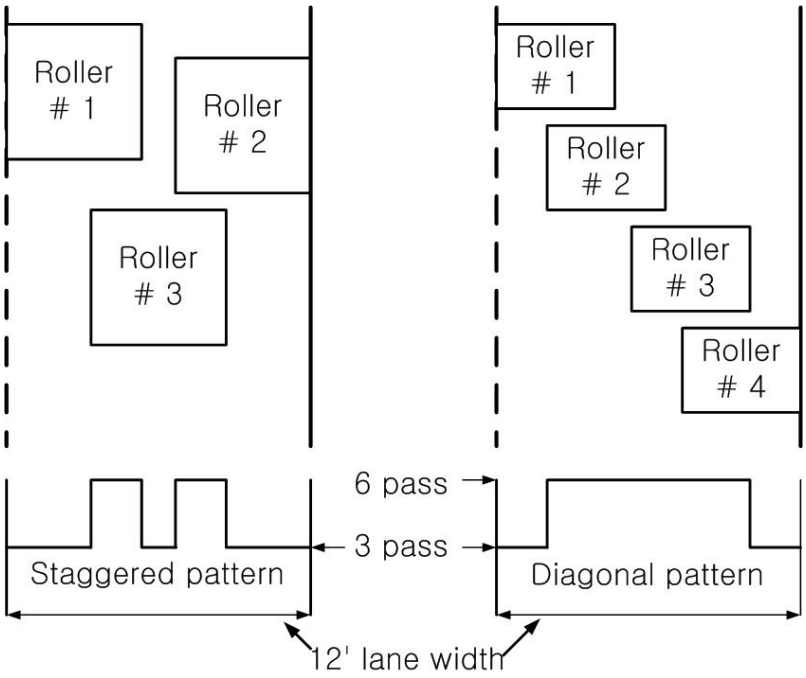

Figure 2-7 Rolling pattern and roller coverage for three and four pneumatic tire rollers (Gransberg et al. 2004)

2.4 Test of Chip Seal Performance

Performance measurements of HMA pavements are not appropriate for measuring chip seal performance because the chip seal surface is constructed in a different way than HMA pavements are constructed. Therefore, chip seal performance needs to be based on a different set of evaluation methods than is used for evaluating HMA pavements.

Stroup-Gardiner et al. (1990) tried to identify potential construction problems that may influence the performance of a chip seal surface. Problems related to construction, such as aggregate pick-up by the rollers, may damage a section of road even before it is opened to traffic. The Vialit test in the laboratory is used to evaluate existing excess aggregate and the set rate of the emulsion. Samples for the Vialit testing were fabricated on a small scale similar to that found in field construction and tested at various curing times.

Yazgan et al. (2004) researched a new test protocol using a performance-based method to determine the aggregate-binder compatibility for a seal coat using the Vialit test. Approximately one year after construction, they evaluated the performance of each test section and rated the field conditions on a scale of 1 to 5, with 5 being the best. At the same time, specimens taken from field test sections during construction were stored under laboratory conditions. Eleven of the twelve test sections showed agreement between field performance and field specimen test results using this new testing protocol. Consequently, the new testing protocol appears to predict the field performance of seal coats.

Davis et al. (1991) have researched the correlation between the Vialit test results from the laboratory and field tests made three months after construction and again after eleven months. The Vialit test samples from the field were collected from the pavement 6 ft from the center line after the last roller had passed and before the brooming process. In order to prevent the metal plates flipping up and damaging samples in the field, the roller speed was reduced to half its normal speed. A comparison of the aggregate retention results provided by the Vialit test between laboratory and field testing shows that the differences in aggregate loss range from 10% to 35%. In this study, field evaluations were also conducted near the field testing sites. A composite condition index, on a scale of 1 to

10 with 10 being best, was developed based on overall condition, bleeding, and aggregate retention results.

Petrie et al. (1990) found that the depth of the emulsion around the chip typically indicates about a 50% embedment after the initial rolling and about a 70% embedment after two or more weeks of traffic. Also, they recommend that the rolling procedure should begin immediately after the aggregate is distributed to ensure proper embedment of the chip seal, because more rolling is required as the emulsion cools. Skilled and experienced construction and inspection personnel also constitute an important factor in a quality chip seal program.

Roque et al. (1991) evaluated the adequacy of existing seal coat design procedures, quality control procedures, and seal coat performance measuring techniques. The evaluations were based on actual field measurements and led to numerous recommendations for improvements in seal coat design methods. In Roque's research, the mean texture depth (MTD), as measured by the sand patch test, was used to evaluate the performance and to measure aggregate wear and embedment rates under a controlled field condition. The wear rate is calculated as the loss in MTD per wheel pass during cool months; the embedment rate is computed as the loss in MTD per wheel pass during warm months minus the calculated wear prediction model to evaluate the effects of different variables on the expected seal coat life.

Ksaibati (2000) studied the effect of aggregate and binder types on the performance of surface treatments. Field distress data were obtained from test sections in both 1995 and 1996. Two pavement condition indices (PCI) were calculated for each of the test sections. The second performance measure included in the analysis is a friction measurement taken with the use of a locked wheel trailer, as described in ASTM E-274.

Milne et al. (2005) developed a method of evaluating the seal performance of different seal binders under similar imposed loads and environments. This test method was developed using the Third-scale Model Mobile Load Simulator (MMLS3) to provide traffic loading. A finite element method (FEM) prototype model of a single seal was developed and was able to evaluate the performance of the surface seal's behavior.

Lee (2007) presented a new test protocol for the performance evaluation of bituminous surface treatments (BSTs) using the MMLS3. This new MMLS3 test method evaluates the effects of various mix parameters on aggregate retention and bleeding; these parameters include aggregate and emulsion application rates (AARs and EARs), fines content and aggregate gradation.

3. EXPERIMENTAL TEST PROGRAM AND METHOD

3.1 Experimental Program

The primary objective of this research is to improve the compaction protocol in chip seal construction. In order to evaluate such a protocol, it is crucial to test samples that are obtained directly from field construction. Thus, a field experimental program has been developed. Numerous factors must be considered for the rolling protocol; Figure 3-1 describes the factors considered in this research.

Each factor has many variables as well as reciprocal factors, such as the correlation between the rolling pattern and the number of rollers. The rolling pattern is decided based on the number of rollers used in construction and the target number of coverages. It is noted that the term *number of coverages* is used for the number of compactions experienced by a section of road. For example, Figure 3-2 shows one roller that passes three times to cover the entire lane with minimal overlap. In this case, the number of passes is three, but the number of coverages is only one.

It is difficult to design a systematic field experimental program with so many unknown factors. Therefore, several phases are designed for the evaluation of field compaction protocols. These phases, shown in Table 3-1, are designed to evaluate one or two compaction factors at a time while the other factors are kept constant. Phase I focuses on the determination of optimal roller types. Phase II determines the optimal number of coverages using inputs found from Phase I. Phase III is designed to study the coverage distribution of a multilayered seal. Finally, Phase IV examines the rolling pattern using results from the previous phases.

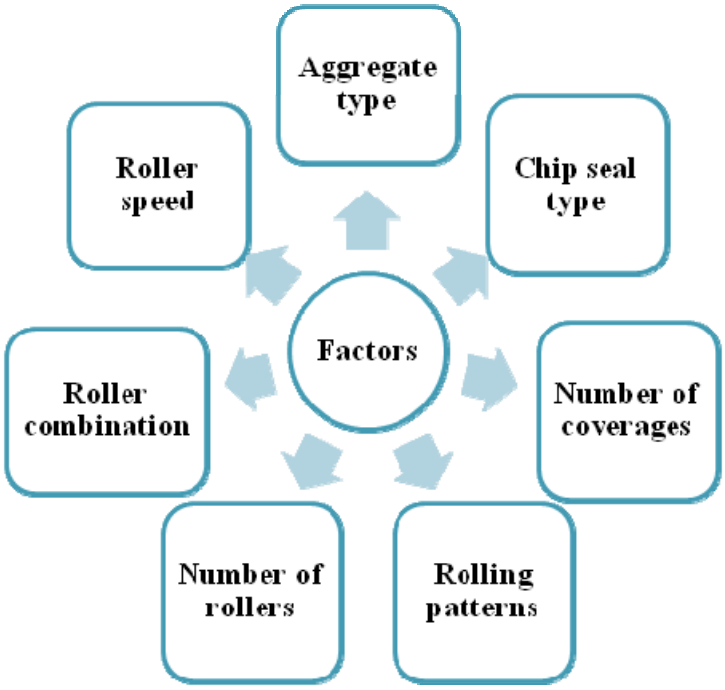

Figure 3-1 Factors to be considered in chip seal compaction

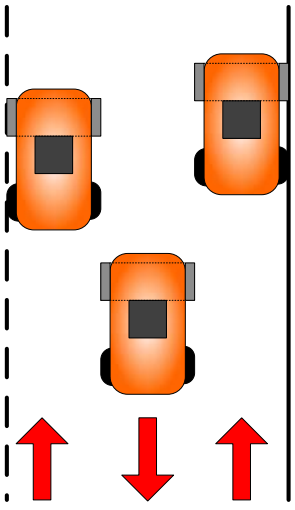

Figure 3-2 Schematic diagram of three passes of one roller

The number of coverages adopted in Phase I for the determination of the optimal roller type is three coverages, based on a literature review. For example, a study of rolling practices conducted in New Zealand found that three passes is the most effective. Also, three passes is the specified number of minimum passes in the standard specifications of a few states, such as Arizona and Louisiana. Using two rollers in a parallel pattern covers an entire lane at the same time, thus optimizing the process. Three different rollers were used to find the optimal roller type in Phase I.

Phase II is designed to determine the optimal number of coverages for chip seal construction. The number of coverages is important in the rolling process to achieve proper aggregate embedment and to interlock the aggregate particles.

Phase III is designed to observe the effects of different coverage distributions on each layer of multilayered chip seals. The current practice in North Carolina (NC) for general coverage distribution is a single coverage on each layer.

Table 3-1 Field Test Program

Phase	Research Purpose and Factors
I	Determination of optimal roller type • Using three different rollers • Using straight seal • Using three coverages
II	Determination of optimal number of coverages • Using two combination rollers • Using straight and split seal • Using parallel rolling pattern
III	Determination of optimal coverage distributions • Using pneumatic tire roller and combination roller • Using split and triple seal • Using parallel rolling pattern
IV	Determination of optimal rolling patterns • Using two pneumatic tire roller and two combination rollers • Using straight seal • Study delayed initial rolling time

However, the New Zealand Chip Seal Rolling Study recommends three coverages on the top layer of a chip seal without any rolling on the sublayers. In order to evaluate the effect of the distribution number of coverages on each layer, the four cases shown in Figure 3-3 are selected. This figure shows a schematic diagram of the distributed coverage for each layer, as follows: Figure 3-3 (a) shows the New Zealand practice for the split seal; Figure 3-3 (b) shows the NC practice for the split seal; Figure 3-3 (c) shows a combination of the New Zealand and NC practices for triple seals; and Figure 3-3 (d) shows the current NC practice for triple seals. It is expected that these four cases will create different structures of the aggregate and, therefore, will illustrate different levels of performance.

The purpose of Phase IV is to determine the optimal rolling patterns for chip seal construction based on the results obtained from the previous phases. Five rolling patterns were designed based on the current NCDOT patterns and on the number of rollers.

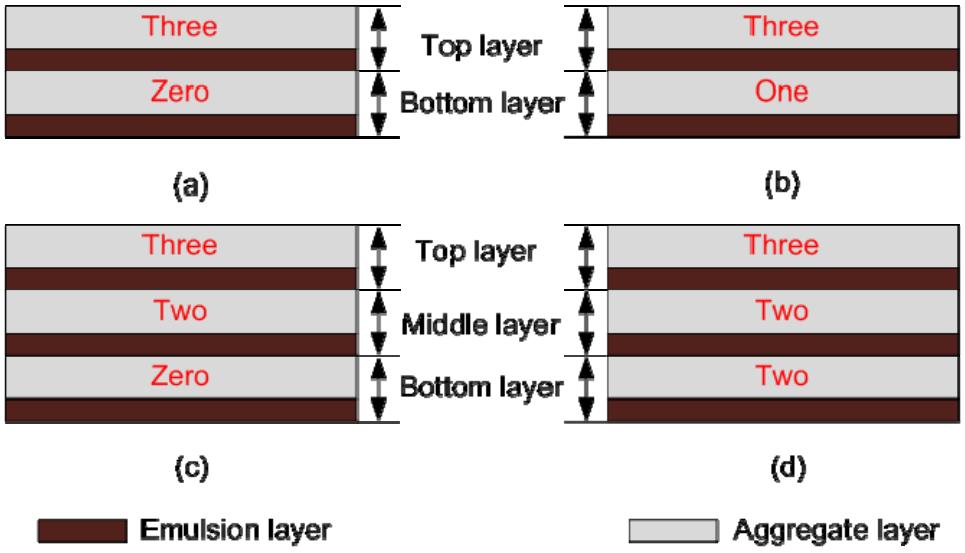

Figure 3-3 Distributed rolling coverage on each layer: (a) New Zealand practice for split seal; (b) NC practice for split seal; (c) a combination of New Zealand and NC practices for triple seal; (d) NC practice for triple seal

3.2 Specimen Fabrication

One of the critical procedures in this research is fabricating the field samples so that they correspond to the actual construction sequence. Thus, establishing the field sampling procedure is of utmost importance to this study. Figure 3-4 describes the developed sampling procedure. Figure 3-4 (a) shows the placement of the templates on the existing pavement. Templates for the flip-over test (FOT), Vialit test, and for the Third-scale Mobile Model Load Simulator (MMLS3) are affixed in the longitudinal direction to the ground paper that covers the existing pavement. The longitudinal layout helps to avoid the sample-to-sample variation in the transverse direction. Figure 3-4 (b) and Figure 3-4 (c) show spraying emulsion and spreading aggregate over the felt disks on the existing pavement, respectively. Except for the rolling pattern in Phase IV, the rolling pattern is a parallel pattern that uses two rollers to avoid overlapping coverage within a section, as shown in Figure 3-4 (d). Figure 3-4 (e) shows gathering the samples for delivery. In order to reduce the disturbance of aggregates on the sample during the collection of the samples, the samples were cured for 30 minutes at ambient temperature after completion of the rolling operation. Thus, the chip seal specimens were much more stable while they were being gathered due to the fact that the water in them had evaporated, thus causing an improved mechanical bonding between the emulsion and the aggregate. As shown in Figure 3-4 (e), samples are placed on a wooden plate to minimize disturbance during the delivery. Collected samples on the wooden plates are stored on racks, as shown in Figure 3-4 (f).

Figure 3-4 Sample fabrication procedure: (a) affixed felt disks on the existing pavement; (b) spraying emulsion; (c) spreading aggregate; (d) compacting with rollers; (e) gathering samples; (f) delivering samples to laboratory

3.3 Materials

This section describes the materials selected for testing and the physical properties of the component materials.

3.3.1 Material Selection

Two types of aggregate were selected for use with the CRS-2 emulsion: Stalite with a 5/16 in. nominal maximum aggregate size (NMAS), and granite No. 78M. The granite aggregate comes from the Hanson quarry; the Stalite is produced by the Carolina Stalite Company using a rotary kiln expanded, slate, light-weight aggregate. The CRS-2 emulsion is obtained from SemMaterials, L.P.

3.3.2 Gradation of Aggregate Particle Size

Dry sieve analyses were performed on both the aggregate types in accordance with ASTM C 117. Figure 3-5 shows the gradations for the two aggregate types plotted on the 0.45 power chart.

3.3.3 Flakiness Index

The Flakiness Index (FI) is a measure of the percentage, by weight, of flat particles. It is determined by testing a small sample of aggregate particles for their ability to fit through a slotted plate (Figure 3-6). There are five slots for five different fractions of the aggregate (Table 3-2). If the aggregate particles fit through the slotted plate, they are considered to be flat. If not, they are considered to be cubical.

The weight of the materials passing all of the slots is divided by the total weight of the sample to give the percentage, by weight, of the flat particles; this percentage is the Flakiness Index. The lower the FI, the more cubical the aggregate. The Alaska DOT and Minnesota DOT specify the FI as a maximum of 30% for the chip seal and a maximum

20% for high volume roadways. (Mchattie 2001, Janisch et al. 1998) The tolerance limits for the flakiness of the aggregate are controlled in accordance with traffic but generally should be less than 30 (Croteau et al. 2005).

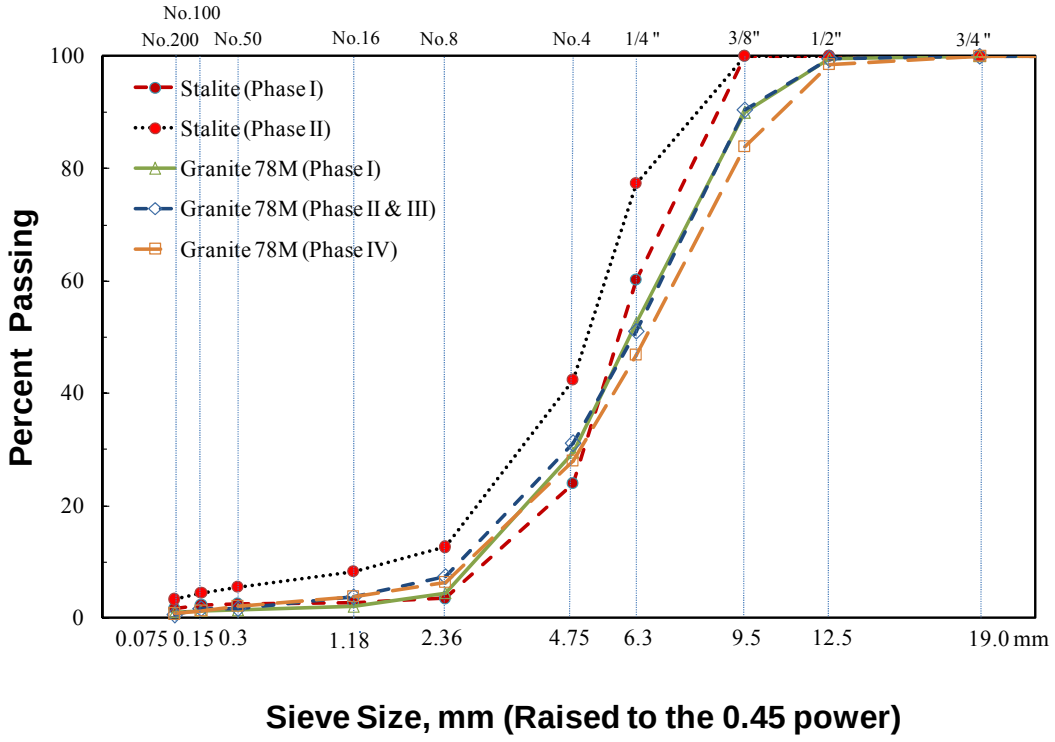

Figure 3-5 Aggregate particle size gradations

Table 3-2 Slot Size Required for Different Fractions (Mchattie 2001)

Size of Aggregate		Slot width, in.
Passing	**Retaining**	
1 in.	3/4 in.	0.532
3/4 in.	1/2 in.	0.384
1/2 in.	3/8 in.	0.258
3/8 in.	1/4 in.	0.184
1/4 in.	No. 4	0.123

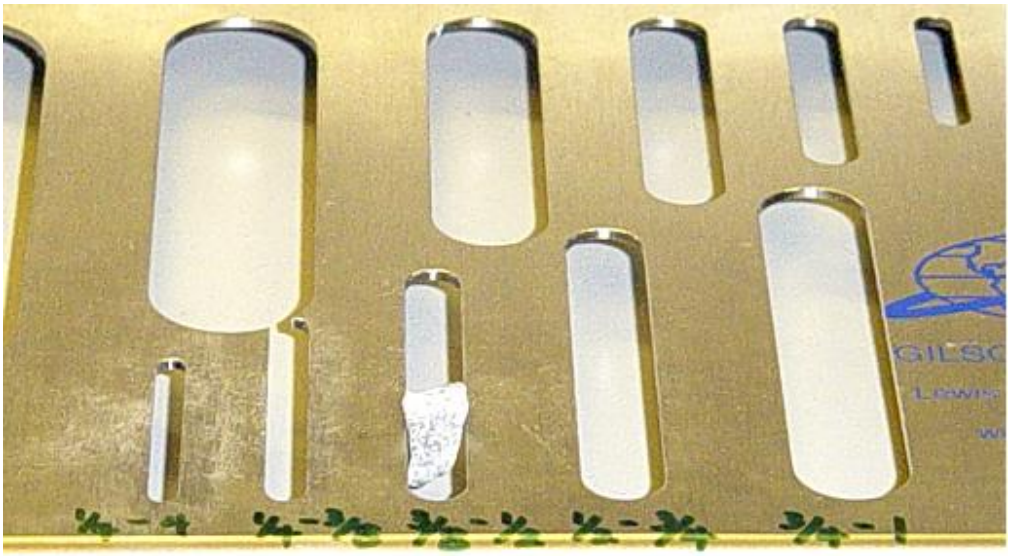

Figure 3-6 Flakiness Index plate gauge

3.4 Experimental Test Method

3.4.1 Vialit Test Procedure

The Vialit test was developed by the French Public Works Research Group and standardized in BS EN 12272-3. This test method is an indicator of aggregate retention for chip seals using Vialit testing apparatus, as shown in Figure 3-7. A stainless steel ball is dropped three times from a height of 19.7 in. onto inverted chip seal trays. The percentage of aggregate loss after three ball drops is used for the evaluation of aggregate retention.

The AST specimens obtained from the field were cured at 95°F (35°C) for 24 hours. Three or six replicates were tested, and Equation (1) and Equation (2) were used to calculate the percentage of aggregate loss using the results from replicated tests. It is noted that the weights used in Equation (1) are those of chip seal specimens, i.e., the combined weights of the emulsion and aggregate. The use of the combined weights was necessary

because the emulsion weight and the aggregate weight could not be determined separately. Equation (2) uses the only aggregate weight that was measured after the mixture was burned in the ignition oven.

$$Aggregate\ Loss\ (\%) = \frac{W_{B,mixture} - W_{A,mixture}}{W_{B,mixture}} \times 100\,, \tag{1}$$

where

$W_{B,mixture}$ = weight of emulsion and aggregate on chip seal specimen before the test and

$W_{A,mixture}$ = weight of emulsion and aggregate on chip seal specimen after the test.

$$Aggregate\ Loss(\%) = \frac{W_{B,agg} - W_{A,agg}}{W_{B,agg}} \times 100\,, \tag{2}$$

where

$W_{B,agg}$ = weight of aggregate on chip seal specimen before the test and

$W_{A,agg}$ = weight of aggregate on chip seal specimen after the test.

Figure 3-7 Vialit test apparatus

3.4.2 Flip-Over Test

The flip-over test (FOT) measures the amount of excess aggregate on the specimens and is part of the sweep test procedure (ASTM D 7000). The samples obtained from the test sections were stored at room temperature and were fully cured at 95°F (35°C) for 24 hours before the test. The specimen was turned vertically, and any loose aggregate was removed by lightly brushing the specimen. Equation (2) was used to calculate the percentage of aggregate loss from the six replicated tests results.

3.4.3 Ignition Oven Test

The Ignition Oven method, which is specified in ASTM D 6307 (ASTM), is adopted to determine the weight of residual aggregate and emulsion. This test method determines the amount of asphalt in hot mix asphalt (HMA) by burning the asphalt cement in an ignition furnace. The amount of emulsion is calculated by the difference in the weight of the original chip seal sample and the residual aggregate. It is noted that the type of aggregate in the bituminous paving mixture may affect the results of this test method. Different aggregates may lose mass to varying degrees due to the pyrolytic action. Accordingly, a correction factor, as shown in Table 3-3, is determined for each type of aggregate. This correction factor is applied to calculate the aggregate weight after burning the specimen.

Table 3-3 Correction Factors for Each Type of Aggregate

Type of aggregate	Correction factor (%)
Granite 78M	0.26
Stalite	0.27

3.4.4 Embedment Depth

In chip seal construction, the purpose of rolling is to achieve proper aggregate embedment to resist traffic loading. Therefore, the rolling operation must follow as closely behind the aggregate spreader as possible to avoid failure. In order to evaluate the embedment of the aggregate, the sand circle method is often employed to measure the exposure depth of the aggregate in the chip seal system based on a volumetric technique.

In this study, a modified sand circle method has been developed to measure the actual embedment depth of the aggregate into the emulsion film. This method is described below in detail.

3.4.4.1 Sample preparation

In order to directly measure the embedment depth of the aggregate, the emulsion must be eliminated from the chip seal structure. The following special specimen preparation technique has been developed by modifying the standard specification found in *Austroad T 253 Seal Behavior*:

1) Pour epoxy onto the specimen, ensuring complete coverage of all the aggregate particles to a sufficient depth.
2) Do not disturb the specimen until the epoxy has set; allow approximately 24 hours.
3) Place the specimen covered with epoxy in a tray with sufficient kerosene to completely submerge the remaining surface seal that is attached to the epoxy; allow the specimen to soak for a minimum of 12 hours.
4) Wash any remaining binder off the specimen with Citra-solve.
5) Allow all solvent to evaporate from the specimen.
6) Ensure that the area to be tested is dry and free from detritus. Brush any fine material from the surface.

3.4.4.2 Modified sand circle method

A modified sand circle method based on *Roads and Traffic Authority Test Method T 240: Texture Depth of Coarse Textured Road Surfaces* has been developed that describes the procedure for measuring the average textural depth of a chip seal. This method adopts the use of a loose unit mass of sand to calculate the average texture depth, as opposed to the method used for the sand patch test (ASTM E 965). After pouring the sand on the specimen, the sand is carefully spread into a circle. However, it is difficult to maintain a circular form as the diameter of the circle increases. Thus, a ring is used to confine the spread of the sand within the circle.

Both the calculation of the loose unit mass of sand and the sand circle test procedure are described below.

3.4.4.3 Calculation of loose unit mass of sand

1) Determine the internal volume (V) in ml of the calibrating container either from the quantity of water necessary to fill the container or by calculation based on internal dimensions measured to the nearest 0.2 mm.
2) Clean and dry the calibrating container and determine its mass to the nearest 0.1 g (M_1).
3) Fill the calibrating container with sand by pouring the sand from a pouring can into the container in an even stream, keeping the pouring spout approximately 25 mm above the surface of the sand to form a central cone. Slightly overfill the container and carefully screen off the excess with a straightedge to provide a surface level with the top of the container. Determine the mass of the container plus its contents to the nearest 0.1 g (M_2). Care is necessary to ensure that the calibrating container is not vibrated or knocked during this operation.
4) Compute the loose unit mass of the sand as follows:

   Loose unit mass (C) $= \frac{M_2 - M_1}{V}$ g/ml

5) Repeat these measurements at least three times and determine the mean of the loose unit mass in g/ml. The range of the loose unit mass obtained by the operator should not exceed 0.01 g/ml.

3.4.4.4 Sand circle test procedure

1) Measure the weight of sand that fills the ring to the nearest 0.1 g (W_1).
2) Put a ring on the specimen.
3) Pour the sand into the ring in an even stream, keeping the pouring spout approximately 25 mm above the surface of the sand to form a central cone. Slightly overfill the container and carefully screen off the excess sand with a straightedge to provide a surface level with the top of the ring.
4) Determine the weight of the sand remaining in the ring to the nearest 0.1 g (W_2). Care is necessary to ensure that the ring is not moved or knocked while removing the excess sand.
5) Determine the weight of the sand filling the voids of the specimen by subtracting W_1 from W_2.
6) Calculate the average embedment depth as follows:

   Average embedment depth = $\frac{1272M}{Dd^2}$,

   where

   D = loose unit mass of the sand (g/cm3);

   d = diameter of the ring (mm); and

   M = mass of the sand (W_2-W_1) (grams).

Figure 3-8 shows the steps of determining the embedment depth of the chip seal using the modified sand circle method. First, the emulsion in the chip seal structure is eliminated. Figure 3-8 (a) shows the bottom surface of the chip seal specimen, free of emulsion. Next, the specimen is covered with Tyvek, which has a hole with the same diameter as the ring. Figure 3-8 (b) shows the ring seated on the Tyvek. The exposed area

seen in Figure 3-8 (b) is used to measure the embedment depth. Figure 3-8 (c) shows the sand that is on top of the surface of the specimen, overfilled to create a central cone form. Next, the excess sand is carefully screened off with a straightedge to provide a surface level with the top of the ring, as seen in Figure 3-8 (d). Figure 3-8 (e) shows the screened-off sand. Finally, the excess sand is completely removed, as shown in Figure 3-8 (f), so that the sand remaining within the ring can be weighed.

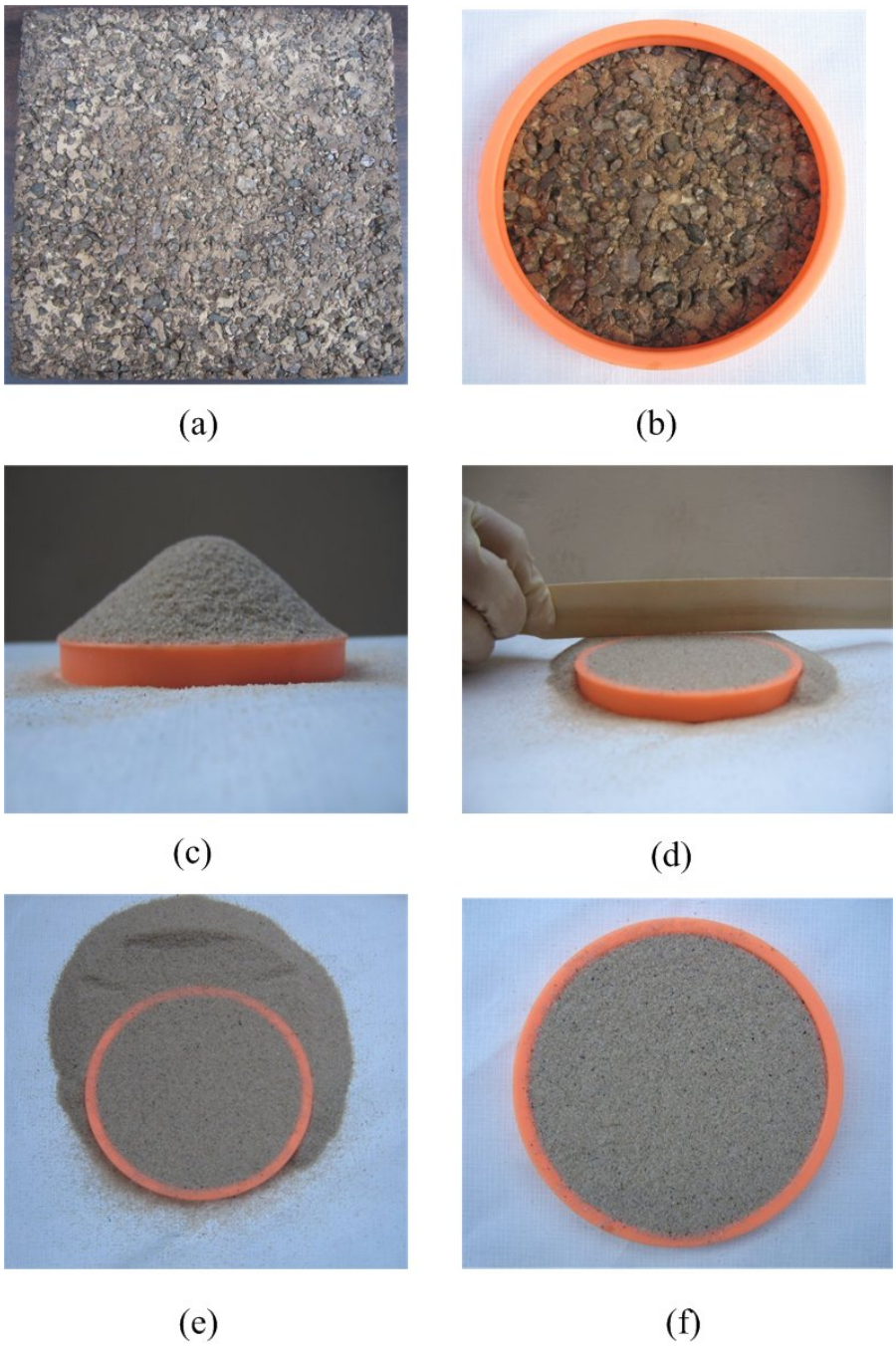

Figure 3-8 Modified sand circle test procedure: (a) surface texture after emulsion is dissolved and eliminated; (b) ring on surface of specimen (c) poured sand in ring; (d) leveling off excess sand with a straightedge (e) excess sand removed from circle (f) excess sand cleaned from sample

3.4.5 MMLS 3 Performance Test Procedure

The MMLS3 is a third-scale unidirectional vehicle load simulator that uses a continuous loop for trafficking. It is comprised of four bogies with only one wheel per bogie. These wheels are pneumatic tires that are 11.8 inches in diameter, approximately one-third the diameter of a standard truck tire. The wheels travel at a speed of about 5,500 wheel applications per hour, which corresponds to a dynamic loading of 3.3 Hz on the pavement surface. This loading consists of a 0.3 sec. haversine loading time and a rest period of 0.3 sec. The dynamic load on the pavement surface by the MMLS3 in motion is measured by a Flexiforce® pressure sensor. The mean value of maximum dynamic loads from the four wheels is approximately 802.6 lbf. The contact area is approximately 5.27 $in.^2$ measured from the footprint of one MMLS3 wheel inflated to 101.5 psi, thus resulting in a surface contact stress of approximately 152.1 psi (Lee 2004).

The major steps in the MMLS3 test preparation are shown in Figure 3-9. Figure 3-9 (a) shows the trimmed specimen, 7.1 in. wide and 14 in. long, for the MMLS3. For chip seal testing under the MMLS3, specimens are attached to thin steel plates that are fastened to a steel base plate, as illustrated in Figure 3-9 (c). MMLS3 loading was applied after a 3-hour temperature preconditioning period at 77°F (25°C). The weight of the specimen attached to the steel plate was measured before and after the MMLS3 loading to determine the aggregate loss. The aggregate loss during the initial traffic loading in the field (normally occurring within half a day) was measured after one wandering cycle of the MMLS3 loading. Then, MMLS3 loading was applied, and the weight measurements were taken periodically over a 2-hour period (equivalent to 11,820 wheel loads) to evaluate the aggregate retention performance of the chip seal under traffic (Kim et al. 2005).

The complete MMLS3 test procedure involves the following steps (Kim et al. 2005):

1) curing the specimens in a forced mechanical convection oven for 24 hours at 95°F (35°C) and 30 ± 3% RH, as specified by the ASTM D7000;

2) measuring the initial specimen weight;
3) conditioning specimens at 77°F (25°C) for 3 hours for the aggregate retention test;
4) MMLS3 loading for 10 minutes, which is the time required for the MMLS3 to complete one wandering cycle, and then measuring the specimen weight;
5) MMLS3 loading for 2 hours with periodic measurements of the specimen weight; and measuring the final specimen weight.

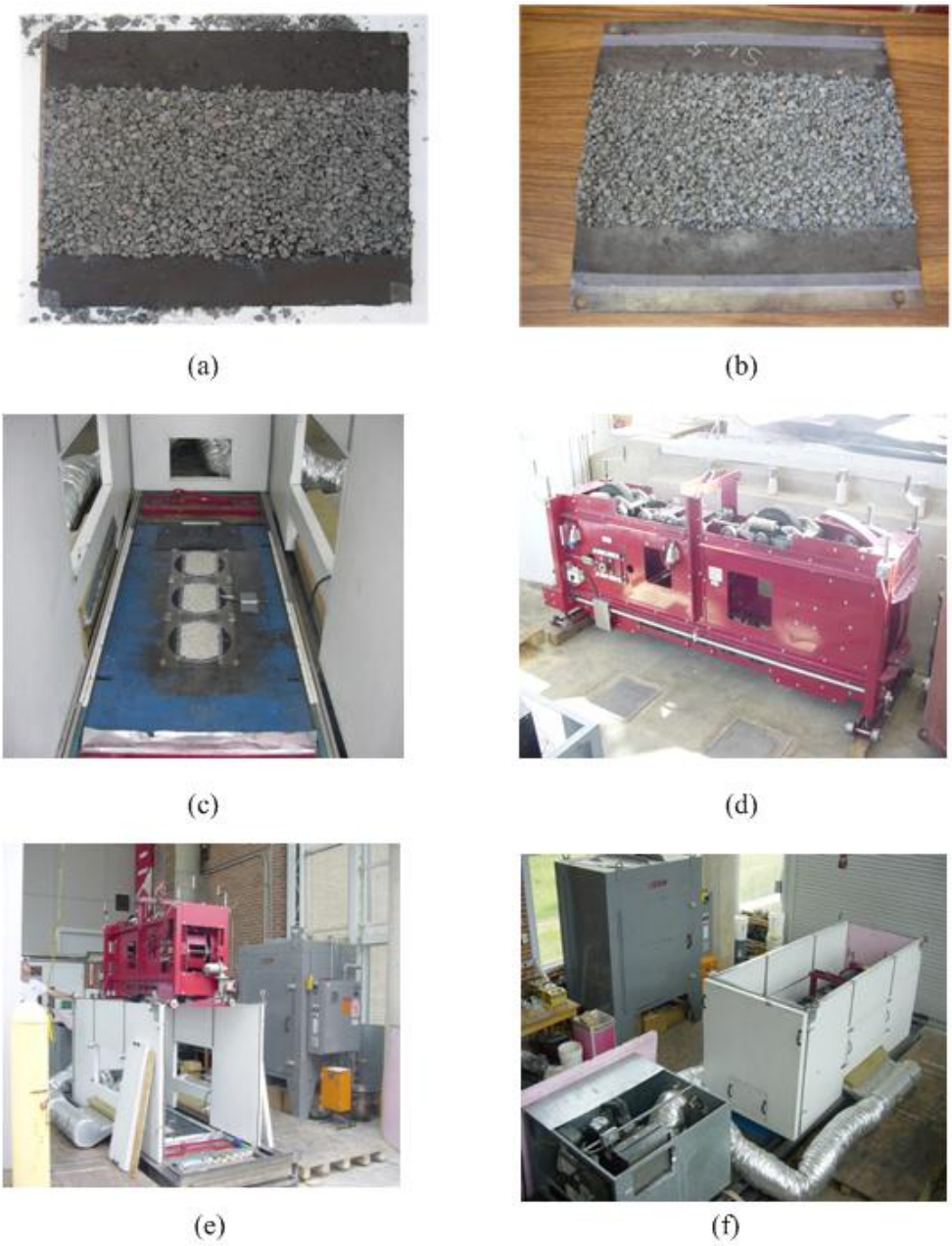

Figure 3-9 MMLS3 test preparation: (a) trimmed specimen; (b) MMLS3 test specimen; (c) installation of specimens on a steel base; (d) side view of MMLS3; (e) positioning MMLS3 in the temperature chamber; (f) complete MMLS3 test setup for chip seal testing

3.4.6 Digital Imaging of Cross-section of Epoxy-reinforced Asphalt Surface Treatment (AST)

In order to evaluate the relationship between the texture condition of the previous layer and the aggregate retention performance of multiple layers, digital image processing (DIP) is employed. DIP is comprised of three basic steps: (a) digital image acquisition of the cut surface of a chip seal specimen; (b) creation of a profile of the cut surface using MATLAB® R2007a; and (c) data analysis to calculate roughness. Two types of chip seals, split seals and triple seals, were used to evaluate the correlation of the texture with the aggregate loss performance.

Both split seal and triple seal specimens have two conditions, *No Traffic* load and *After Traffic* load. A prepared cut surface is scanned by a Hewlett Packard digital scanner (HP Scanjet 4850) as a color BMP file with a resolution of 300 dpi. Using Adobe Photoshop®, the Stalite 5/16" aggregate was manually eliminated from the original digital image using the Quick Selection tool. The digital image was converted from a color scale to an 8-bit grayscale before and after removing the Stalite 5/16" aggregate from the original image. The 8-bit grayscale digital image consists of a single plane of pixels. Each pixel is encoded using a single number representing grayscale values from 0 to 225.

To scan the cut surface of the chip seal image for DIP, various steps are required, as follows:

1) Remove excess aggregate from the original sample.
2) Pour epoxy onto the specimen, ensuring complete coverage of all the aggregate to a sufficient depth.
3) Do not disturb the specimen until the epoxy has set; allow approximately 24 hours.
4) Cut the specimen with an electric saw.
5) Dry the sample for 24 hours.

4. ROLLER TYPES

4.1 Experimental Program

Two types of rollers, the steel wheel roller and the pneumatic tire roller, are generally used in the United States to roll the aggregate during chip seal construction. A combination roller that combines the use of a rubber-coated steel wheel drum on one axle with a single row of rubber tire wheels on the rear axle is used in chip seal construction in New Zealand (Transit New Zealand 2005) and Canada (Croteau et al. 2005).

The primary objective of the Phase I experimental program is to determine an optimal roller type for the chip seal. In order to estimate roller performance, it is critical to test samples that are obtained directly from field construction. Test sections were constructed on New Sandy Hill Church Road (SR 1131) near Bailey in Wilson County, NC on June 12th 2007 to evaluate the effect of the different roller types. The experimental program includes a single seal type (straight seal) for the three test sections and three different types of rollers: the steel wheel roller, the pneumatic tire roller, and the combination roller.

Figure 4-1 shows a schematic diagram for determining the optimal roller type for chip seal construction. It shows the layout of the three different roller types in a 1000 ft. long section, which is divided into three 300 ft. long sections, one section per roller type, with a remaining 100 ft. section used for start-up. These 300 ft. long sections were used to fabricate samples, as follows. Once the templates are affixed onto the existing pavement for the entire 1000 ft. length, the emulsion sprayer sprays emulsion. Next, the aggregate spreader spreads aggregate over the emulsion. Then, the three different roller types roll the aggregate immediately after the aggregate spreader has passed the start of each divided section. Each section receives three coverages. The aggregate and emulsion application rates (AARs and EARs) were determined from visual observations made by the North

Carolina Department of Transportation (NCDOT) Division Supervisors from a trial construction. The AAR and EAR for the straight seal are 17 lb/yd^2 and 0.35 gal/yd^2, respectively.

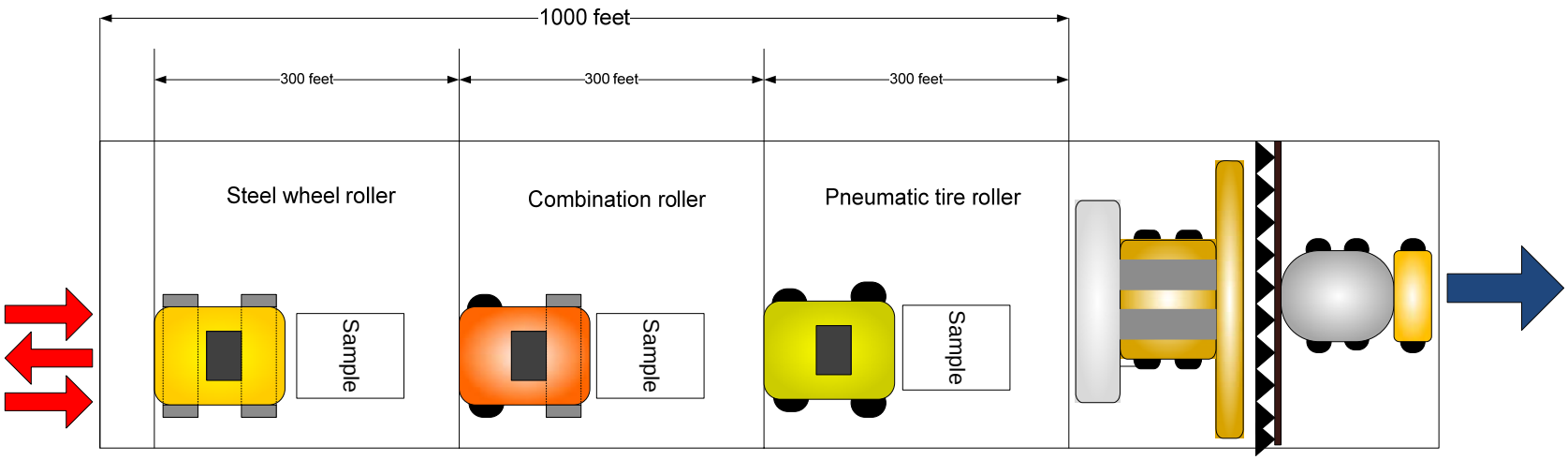

Figure 4-1 Schematic diagram for determination of optimal roller type

4.2 Sample Weight Variations

Samples fabricated in the field have a natural variability. Due to the specimen-to-specimen variability, statistical methods are used to determine if the weight of the mixtures or aggregate are similar or different. The statistical test chosen for this comparison is the equal variance two-tailed paired t-test, or analysis of variance (ANOVA). The null hypothesis is that the mixture or aggregate weights are the same. One challenge with using this method is that it determines significance based on the pooled variances of all the inputs. Some comparisons involve one set of data with low variability for one group and high variability for another. This difference means that some p-values are more precise than others. To compensate for this discrepancy, the variance was pooled for a given test method, e.g., the Vialit test. The variability of each group was taken into account by dividing each result by the standard deviation of the group (i.e., the modified z-test). The z-values were multiplied by the pooled standard deviation and added to the group mean. The t-test or ANOVA against the group number (two or three) was performed on the modified values (LaCroix et al. 2008).

Table 4-1 shows both the basic statistical analysis and a comparison with the ANOVA results. A significance level of 0.05 was used for the ANOVA test. From the ANOVA test results, as shown in Table 4-1, all the p-values for the F-test are larger than 0.05. Thus, no significant difference is evident in the sample weight per each test method for the three roller type groups.

Figure 4-2 plots the distribution of both mixture and aggregate weights to find an optimal roller type using the three different rollers. Figure 4-2 has three symbols, a filled symbol, an empty symbol, and a large empty circle symbol. The large empty circle symbol indicates the averages of the data for each roller type. The mixture weight is represented by the filled symbol, and the aggregate weight is represented by the empty symbol. The aggregate weight, as shown in Figure 4-2, was determined after the chip seal samples were burned in the ignition oven. The relatively small variations and close distribution of weights are shown in Figure 4-2.

Table 4-1 Results of Statistical Analysis of Sample Weights

Test Method	Type of weight	Type of rollers	Mean	Variance	Std. Dev.	F-Stat	P-value	Conclusion
Vialit	Mixture	Steel	349.7	655.8	25.6	2.24	0.14	**Accept H_o**
		Combo	324.0	364.8	19.1			
		Pneumatic	324.7	424.2	20.6			
	Aggregate	Steel	301.2	355.7	18.9	0.87	0.44	**Accept H_o**
		Combo	279.8	285.3	16.9			
		Pneumatic	281.5	484.7	22.0			
FOT	Mixture	Steel	640.2	816.8	28.6	2.55	0.11	**Accept H_o**
		Combo	605.5	736.5	27.1			
		Pneumatic	615.8	225.5	15.0			
	Aggregate	Steel	574.0	766.5	27.7	3.16	0.07	**Accept H_o**
		Combo	540.0	750.7	27.4			
		Pneumatic	539.9	52.5	7.2			
MMLS3	Mixture	Steel	594.8	388.0	19.7	2.55	0.10	**Accept H_o**
		Combo	587.8	523.8	22.9			
		Pneumatic	608.8	148.7	12.2			
	Aggregate	Steel	530.0	363.0	19.1	2.24	0.14	**Accept H_o**
		Combo	520.4	879.1	29.6			
		Pneumatic	540.5	148.3	12.2			

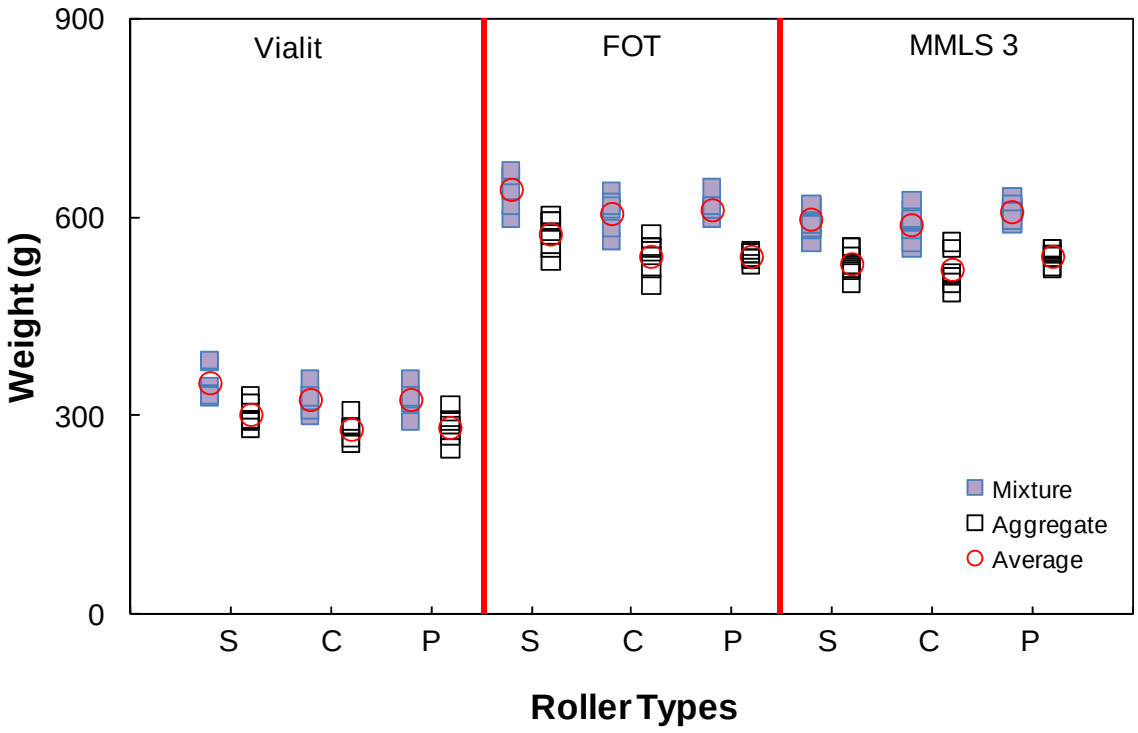

Figure 4-2 Aggregate distribution: S is steel wheel roller; C is combination roller; P is pneumatic tire roller

4.3 Test Results

4.3.1 Flip-Over Test

The flip over test (FOT) measures the amount of excess aggregate on the specimen. Details regarding specimen curing and FOT procedures are described in Chapter 3 and, therefore, a detailed description is not included here. From the statistical analysis, as explained in Section 4.2, the variance of sample weights was narrowed, as shown in Figure 4-2. Figure 4-3 shows the percentage of aggregate loss from the FOT of the straight seal in terms of the three different roller types. The percentage of aggregate loss represented in Figure 4-3 is determined using the weight of the aggregate using Equation (2). A large circle empty symbol indicates the average of the data for each roller type. The small variation of sample weights, as shown in Figure 4-2, diminishes the range of the

percentage of the aggregate loss, as shown in Figure 4-3. The percentages of aggregate loss of the combination roller and the pneumatic tire roller show a larger variation than that of the steel wheel roller, ranging from 4.4 % to 8.7%, as shown in Figure 4-3. The range of the percentage of the aggregate loss seen in Figure 4-3 is below the maximum allowable aggregate loss specified, 10%, in the Alaska chip seal guide. The pneumatic tire roller shows the lowest percentage of aggregate loss, 4.4%, among the three different rollers.

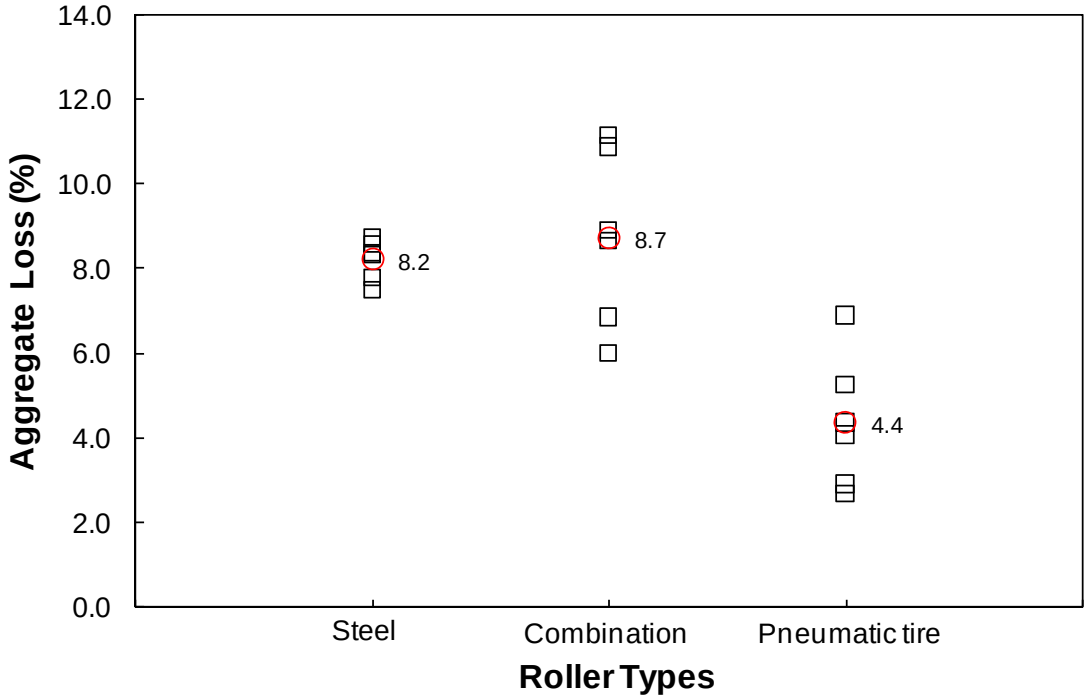

Figure 4-3 Aggregate loss of a straight seal obtained from FOT samples

4.3.2 Vialit Test

The Vialit test is used to measure the adhesion between the aggregate and the emulsion for the evaluation of aggregate loss performance. The details of the Vialit test procedure are explained in Chapter 3 and, therefore, are not provided here. The Ignition Oven method, likewise described in detail previously, is used to determine the emulsion

weight in the chip seal mixture. To determine the aggregate weight of the Vialit test sample, the Vialit test sample mixture is removed from the Vialit steel plate and then put into the ignition oven to burn off the emulsion. Finally, the emulsion weight is determined by subtracting the weight of the residual aggregate after the Ignition Oven test. This emulsion weight is then subtracted from the weight of the chip seal specimen before testing to determine the weight of the aggregate in the original, untested chip seal specimen. Figure 4-2 shows the aggregate weight distributions of the Vialit samples after burning.

As explained in the previous statistical analysis, no significant difference was found in the sample weights from the Vialit test. The aggregate loss performance was calculated using Equation (2) and is presented in Figure 4-4 in terms of the different roller types.

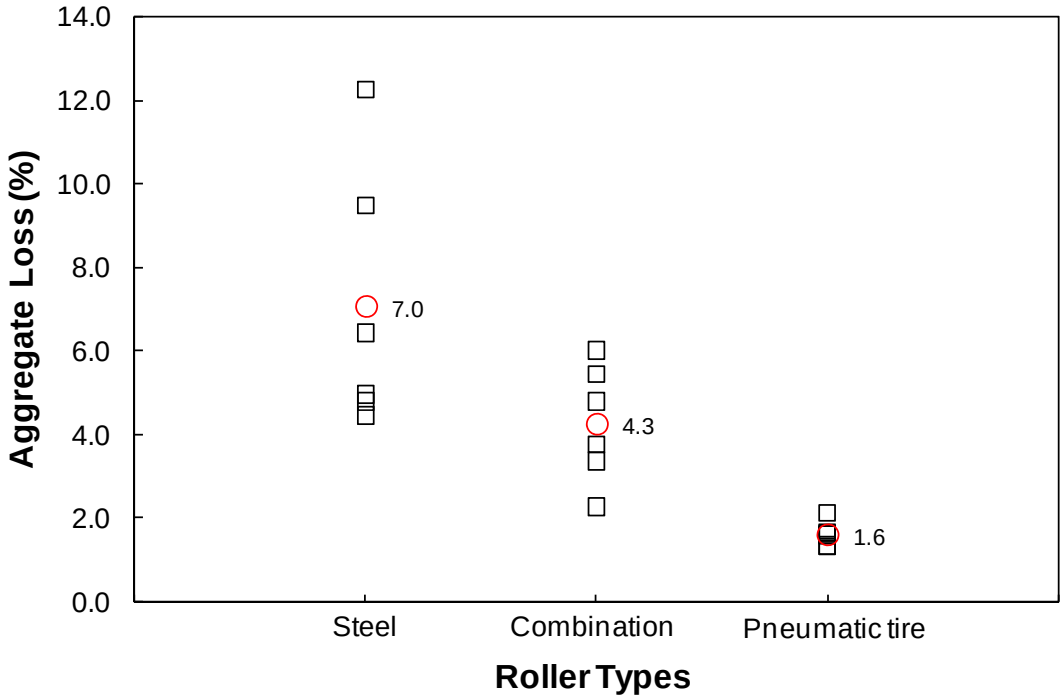

Figure 4-4 Aggregate loss of a straight seal from Vialit test samples

The largest variance of aggregate loss occurred from the steel wheel roller, which is contrary to the FOT result. It is clearly seen in Figure 4-4 that the aggregate loss

performance indicates a significant decrease in aggregate loss, although those values are below the maximum allowable aggregate loss specified, 10%, in the Alaska chip seal guide **(**Mchattie 2001). The pneumatic tire roller shows the best aggregate loss performance, which is the same result as that from the FOT.

4.3.3 MMLS3 Test

Figure 4-2 indicates a small variation in the straight seal sample weights for the different roller types for the third-scale Model Mobile Loading Simulator (MMLS3) test, which is a similar result to that found in both the FOT and the Vialit test.

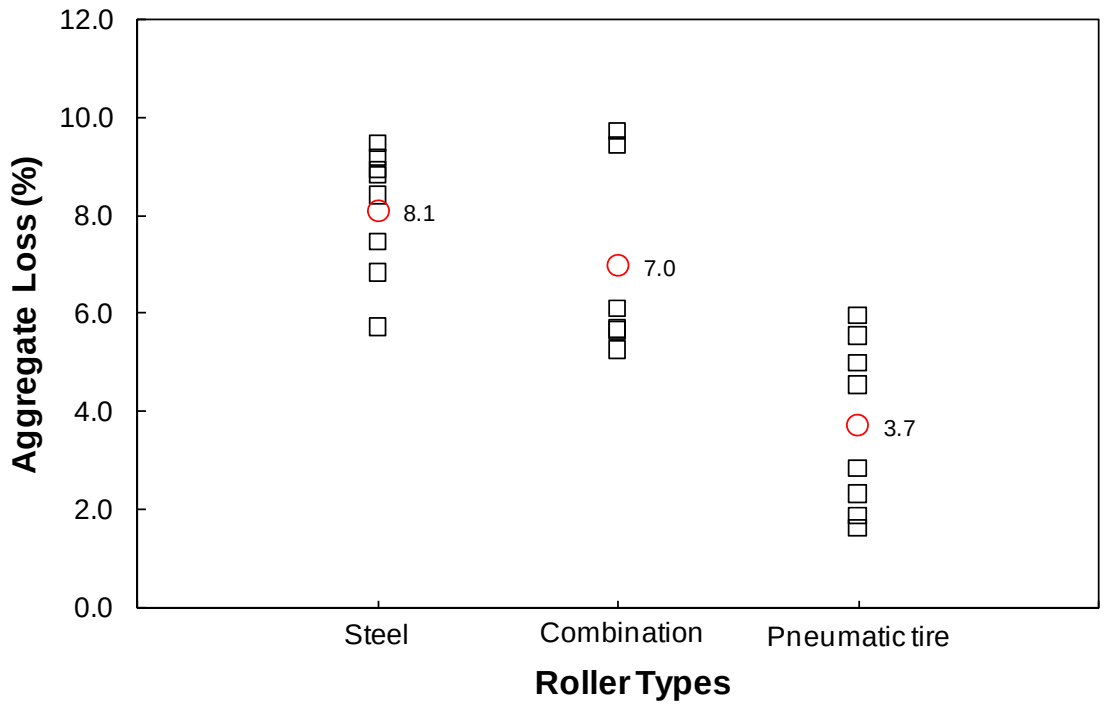

Figure 4-5 Aggregate loss of a straight seal from MMLS3 samples

Figure 4-5 shows the performance of aggregate loss after a trafficking load for 2 hr. 10 min. (12,940 wheel passes) using the MMLS3. Equation (2) was used to calculate the percentage of aggregate retention. A similar trend to that found from other aggregate

retention tests (Figure 4-3 and Figure 4-4) is observed in Figure 4-5. The sample that was rolled by a pneumatic tire roller shows the lowest percentage of aggregate loss (3.7%).

This percentage is nearly half of the others, 7.59% and 6.16%. These results indicate that a pneumatic tire roller shows better aggregate retention performance than the other two rollers, as was found also in the FOT and the Vialit test.

4.3.4 Comprehensive Analysis

Figure 4-2 shows the ANOVA test results for the aggregate retention performance that is used to determine an optimal roller type. All of the p-values from the ANOVA test are less than 0.05, which indicates that significant differences exist among the three groups per test method, i.e., Vialit, FOT, and MMLS3.

Table 4-2 Results of ANOVA: Different Roller Types

Test Methods	F-Test	P-Value	Conclusion
Vialit	5.078	0.021	Reject H_o
FOT	19.727	<0.0001	Reject H_o
MMLS3	8.022	0.002	Reject H_o

Table 4-3 Summary of Average Percentage of Aggregate Loss

Test Methods	Roller Types		
	Steel	Combination	Pneumatic tire
FOT	8.2	8.7	4.4
Vialit	7.0	4.3	1.6
MMLS3	8.1	7.0	3.7

Table 4-3 summarizes the percentage of average loss from the three aggregate retention tests. The steel wheel roller shows the poorest aggregate retention performance.

It is known that the use of a steel wheel roller on chip seals can result in an unequal compaction force distribution across a lane because the surface of the steel roller drum is straight along the wheel axle direction, and an existing pavement surface can be uneven across a lane. Also, the steel wheel roller compaction force is concentrated on the hump (the highest area), thus causing the aggregate at those locations to break. Such breakage is usually found in the area next to the wheel path. The breakage is also related to aggregate quality, because poor quality aggregate has a greater potential to break. Figure 4-6 shows photographs taken at one of the secondary roads in Division 3 of an uneven rolling distribution. Based on these observations, the use of the steel wheel roller has been removed from future consideration.

The roller that offers the lowest aggregate loss is the pneumatic tire roller, as indicated in Table 4-3. However, a visual observation of the chip seal surface rolled only by the pneumatic tire roller during the Phase I study reveals that the surface is much rougher than surfaces rolled either by a steel wheel roller or by a combination roller. These observations suggest the benefit of using both the pneumatic tire and combination rollers.

Figure 4-6 Uneven compaction under steel wheel roller

4.4 The Effect of Aggregate Shape with Roller Types

An interesting observation was found that, in this study, the aggregate shape is flatter than that used in the study of number of coverages. Aggregate particles are said to be *flaky* when their thickness is less than 0.6 of their mean size. Thus, the Flakiness Index (FI) of the aggregate used in the other Phases is shown in Table 4-4. The lower the FI, the more cubical the aggregate. The Alaska DOT and Minnesota DOT specify the maximum FI to be 30% for the standard aggregate quality requirements for a seal coat and double-layer chip seal (Mchattie 2001; Janisch et al. 1998). As shown in Table 4-4, the FI for all the aggregates is lower than 30%. However, the FI from Phase I is twice as large as that of Phase II with the same aggregate type. The FI of the Stalite 5/16" aggregate is

approximately three times smaller than that used in Phase I. This large value indicates a flatter aggregate shape. The relationship between aggregate shape and roller type was investigated using the Stalite 5/16" cubical.

Table 4-4 Flakiness Indices of Aggregates Used in Different Phases

Phase	Aggregate Types	Flakiness Index (%)
I	Granite 78M	24.26
II	Granite 78M	12.82
II	Stalite 5/16	8.28

4.4.1 Experimental Program

In order to evaluate the relationship between aggregate shape (FI) and roller type, the Division 5 crew constructed a small-scale field site on Hamlin Road (SR 1633) in Durham County on July 18th, 2007. In order to use cubical aggregate instead of the flatter aggregate, Stalite 5/16" aggregate was chosen for this study. Figure 4-7 compares the gradation of Stalite 5/16" aggregate with the granite 78M aggregate used in the previous test.

Table 4-5 shows the FI results from the two types of aggregate. The FI value of the Stalite 5/16" aggregate is smaller than that of the granite 78M, thus indicating that the granite 78M aggregate used in the previous section is a flatter aggregate shape. Two different types of rollers, the pneumatic tire roller and the combination roller, were used for this study. The construction sequence that was followed to fabricate samples in the field is the same as shown in Figure 4-1. Two rollers rolled the aggregate immediately after passing the aggregate spreader. CRS-2P emulsion was used because it is the emulsion that Division 5 commonly uses. The AAR and EAR employed are 11 lb/yd^2 and 0.25 gal/lb, respectively.

Table 4-5 Flakiness Indices of Two Aggregates Types

Aggregate Types	Flakiness Index (%)
Stalite 5/16	8.56
Granite 78M	24.26

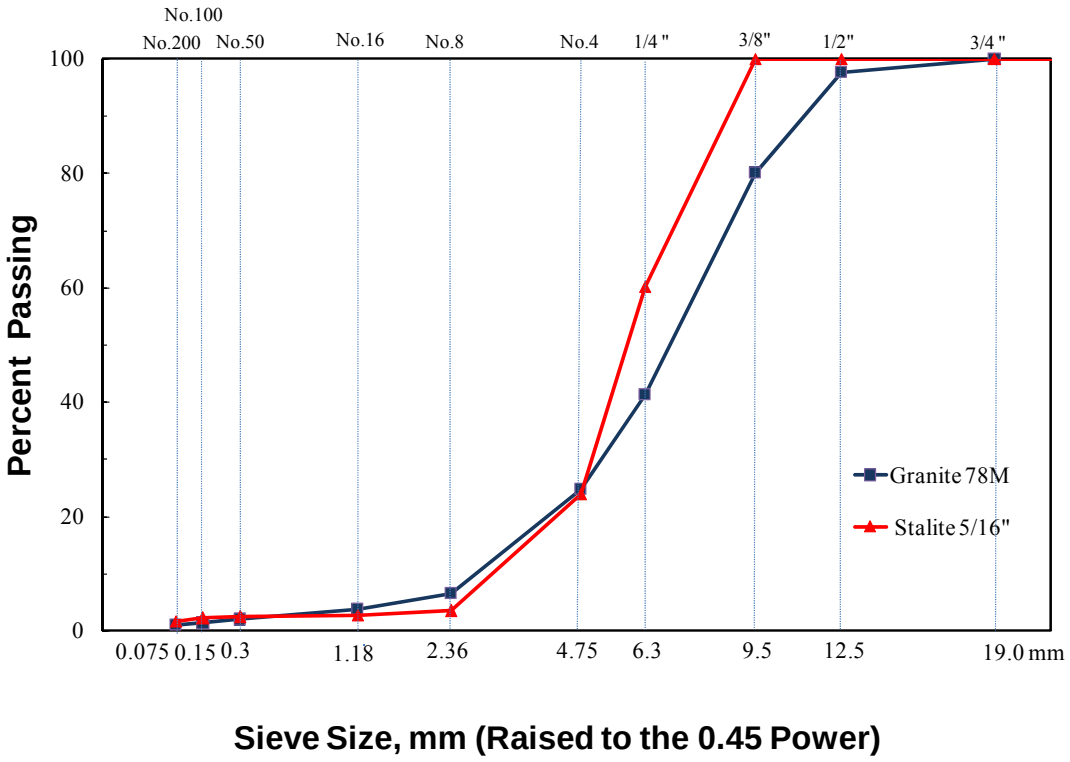

Figure 4-7 Aggregate gradation for straight seal construction

4.4.2 Comparison Sample Variation with Statistical Analysis

Due to specimen-to-specimen variability, statistical methods are used to determine if the weights are similar or different. The statistical test chosen for this comparison is the

equal variance two-tailed paired t-test. The null hypothesis is that the mixture or aggregate weights are the same. Table 4-6 shows the results of the statistical analysis of sample weights from two groups, the pneumatic tire roller and the combination roller.

A t-test with significance levels of 0.05 was performed to evaluate whether there are differences in the variances of sample weights between two sections as a function of roller type. Table 4-6, which summarizes the results of the tests, shows p-values that are bigger than 0.05. Thus, the means of the weights between the two groups is not different. Figure 4-8 displays the distribution of sample weights of the two sections as a function of the three different tests.

Table 4-6 Results of Statistical Analysis: Sample Weight

Test Methods	Types	Roller types	Mean	Variance	Std. Dev.	t-test	p-value	Conclusion
Vialit	Mixture	Pneumatic tire	132.3	216.2	14.7	1.21	0.25	**Accept H_o**
		Combination	141.6	124.2	11.1			
	Aggregate	Pneumatic tire	112.1	172.9	13.1	-0.75	0.47	**Accept H_o**
		Combination	117.0	86.0	9.3			
FOT	Mixture	Pneumatic tire	333.3	398.5	20.0	-0.56	0.59	**Accept H_o**
		Combination	339.9	447.3	21.1			
	Aggregate	Pneumatic tire	284.4	354.9	18.8	-0.46	0.66	**Accept H_o**
		Combination	289.4	310.1	17.6			
MMLS3	Mixture	Pneumatic tire	337.0	165.6	12.9	-1.59	0.13	**Accept H_o**
		Combination	327.1	150.1	12.3			
	Aggregate	Pneumatic tire	279.8	184.5	13.6	0.46	0.65	**Accept H_o**
		Combination	277.2	116.1	10.8			

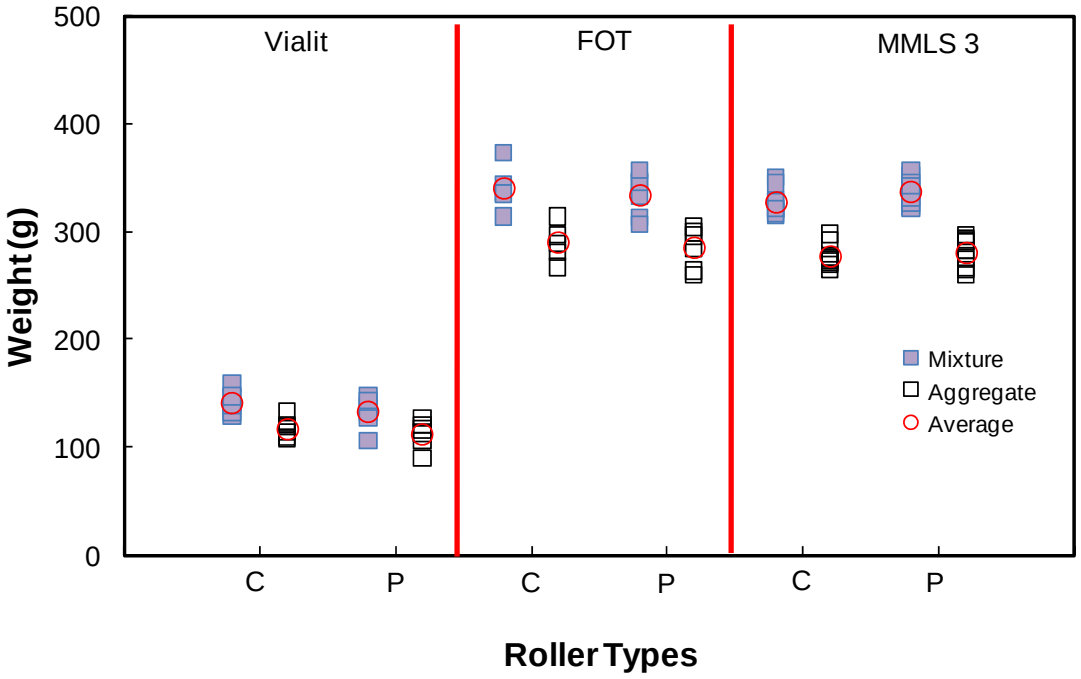

Figure 4-8 Distribution of sample weights from two sections: C is combination roller, P is pneumatic tire roller

4.4.3 Test Results

The Vialit test, FOT, and MMLS3 test were conducted to evaluate aggregate loss performance using Stalite 5/16"aggregate with two different roller types. Detailed information regarding these three tests is provided in Chapter 3. Figure 4-9 shows the results of the aggregate loss performance obtained from the three aggregate retention tests. As described in Figure 4-9, the trend of aggregate retention performance using the combination roller is slightly better than that using the pneumatic tire roller. The variance of the percentage of aggregate loss between the two groups is close. Thus, statistical analysis is required to recognize the significant difference between the two sections. Table 4-7 shows the results of the t-test, which is commonly used to compare two groups.

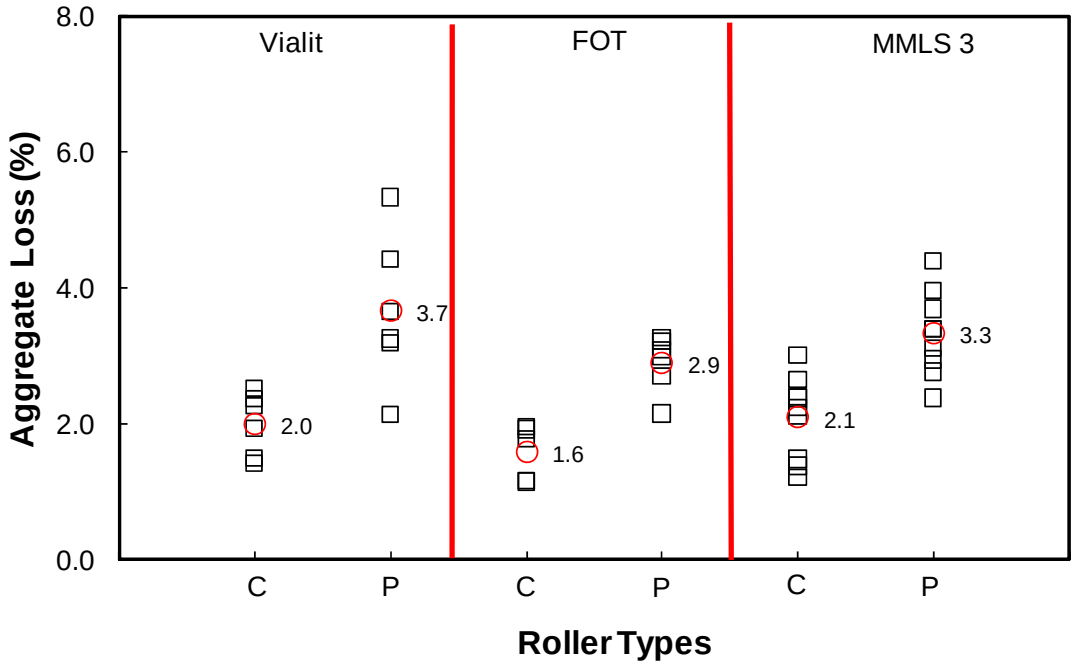

Figure 4-9 Results of aggregate loss performance: C is combination roller; P is pneumatic tire roller

From the t-test results shown in Table 4-7, the percentages of aggregate loss of the two different roller types are statistically different from each other because their p-values are less than 0.05, which is the alpha value. This result is contrary to the previous results using granite 78M aggregate where the pneumatic tire roller showed the best aggregate retention performance. It appears that the variability of aggregate gradations affects the aggregate loss performance that was reported in the previous NCDOT research report, "Optimizing Gradation for Surface Treatments." That is, in the optimal gradation research, the aggregate retention performance is affected by the variations in aggregate gradation (Kim and Lee 2005).

The pneumatic tire roller tends to leave a rougher surface texture than the steel wheel and combination rollers from observation of the field chip seal construction. The rougher surface texture results in more aggregate loss under traffic. The Stalite 5/16" aggregate used in this study has a more cubical shape and a more uniform gradation than

the granite 78M aggregate used in this study. Therefore, the combination of the pneumatic tire roller that produces a rough finish and the cubical shape and uniform gradation of the Stalite 5/16" aggregate could show a greater aggregate loss from the pneumatic tire roller. These observations suggest that the aggregate shape and gradation affects the aggregate retention performance, depending on roller type. Based on the results from this study, both the pneumatic roller and the combination roller are recommended for rolling the aggregate for chip seal construction. Due to the rough finish attributed to the pneumatic roller, it is recommended that the rolling should start with the pneumatic tire roller and finish with the combination roller.

Table 4-7 Results of Statistical Analysis Using Stalite 5/16"

Test Methods	Roller types	Mean	Variance	Std. Dev.	t-Test	p-value	Conclusion
Vialit	Pneumatic tire	3.66	1.22	1.10	2.27	0.047	Reject H_0
	Combination	1.99	0.22	0.47			
FOT	Pneumatic tire	2.89	0.18	0.42	2.74	0.027	Reject H_0
	Combination	1.58	0.17	0.41			
MMLS3	Pneumatic tire	3.34	0.39	0.62	2.99	0.009	Reject H_0
	Combination	1.77	0.27	0.52			

5. OPTIMAL NUMBER OF COVERAGES

5.1 Experimental Program

In order to evaluate compaction protocols, it is critical to test samples that are obtained directly from field construction. Test sections were constructed on SR 1131 near Bailey, NC in September 2006 to evaluate the effect of the number of coverages without being affected by the time delay between coverages. The experimental program includes the two seal types (straight seal and split seal) and three numbers of coverage (1, 3, and 5), resulting in six sections. A schematic diagram of the number of coverages is shown in Figure 5-1. The number of coverages is designed using odd numbers, i.e., 1, 3, and 5, because rollers must move forward during the last pass in the actual construction procedure in the field, as illustrated by the arrows seen in Figure 5-1. Each of the six test sections was divided into two groups according to chip seal type, and each of the two groups was composed of three sections so that the effects of the three coverages on the aggregate loss performance could be evaluated. Two combination rollers, which combine the use of a steel wheel drum on the front axle with four rubber tire wheels on the rear axle, were used side by side to cover an entire lane.

Granite 78M aggregate was used for the straight seal construction. For the split seal construction, granite 78M and Stalite 5/16" were used for the bottom and top layers, respectively. Only one rolling coverage was applied to the bottom layer of the split seal using the combination roller. Three different numbers of coverage (1, 3, and 5) were applied on top of the straight seal and split seal. The AARs and EARs were determined from visual observations made by the North Carolina Department of Transportation (NCDOT) Division Supervisors from a trial construction. The AAR and EAR for the straight seal were 17 lb/yd^2 and 0.35 gal/yd^2, respectively. The AARs for the split seal

were 17 and 9 lb/yd^2 for the bottom (granite 78M) and top (Stalite) layers, respectively. The same EAR of 0.25 gal/yd^2 was used for both layers in the split seal.

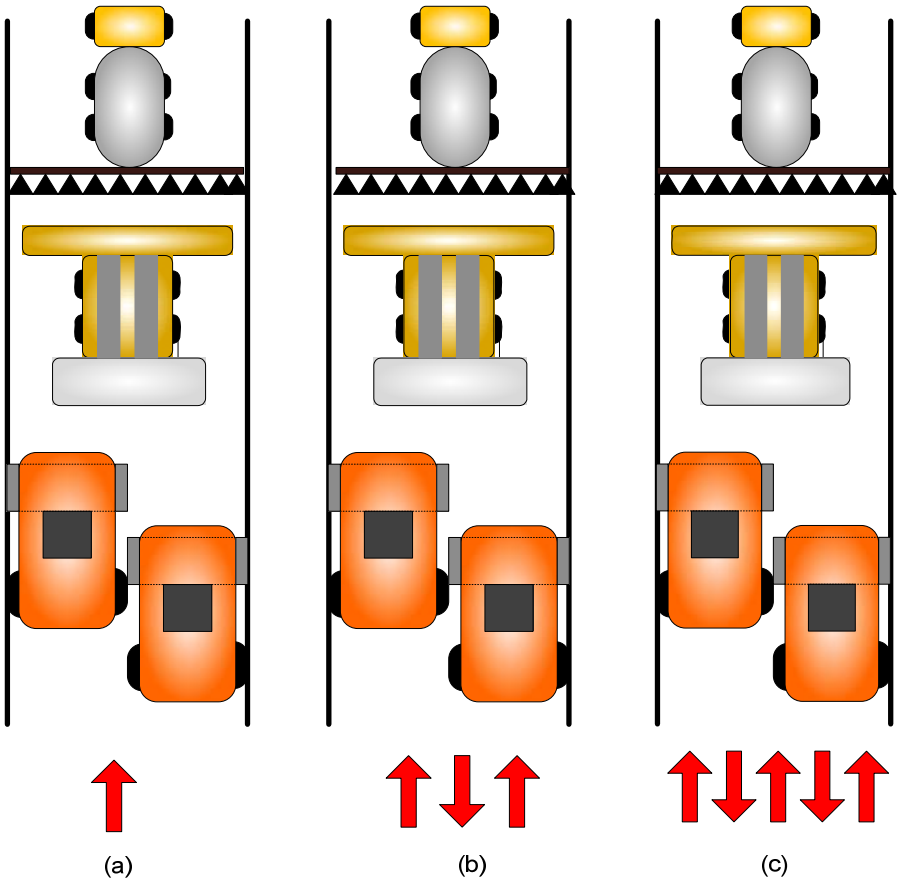

Figure 5-1 Schematic diagram of number of coverages

5.2 Sample Weight Variations

The samples for this number of coverages study have a certain fundamental sample variance because they were obtained directly from field construction. Thus, statistical analysis is required to estimate the distribution of the sample weights. For the statistical analysis of the sample variance against three different numbers of coverage, the

analysis of variance (ANOVA) was used to test the hypothesis that the means among the three groups are equal. The FOT and MMLS3 test show the same distribution, i.e., that the sample weights for three coverages is slightly higher than that for one and five coverages.

Table 5-1 shows the summary of the statistical analysis and ANOVA results of the mixture weights. In the ANOVA test, a significance level of 0.05 was used. In the straight seal case, one of those groups has a different means from that of the ANOVA test because the p-value is less than 0.05. In the split seal case, the means among the three different numbers of coverage are equal except in the case of the FOT.

Table 5-1 Statistical Analysis Summary

Method	Seal Type	Number of Coverages	Mean	Variance	Std. Dev.	F-Stat	P-value	Conclusion
Vialit	Straight	One	331.23	151.85	12.32	9.83	0.01	Reject H_0
		Three	349.77	36.14	6.01			
		Five	379.90	164.19	12.81			
	Split	One	564.17	334.40	18.29	0.86	0.47	Accept H_0
		Three	512.23	4751.16	68.93			
		Five	542.50	2028.64	45.04			
FOT	Straight	One	732.15	219.41	14.81	6.78	0.01	Reject H_0
		Three	782.78	396.83	19.92			
		Five	708.33	260.77	16.15			
	Split	One	1052.13	366.09	19.13	4.99	0.02	Reject H_0
		Three	1040.40	1208.69	34.77			
		Five	1096.27	1552.27	39.40			
MMLS3	Straight	One	751.49	375.20	19.37	17.84	<0.0001	Reject H_0
		Three	777.18	91.68	9.57			
		Five	727.68	251.55	15.86			
	Split	One	1059.05	194.52	13.95	0.34	0.72	Accept H_0
		Three	1064.43	656.06	25.61			
		Five	1065.94	552.12	23.50			

Figure 5-2 and Figure 5-3 show the sample weight distribution as a function of the chip seal type, i.e., the straight seal and the split seal. The split seal describes the variance as a narrow band of the sample weight. However, the straight seal shows a slightly fluctuant sample variance. The FOT and MMLS3 test show the same distribution, i.e., that the sample weight for three coverages is slightly higher than that for one and five coverages.

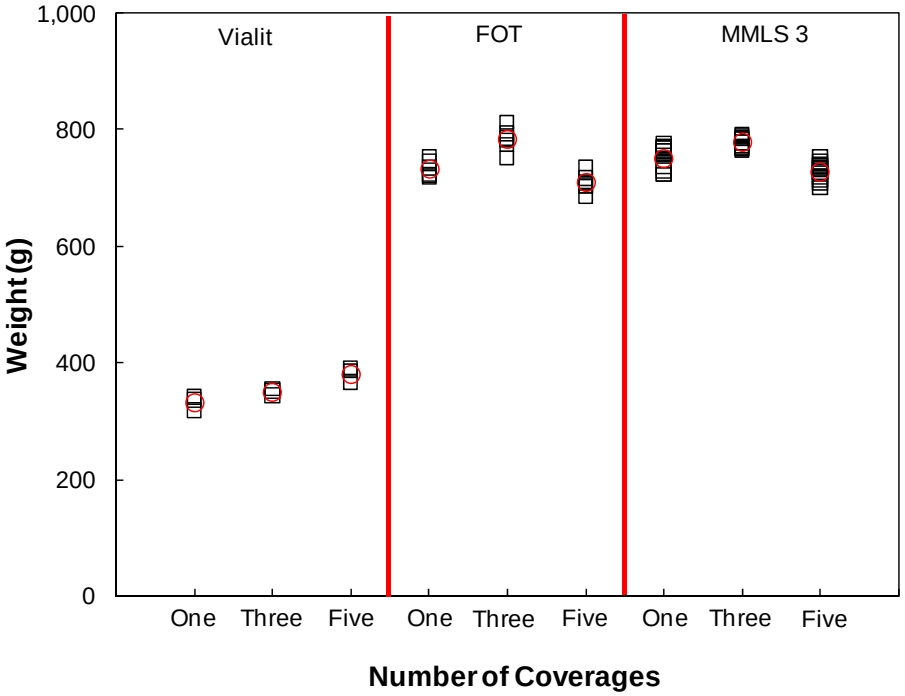

Figure 5-2 Mixture weight distributions of the straight seal

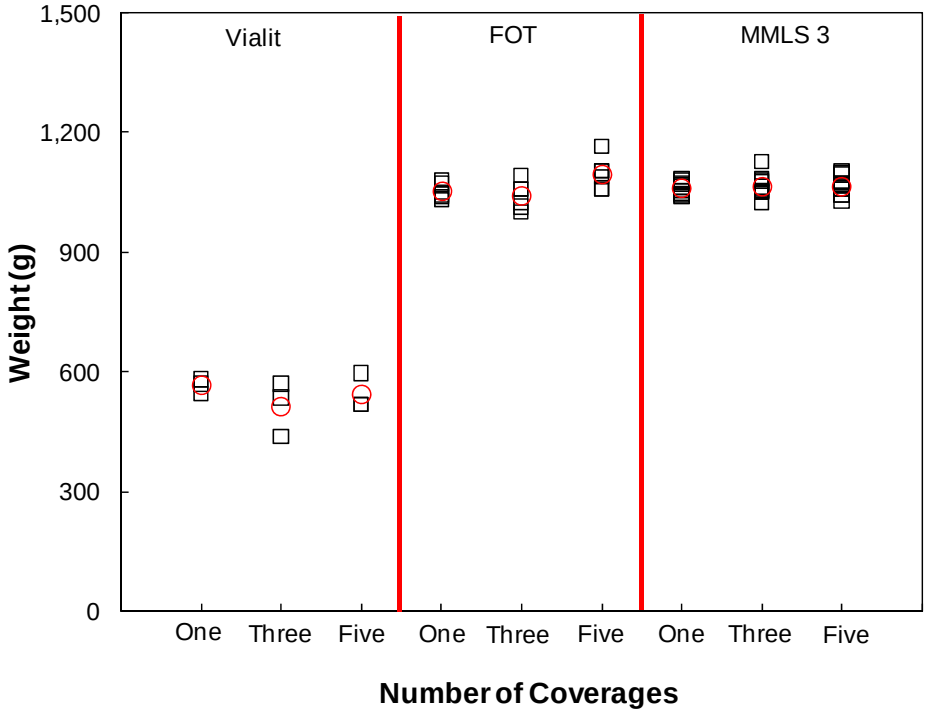

Figure 5-3 Mixture weight distributions of the split seal

5.3 Test Results

Laboratory tests were conducted on the samples obtained from the field test sections. The aggregate embedment depth of the chip seal was measured using the modified sand circle method. The aggregate loss performance was determined using the Vialit test, FOT, and the MMLS3 test.

5.3.1 Ignition Oven Test and Determination of Aggregate Weight

The total weight of the cured straight seal specimen obtained in the field is composed of three separate weights, i.e., the weight of the felt disk, the weight of the residual asphalt, and the weight of the aggregate. Because the weight of the felt disk is measured prior to chip seal sample fabrication, the aggregate weight before testing can be determined, if the asphalt weight is known. The asphalt weight is determined using the

Ignition Oven test by subtracting the weight of the residual aggregate after the Ignition Oven test and the weight of the felt disk from the weight of the tested specimen before the Ignition Oven test. Thus, the weight of the aggregate in the original, untested chip seal specimen can be determined once the weight of the asphalt and the weight of the felt disk are subtracted from the weight of the original chip seal specimen.

This concept becomes more complex with the split seal because the residual aggregate from the Ignition Oven test is composed of aggregates from both the bottom (granite 78M) and top (Stalite 5/16″) layers, whereas the weight of the aggregate to be used in the percentage of aggregate loss calculation should be only the weight of the top layer aggregate in order to be consistent with the values from the straight seal. The following method was developed to estimate the weight of the aggregate in the top layer of the split seal. It was found from the straight seal experiments with granite 78M specimens that a strong correlation exists between the total aggregate weight and the weight of aggregate retained on a ¼" sieve. This relationship is depicted in Figure 5-4 and presented as follows based on regression analysis:

$$W_{Total} = 1.2706 \times W_{1/4} + 294.63, \quad (3)$$

where W_{Total} and $W_{1/4}$ are the weights of the total aggregate and the aggregate retained on a 1/4″ sieve, respectively.

Chip seal specimens after testing were burned in the ignition oven to determine the weight of the asphalt and aggregate. To determine the weight of the aggregate from the top layer (i.e., Stalite 5/16") only, the residual aggregate is first sieved through a $\frac{1}{4}$" sieve. Then, the granite 78M aggregate is separated from the residual aggregate retained on the ¼" sieve according to the difference in color between the two aggregates. Once the weight of the granite aggregate retained on the ¼" sieve is determined, this weight is used in Equation (3) to determine the weight of the total granite aggregate. Because the granite 78M aggregate is used in the bottom layer, it is reasonable to assume that no loss of this aggregate occurs on the surface during testing. Finally, the weight of the granite 78M

aggregate, the weight of the residual asphalt, and the weight of the felt disk are subtracted from the weight of the chip seal specimen before testing to determine the weight of the Stalite 5/16" aggregate in the original specimen before testing.

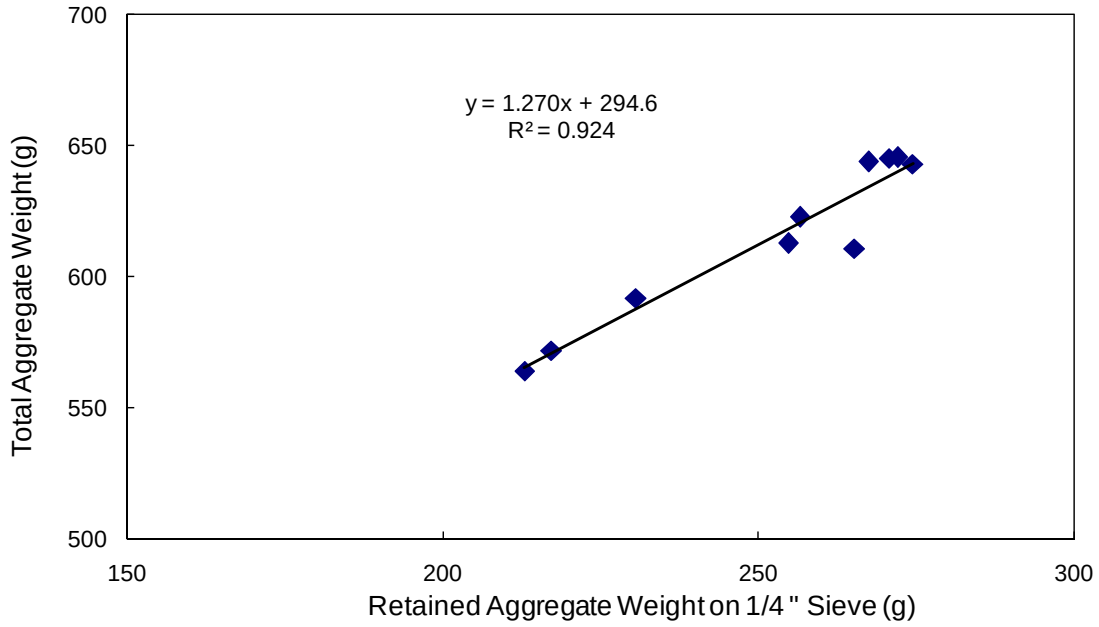

Figure 5-4 Correlation between total aggregate weight and retained aggregate weight on 1/4" sieve for granite 78M aggregate

5.3.2 Vialit Test

The Vialit test measures the adhesion between the binder and aggregate. The adhesion is evaluated as the measurement of aggregate loss due to the shock of impact. The average aggregate loss of the three replicates from the Vialit test was calculated and is plotted in Figure 5-5 against the number of coverages. It must be noted that the aggregate loss determined from the Vialit test using Equation (1) is based on the mixture weight, i.e., the combined weights of the emulsion and aggregate. The use of the mixture weight is necessary because the emulsion weight and the aggregate weight cannot be determined separately. The Ignition Oven test cannot be applied to the Vialit test because the steel

plate cannot be incinerated in the oven. The aggregate loss based on the aggregate weight is estimated from the FOT data, shown in Figure 5-6 and Figure 5-7. The difference in percentage of aggregate loss due to the difference in the mixture weight and aggregate weight is determined from Figure 5-6 and Figure 5-7. This difference is then applied to the aggregate loss based on the mixture weight determined from the Vialit test to estimate the aggregate loss based on the aggregate weight. The results are presented in Figure 5-5.

For both seal types, the aggregate loss decreases as the number of coverages increases. In the case of the straight seal, a large reduction in aggregate loss is evident between one coverage and three coverages, and only a small change in aggregate loss takes place between three coverages and five coverages.

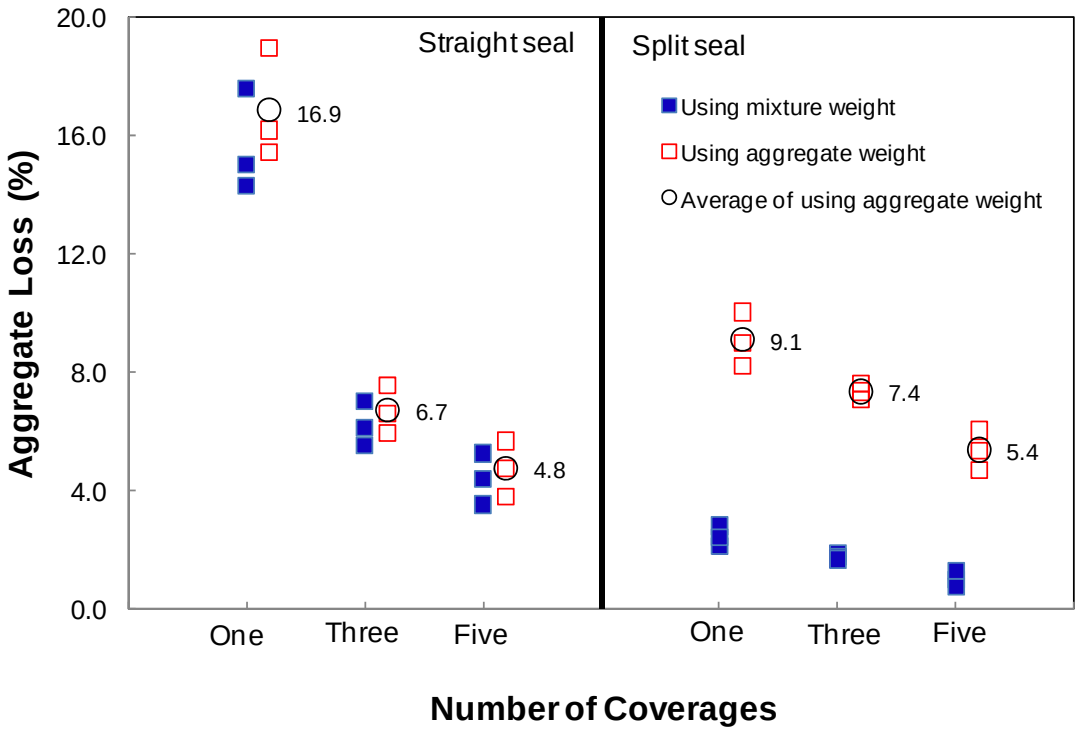

Figure 5-5 Average aggregate loss, determined from Vialit test

This finding indicates that no significant improvement in adhesion between binder and aggregate exists between three coverages and five coverages. Also, it is noted that the

NCDOT specifications specify a 10% aggregate loss as the maximum allowable aggregate loss for chip seals. According to this criterion, both three and five coverages meet the specification. Unlike the straight seal, a large reduction in aggregate loss is not apparent in the trend shown in the split seal data. This difference can be explained by the fact that lost aggregates in the split seal are composed of Stalite 5/16" from the top layer only, whereas in the percentage of aggregate loss calculation in the split seal, the entire weight of both layers is used in the denominator. Based on the results shown in Figure 5-5, three coverages is a proper number of coverages, considering both aggregate loss performance and cost effectiveness.

5.3.3 Flip-Over Test

The FOT measures the amount of excess aggregate on the specimen. The aggregate loss performance is shown in Figure 5-6 and Figure 5-7 as a function of the number of coverages and chip seal types. Both figures have three symbols, a filled symbol, an empty symbol, and a large empty symbol. The large empty symbol indicates the average of the data for each number of coverage. The percentage of aggregate loss, represented by the filled symbol, is determined using the total mixture weight, whereas that represented by the empty symbol is calculated using the weight of the aggregate in the denominator. The percentage of aggregate loss that is calculated using the aggregate weight is slightly higher than the percentage of aggregate loss determined using the mixture weight, because the aggregate weight is smaller than the mixture weight. It is clearly demonstrated in Figure 5-6 that, as the number of coverages increases, the aggregate loss decreases, in this case from 15.0% to 5.3%. The percentage of aggregate loss for three coverages is 10.6%. This percentage is similar to that of the extra aggregate used by the Alaska DOT (Mchattie 2001).

Figure 5-7 shows the aggregate loss performance of the split seal. Two important observations can be made from this figure. First, the values based on the mixture weight are significantly different from those using the aggregate weight. It is noted that the aggregate weight used in calculating the values represented by the empty symbols is the

weight of the aggregate in the top layer only (i.e., Stalite), which is determined using the method presented in Section 5.3.1. Because the denominators represented by the empty symbols (i.e., the aggregate weights) are much smaller than those represented by the filled symbols (i.e., the mixture weights), this trend is obvious. It is interesting that the percentage of aggregate loss for the straight seal is similar to that for the split seal when only the weight of the aggregate in the top layer is used in the percentage of aggregate loss calculation. For example, the percentages of aggregate loss for one coverage and three coverages are about 15% and 10%, respectively, as seen in Figure 5-6 and Figure 5-7. It is not clear why the values for five coverages are quite different.

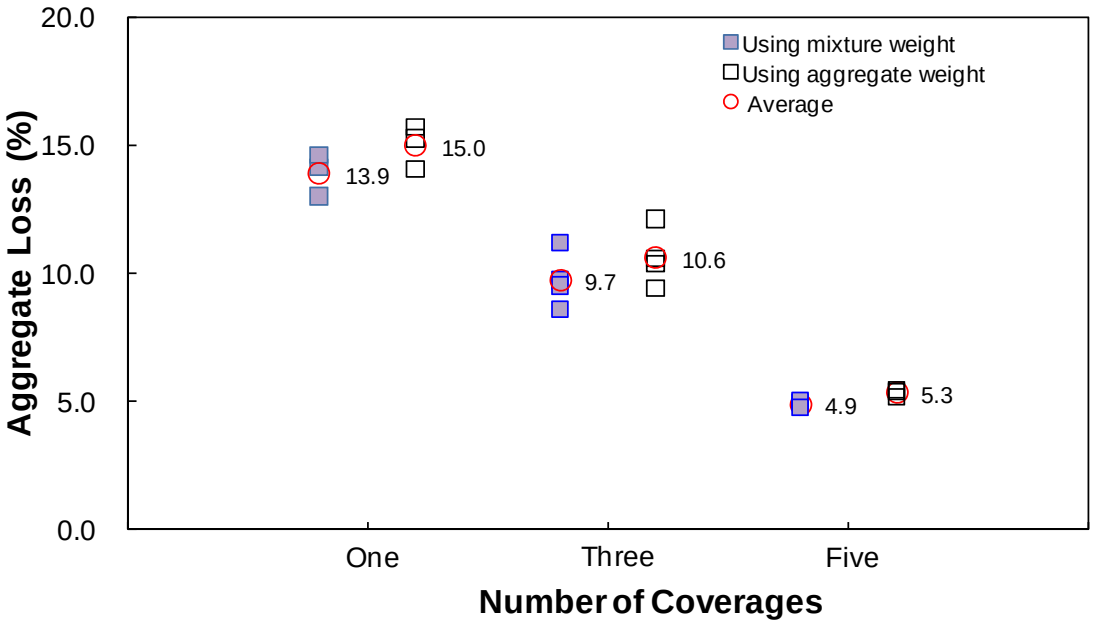

Figure 5-6 FOT results for the straight seal

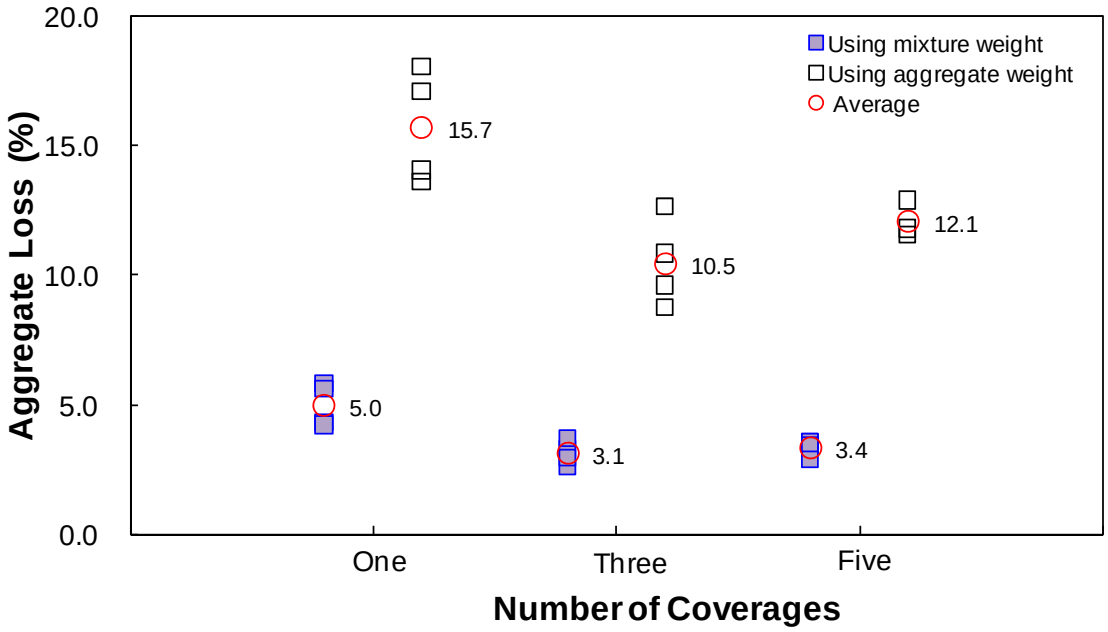

Figure 5-7 FOT results for the split seal

The second observation from Figure 5-7 is that a significant decrease in aggregate loss is evident between one coverage and three coverages, but no significant improvement in aggregate loss performance occurs between three and five coverages. Considering this trend and the economic factors involved in rolling, three coverages seems to be the optimal number of coverages for the split seal. It is noted that about a 10% aggregate loss found in both straight and split is the maximum allowable aggregate loss specified in the Alaska chip seal guide (Mchattie 2001).

5.3.4 Embedment Depth of the Chip Seal

The embedment depth of the straight seal is measured from the FOT and MMLS3 test specimens using the modified sand circle method. The results are shown in Figure 5-8 as a function of the number of coverages. These specimens were compacted in the field using a combination roller. In Figure 5-8, only one FOT sample is available for each number of coverages; therefore, one data point shown in Figure 5-8 is an average of the three replicate measurements for each sample. Figure 5-8 shows a significant increase in

embedment depth between one coverage and three coverages. However, only a slight change in embedment depth is evident between three and five coverages. Figure 5-8 also shows the embedment depth of a straight seal after 2 hr. 10 min. of MMLS3 trafficking. The same trend seen in Figure 5-8 for the FOT results is also evident in the MMLS3 results.

Contrary to our expectation, the embedment depth of MMLS3 specimen is slightly less than that of FOT specimen in Figure 5-8. This unexpected trend results from the MMLS3 test set-up. In the MMLS3 test set-up, the samples of MMLS3 were mounted on the steel plate. The steel plate prevents the penetration of the aggregate particles into the existing surface and therefore the increase of the embedment depth. In typical field conditions, traffic loading causes the aggregate exposure depth to decrease and therefore the aggregate embedment depth to decrease.

As Hudson et al. (1986) found, the surface texture depth changes significantly up to three roller passes. Considering the trends seen in Figure 5-8, three coverages seems to be the optimal number of coverages for the straight seal.

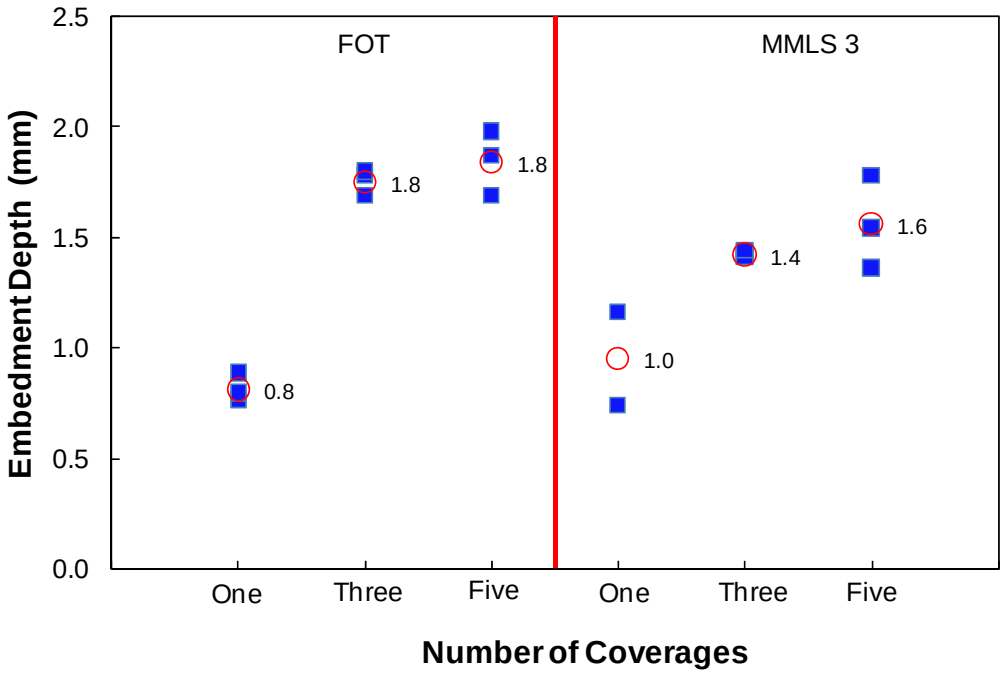

Figure 5-8 Embedment depth of FOT and MMLS3 samples as a function of the number of coverages

5.3.5 MMLS3 Test

To determine the aggregate loss due to MMLS3 loading, the aggregate loss is measured at two separate times: 1) after one wandering cycle of MMLS3 loading to simulate an initial traffic loading in the field, and 2) after a two-hour traffic period to evaluate the aggregate retention performance under traffic. Figure 5-9 and Figure 5-10 show the percentage of aggregate loss during the 2 hr. 10 min. (12,940 wheel passes) duration of the aggregate retention test on straight and split seals, respectively. Figure 5-10 shows the aggregate loss performance of the split seal. The same observation as made in Figure 5-7 is made here. The values of aggregate loss are significantly different as a function of the weights used in the calculations. It is noted that the aggregate weight used in calculating the values represented by the empty symbols is the weight of the aggregate in the top layer only (i.e., Stalite 5/16"), which is determined using the method

presented in Section 5.3.1. Because the denominators represented by the empty symbols (i.e., the aggregate weights) are much smaller than those represented by the filled symbols (i.e., the mixture weights), this trend is obvious. Contrary to the FOT results (seen in Figure 5-7), the significant decrease in aggregate loss is not apparent as a function of the number of coverages. A slight improvement in aggregate loss performance occurs between one and three coverages. For example, the percentages of aggregate loss for one coverage and three coverages are about 14.3% and 13.7%, respectively, as seen in Figure 5-10. It is not clear why the values for the different coverages are slightly different.

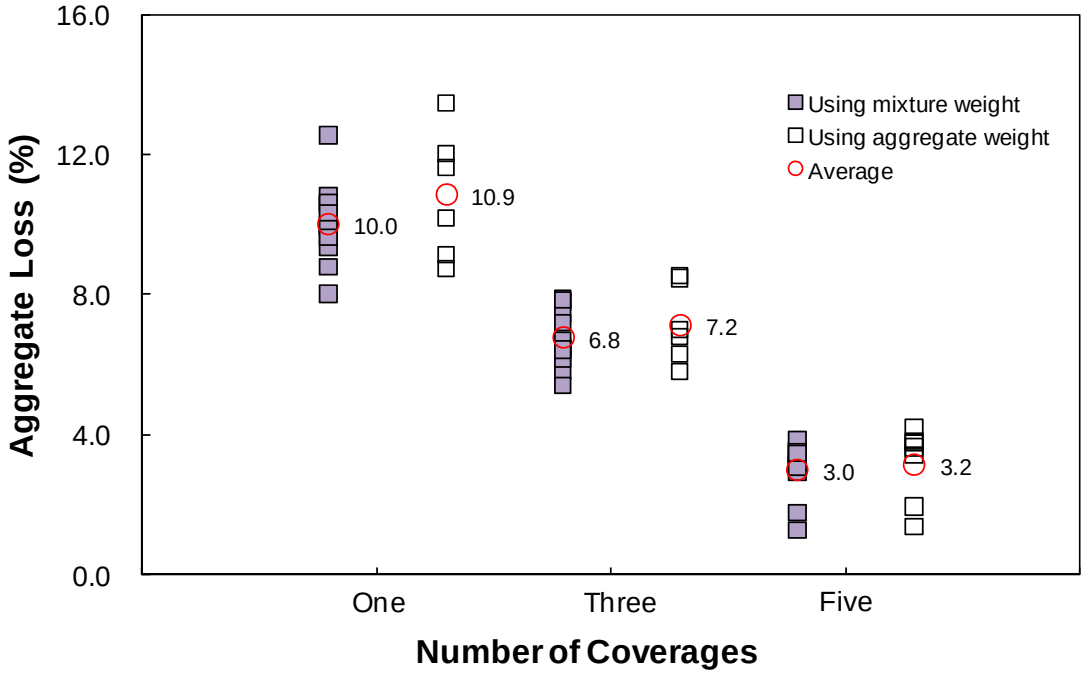

Figure 5-9 Aggregate loss of the straight seal measured from the MMLS3 test after 12,940 wheel passes

5.3.6 Comprehensive Analysis

The objective of Phase II is to determine an optimal number of coverages. A total of six test programs were completed to evaluate the performance of two seal types (straight seal and split seal) under three different numbers of coverages (1, 3, and 5).

Table 5-2 summarizes the percentage of average aggregate loss from three aggregate retention tests and the aggregate embedment depth using MMLS3 and FOT samples. The decrease of aggregate loss against the number of coverages was clearly shown in Table 5-2. Also, the change of aggregate embedment depth as function of the number of coverages indicates that the optimal number of coverage is the three coverages in the straight seal.

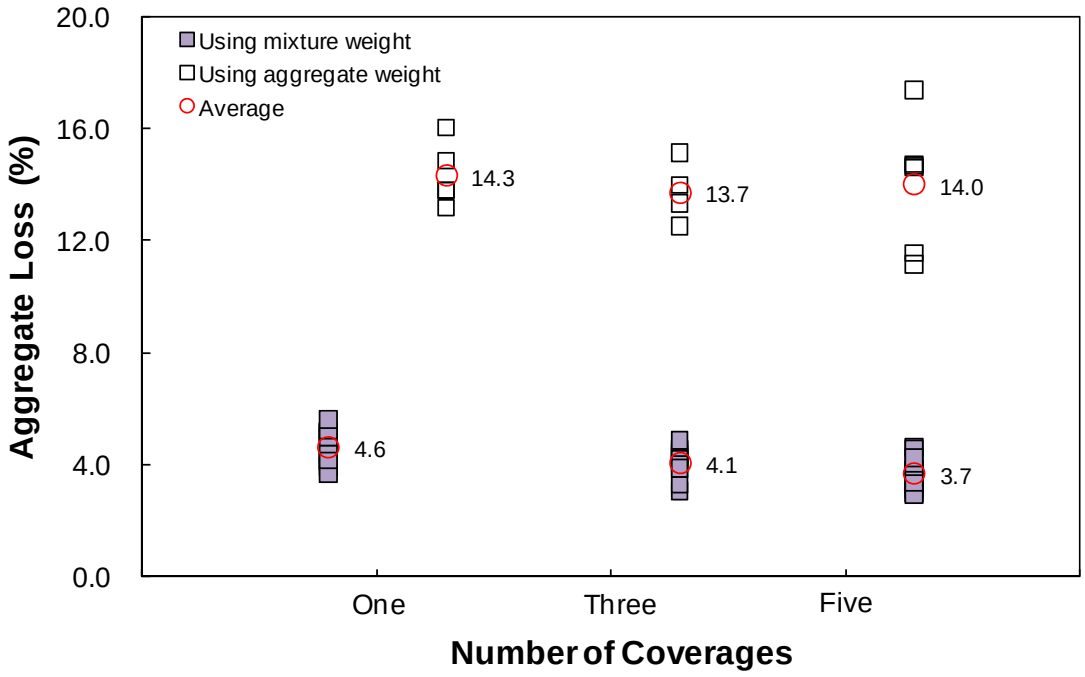

Figure 5-10 Aggregate loss of the split seal measured from the MMLS3 test after 12,940 wheel passes

Statistical analysis was conducted to determine if the differences found in the means are statistically significantly. ANOVA was used to test for differences among the

three groups (1, 3, and 5 coverages). The results of these ANOVA tests are shown in Table 5-3. The differences among the three groups are significant because the p-values are greater than the alpha level of 0.05, with the exception of the MMLS3 result of the split seal. The MMLS3 test of the split seal indicates no significant differences among the three different coverages. It should be noted that the aggregate in a multiple seal layer will become rearranged and compacted under traffic in order to reach a theoretical optimal packing arrangement (Ball et al. 2005). The MMLS3 results of the split seals explain that the top layer of the aggregate (Stalite 5/16") starts to reorient and embed into the underlying layer of aggregate (granite 78M). Due to the compaction mechanism of the split seal under MMLS3 loading, the MMLS3 does not create a difference in the percentage of the aggregate loss. Considering these results and the economic factors involved in rolling, three coverages seems to be the optimal number of coverages for the split seal.

Table 5-2 Summary of Average Percentage of Aggregate Loss and Embedment Depth

Test Method	Chip Seal Type	Number of Coverages		
		One	Three	Five
Vialit	Straight	16.9	6.7	4.8
	Split	9.1	7.4	5.4
FOT	Straight	16.0	10.6	6.3
	Split	15.7	10.5	12.1
MMLS 3	Straight	10.9	7.2	3.2
	Split	14.3	13.7	14.0
Embedment depth	Straight (FOT)	0.81	1.76	1.84
	Straight (MMLS3)	0.95	1.42	1.56

Table 5-3 Summary of Statistical Analysis Results

Test Method	Chip seal types	F-Test	P-value	Conclusion
Vialit	Straight	23.10	0.0015	Reject H_0
	Split	4.74	0.0583	Reject H_0
FOT	Straight	3.49	0.0813	Reject H_0
	Split	144.55	<0.0001	Reject H_0
MMLS3	Straight	7.79	0.0043	Reject H_0
	Split	0.15	0.8664	**Accept H_0**

6. COVERAGE DISTRIBUTION OF MULTILAYERS

6.1 Experimental Program

This study is designed to observe the effects of different coverage distributions per each layer of multilayers. The current practice in North Carolina for general coverage distribution is a single coverage on each layer of multilayers, such as split seal and triple seals. However, the New Zealand Chip Seal Rolling Study recommends three coverages on the top layer of a chip seal without any rolling on the sublayers. In order to evaluate the effects of the different number of coverages for each layer, four cases shown in Figure 6-1 are evaluated in this study.

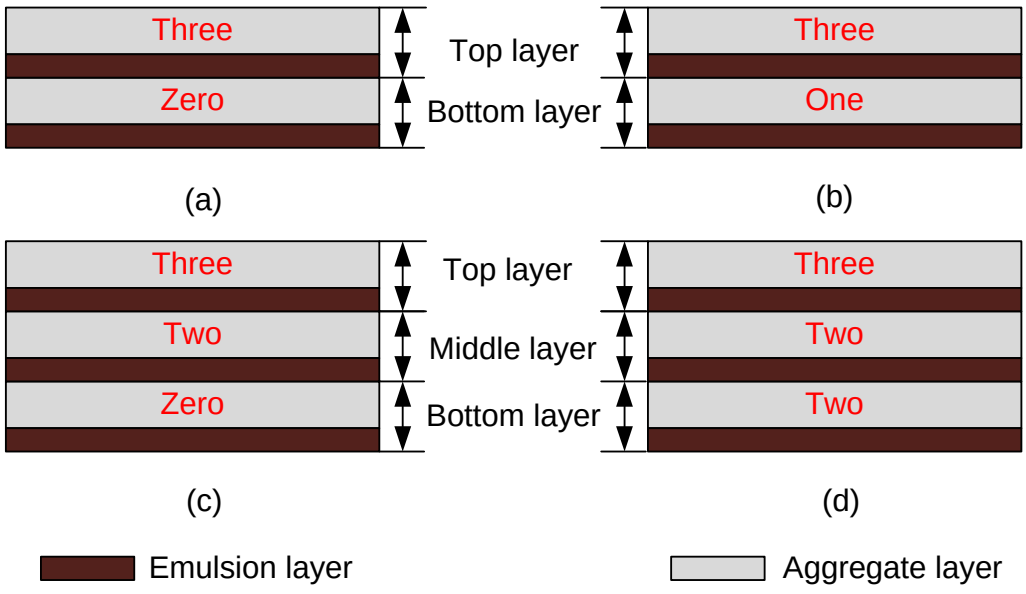

Figure 6-1 Schematic diagram of the coverage distribution per layer

Figure 6-1 shows the coverage distribution of both the split seal and the triple seal. Figure 6-1 (a) is the New Zealand practice; Figure 6-1 (b) is the current North Carolina practice. Figure 6-1 (c) and Figure 6-1 (d) show the coverage distributions of the triple seal. Figure 6-1 (c) and Figure 6-1(d) also show the differences in coverage applied at the bottom layer in the case of the triple seal. Figure 6-1 (c) shows no coverage at the bottom layer; Figure 6-1 (d) shows two coverages at the bottom layer. For the other layers, that is, the middle and the top layers, two coverages and three coverages are applied, respectively. It is expected that these four cases will create different skeletons of the aggregate and also show different aggregate retention performances.

6.2 Split Seal Study

6.2.1 Split Seal Construction

For the split seal construction, granite 78M and Stalite 5/16" aggregates are used for the bottom and top layers, respectively. The aggregate application rates for the split seal are 17 and 9 lb/yd^2 for the bottom (granite 78M) and top (Stalite 5/16") layers, respectively. The same emulsion application rate of 0.25 gal/yd^2 is used for both layers in the split seal. The test sections were constructed on the same road, New Sandy Hill Church Road (SR 1131) near Bailey in Wilson County, NC on June 12th, 2007. Two aggregate spreaders were used for each aggregate type for the split seal. One aggregate spreader provided the spreading aggregate for the bottom layer of the split seal (granite 78M); another aggregate spreader provided the spreading aggregate for the top layer of the split seal (Stalite 5/16"). A single emulsion sprayer was used to spray the emulsion on each layer of the split seal. Two combination rollers rolled the aggregate in a parallel pattern to cover the entire lane at the same time.

6.2.2 Sample Weight Variations

Specimens fabricated during field construction are to be evaluated for their rolling protocol. Thus, it is important to reduce the variation in sample weights among the different sections because the variation in the sample weights affects the measurement of aggregate loss performance. Therefore, statistical analysis of the distribution of the sample weights is necessary prior to the measurement of aggregate loss performance. The t-test, which is a statistical test, is used to investigate whether there are differences in the means of the two sections in terms of weight. T-tests with significance levels of 0.05 were performed to investigate whether there were differences in the means of the weights between zero and one coverage for coverage distributions at the bottom layer of the split seal. The distribution of both the entire mixture and the Stalite 5/16" was examined and plotted, as shown in Figure 6-2.

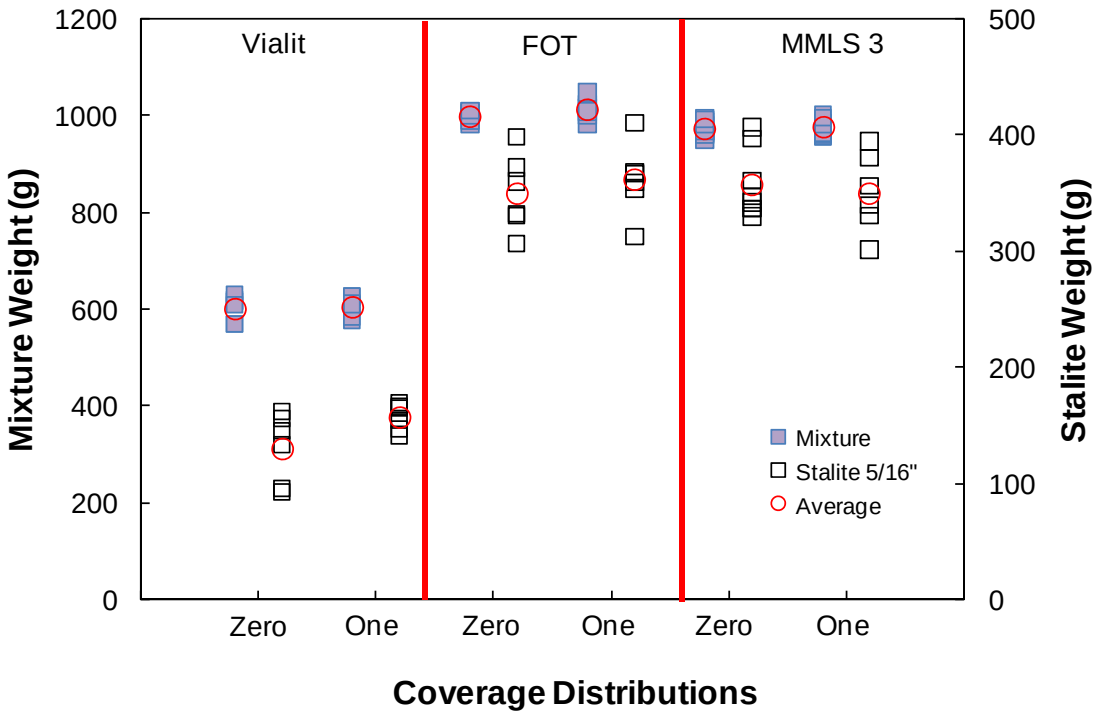

Figure 6-2 Distribution of sample weights

The test results of the statistical analysis of both the entire mixture and the Stalite 5/16" are summarized, respectively, in Table 6-1. The weight of the Stalite 5/16" taken from the split seal samples was calculated by the Ignition Oven method, as explained in the previous section. The Ignition Oven method was used to calculate the Stalite 5/16" aggregate weight that is subtracted from the total aggregate weight, that is, the weight of both the granite 78M and Stalite 5/16" aggregate. As described in Table 6-1, the Stalite 5/16" weight failed to reject the null hypothesis because its p-value is greater than 0.05.

Table 6-1 Results of t-tests for Sample Weights

Test Method	Types	Coverage	Mean	Variance	Std. Dev.	t-Test	p-Value	Conclusion
Vialit	Mixture	Zero	601.6	686.6	26.2	-1.80	0.10	Accept H_0
		One	604.8	397.1	19.9			
	Stalite	Zero	130.4	884.9	29.7	-0.25	0.80	Accept H_0
		One	157.0	127.5	11.3			
FOT	Mixture	Zero	998.8	138.0	11.7	-0.65	0.53	Accept H_0
		One	1012.6	470.7	21.7			
	Stalite	Zero	349.7	1092.1	33.0	-1.32	0.22	Accept H_0
		One	361.5	996.7	31.6			
MMLS3	Mixture	Zero	973.0	236.1	15.4	0.40	0.70	Accept H_0
		One	975.4	293.5	17.1			
	Stalite	Zero	356.7	849.3	29.1	-0.32	0.75	Accept H_0
		One	350.1	1164.9	34.1			

6.2.3 Test Results

6.2.3.1 Ignition oven test for determination of aggregate weight

The total weight of the cured split seal sample fabricated in the field is composed of three separate weights, i.e., the weight of the felt disk, the weight of the residual asphalt, and the weight of the aggregate. Because the weight of the felt disk is measured prior to chip seal sample fabrication, the aggregate weight before testing can be

determined, if the asphalt weight is known. The asphalt weight is determined using the Ignition Oven test by subtracting the weight of the residual aggregate after the Ignition Oven test and the weight of the felt disk from the weight of the tested specimen before the Ignition Oven test. Thus, the weight of the aggregate in the original, untested chip seal specimen can be determined once the weight of the asphalt and the weight of the felt disk are subtracted from the weight of the original chip seal specimen.

This concept becomes more complex with the split seal because the residual aggregate from the Ignition Oven test is composed of aggregates from both the bottom (granite 78M) and top (Stalite 5/16″) layers, whereas the weight of the aggregate to be used in the percentage aggregate loss calculation should be only the weight of the top layer aggregate in order to be consistent with the values from the straight seal. The following method was developed to estimate the weight of the aggregate in the top layer of the split seal. It was found from the straight seal experiments with granite 78M specimens that a strong correlation exists between the total aggregate weight and the weight of aggregate retained on a ¼" sieve. This relationship is depicted in Figure 6-3 and presented as follows based on regression analysis:

$$W_{Total}=1.336 \times W_{1/4}+219.1 \qquad (4)$$

where W_{Total} and $W_{1/4}$ are the weights of the total aggregate and the aggregate retained on a 1/4″ sieve, respectively. Chip seal specimens after testing were burnt in the ignition oven to determine the weight of the asphalt and aggregate. To determine the weight of the aggregate from the top layer (i.e., Stalite 5/16") only, the residual aggregate is first sieved through a ¼" sieve. Then, the granite 78M aggregate is separated from the residual aggregate retained on the ¼" sieve according to color difference. Once the weight of the granite aggregate retained on the ¼" sieve is determined, this weight is used in Equation (4) to determine the weight of the total granite aggregate.

Because the granite 78M aggregate is used in the bottom layer, it is reasonable to assume that no loss of this aggregate occurs during testing on the surface. Finally, the weight of the granite 78M aggregate, the weight of the residual asphalt, and the weight of

the felt disk are subtracted from the weight of the chip seal specimen before testing to determine the weight of the Stalite 5/16" in the original specimen before testing.

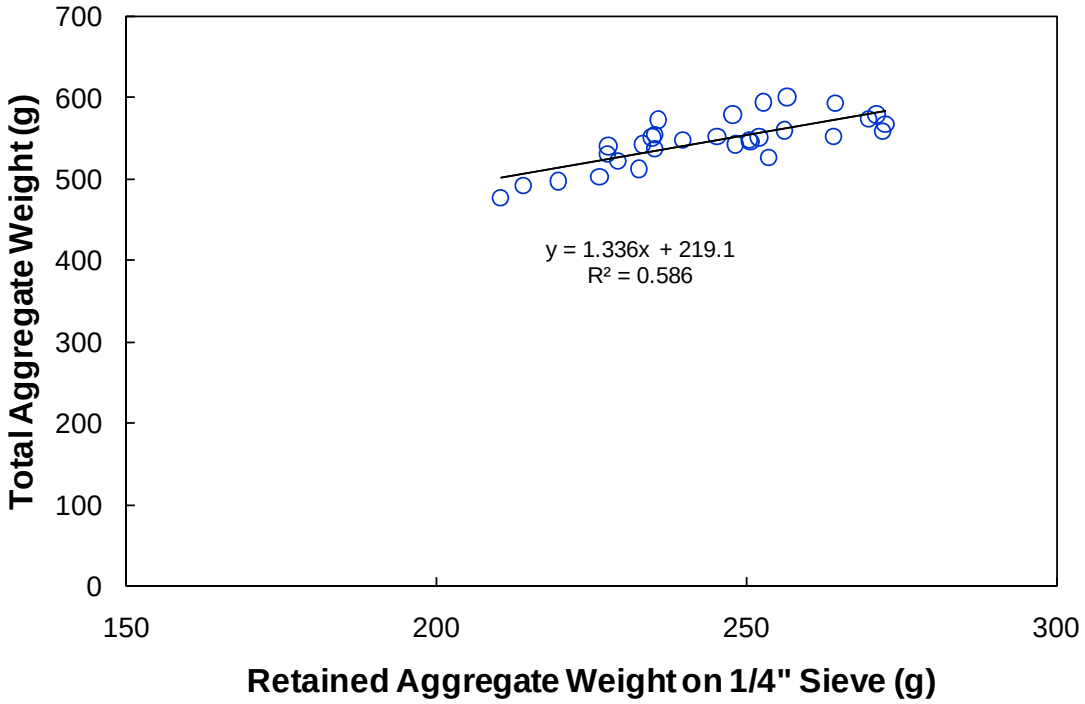

Figure 6-3 Correlation between total aggregate weight and retained aggregate weight on 1/4" sieve for granite 78M aggregate

6.2.3.2 Flip-over test

The flip-over test (FOT) is employed to investigate the effects of different coverage distributions between the bottom and the top layers by measuring the amount of excess aggregate on the split seal specimen. Based on a slightly different aggregate weight per sample, as shown in Figure 6-2, the aggregate loss performance of the split seal is shown in Figure 6-4 as a function of coverage distribution at the bottom layer. Figure 6-4 has three symbols to indicate the calculated aggregate loss using different weights in the denominator. As explained in Chapter 4, the percentage of aggregate loss, which is determined using the mixture weight, is significantly different from that based on the

value of the aggregate loss that is determined using the aggregate weight, as plotted in Figure 6-4.

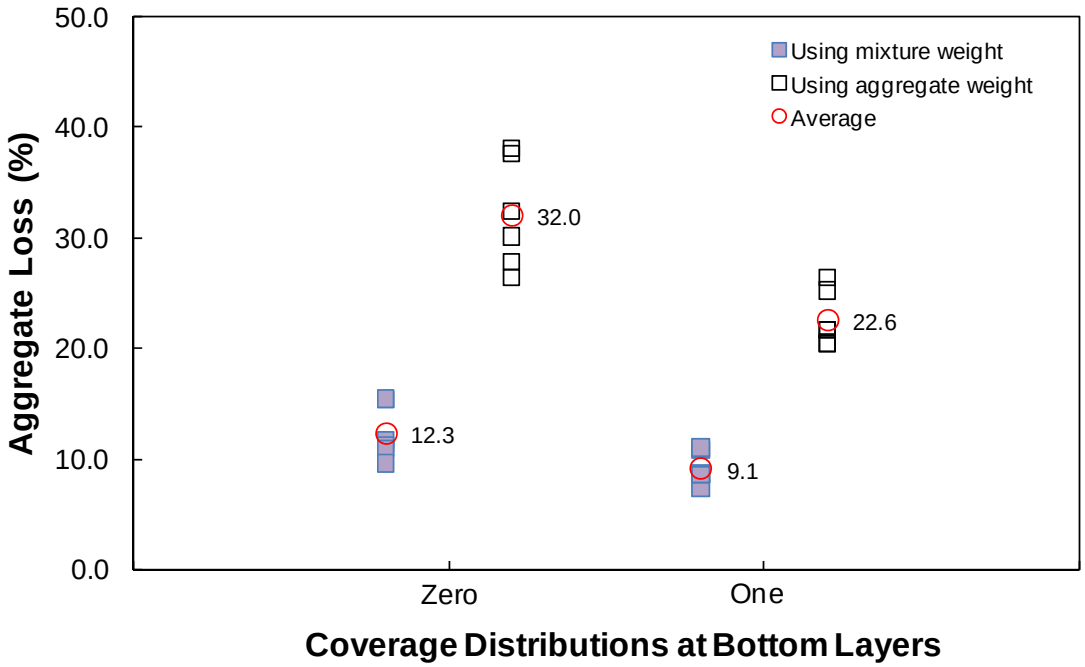

Figure 6-4 Aggregate loss of a split seal from FOT samples

It is noted that the aggregate weight used in calculating the values for the empty symbols is the weight of the aggregate top layer only (Stalite 5/16"). There is an approximately 20% and 13% difference between the filled and empty symbols, respectively. Because the denominators represented in the empty symbols are much smaller than those in the filled symbols (i.e., using the mixture weight), the difference between two values is obvious.

It is clearly demonstrated in Figure 6-4 that, with one coverage at the bottom layer, the aggregate loss decreases, in this case from 32.0% to 22.6%. That is, a significant decrease in aggregate loss is evident between zero coverage and one coverage at the bottom layer. The values shown in Figure 6-4 are too much higher than the expected

because the AAR (aggregate application rate) used by the aggregate spreader is higher than the optimum AAR. Higher AAR causes the higher aggregate loss performance.

6.2.3.3 Vialit test

Of the split seal samples, the Vialit test sample that has the smallest variation of total aggregate weights, i.e., both granite 78M and Stalite 5/16" weights, is shown in Figure 6-3. This figure shows a trend similar to the FOT sample weight distributions. The purpose of the Vialit test is to measure the adhesion between the emulsion and the aggregate in the chip seal structure. The adhesion is estimated as the measurement of aggregate weight loss due to the shock impact. The percentage of aggregate loss performance of the six replicates from the Vialit test is plotted in Figure 6-5 against the rolling operation at the bottom layer of the split seal.

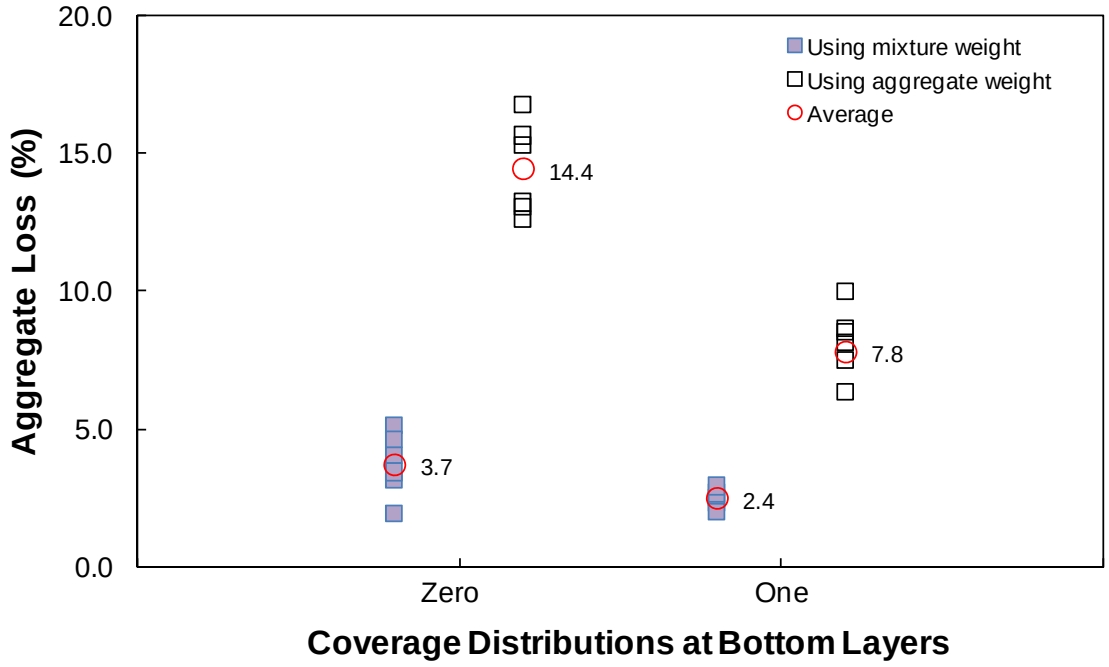

Figure 6-5 Aggregate loss of the split seal from Vialit test samples

The percentage of aggregate loss, represented by three symbols in Figure 6-5, is calculated using both the mixture and the Stalite 5/16" aggregate weights, as shown in Equation (1) and Equation (2), respectively.

The significant difference of the aggregate loss performance versus the coverage distribution at the bottom layer of the split seal can be observed in Figure 6-5. The average aggregate loss using one coverage at the bottom layer of the split seal decreased twice as much as that with zero coverage, in this case from 14.4% to 7.8%. That is, the percentage of aggregate loss determined with zero coverage at the bottom layer of the split seal is 14.4%.

However, the one coverage at the bottom layer displayed a 7.8% aggregate loss performance. The bottom layer's percentage with one coverage is less than a 10% aggregate loss, which is the maximum allowable aggregate loss specified by the NCDOT's specification (North Carolina 2000).

6.2.3.4 MMLS3 test

Table 6-1 describes the variation of the split seal sample weights according to the different rolling operations at the bottom layer. No significant difference is evident in the range of the split seal sample weights between zero and one coverage at the bottom layer. Figure 6-6 shows the percentage of aggregate loss during the 2 hr. 10 min. (12,940 wheel passes) aggregate retention test on the split seal. The percentage of aggregate loss was calculated the same as in the previous tests (i.e., FOT and Vialit). A trend similar to that found from the other aggregate retention tests (Figure 6-4 and Figure 6-5) is observed in Figure 6-6. The average aggregate loss using aggregate weights, symbolized by the empty symbols in Figure 6-6, is clearly different from 27.1% for zero coverage to 19.7% for one coverage. An even more significant difference is observed by using aggregate weight to measure aggregate loss performance, as was done in both the Vialit test and the FOT. With the application of the rolling operation at the bottom layer of the split seal, the percentage of aggregate loss definitely decreases. As explained in the previous FOT section, the high AAR of the Stalite 5/16"of the split seal produced the unusually higher

percent of aggregate loss.

6.2.3.5 Comprehensive analysis of split seal study

The t-test was conducted to assess whether there is a statistical difference of the aggregate loss performance in the means of two sections between the different coverage distributions at the bottom layer of the split seal. To test the significance using the t-test, the alpha value used in this study is generally 0.05. One coverage at the bottom layer shows the besr aggregate retention performance from the three aggregate retention tests. It is clear that, in the case of the split seal, the bottom layer requires the rolling operation to improve the aggregate retention performance.

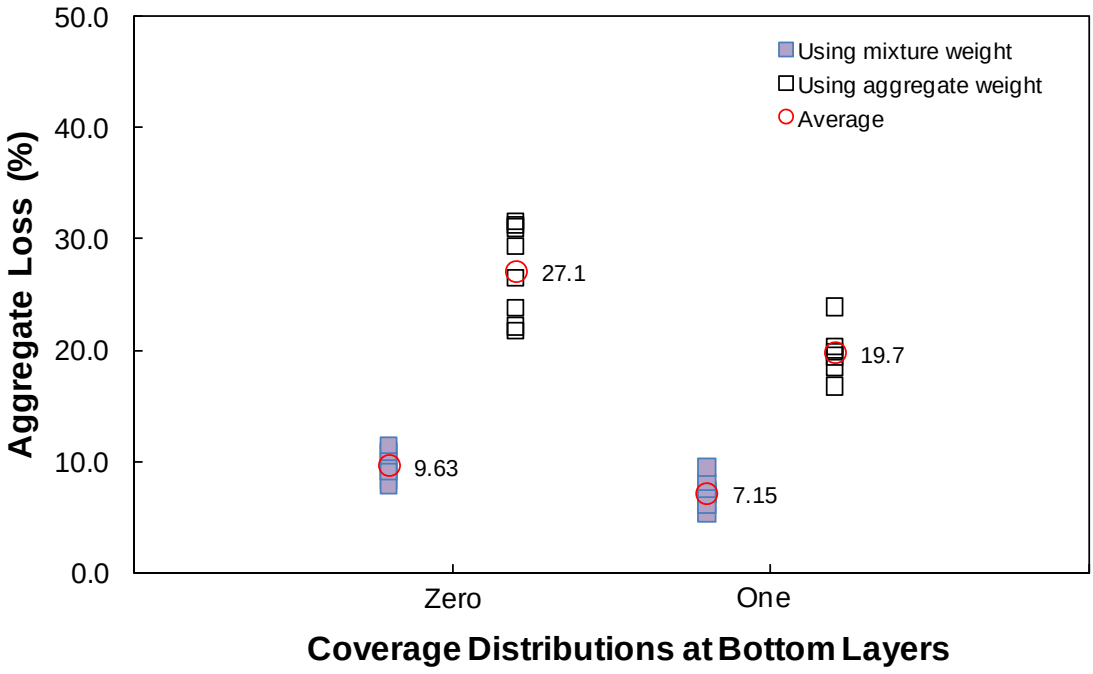

Figure 6-6 Aggregate loss of a split seal from MMLS3 test samples

Table 6-2 summarizes the results of the t-tests for different coverage distributions at the bottom layer. The p-value from the t-test, as shown in Table 6-2, is lower than the alpha value, 0.05. These values indicate that the percentage of aggregate loss performance

between the two sections show significant differences between zero and one coverage at the bottom layer of the split seal. One coverage at the bottom layer shows the best aggregate retention among the three aggregate retention tests. It is clear that, in the case of the split seal, one coverage at the bottom layer of the split seal improves the aggregate retention performance.

Table 6-2 Results of the t-test for the Coverage Distribution of the Split Seal

Statistic	Vialit		FOT		MMLS 3	
	Mixture	Aggregate	Mixture	Aggregate	Mixture	Aggregate
Sample mean	1.06	6.24	3.14	9.42	2.47	7.38
Standard error	0.44	2.05	1.37	3.56	0.82	2.75
t-test	2.40	3.04	2.29	2.64	3.02	2.69
p-value	0.04	0.01	0.05	0.002	0.001	0.02
Conclusion	Reject H_0	Reject H_0	Reject H_0	Reject H_0	Reject H_0	Reject H_0

6.3 Triple Seal Study

6.3.1 Triple Seal Construction

In order to evaluate the effect of the coverage distribution of the triple seal, triple seal test sections were constructed on SR 1725 in Wayne County, NC on August 2nd 2007. For the triple seal construction, granite 78M, granite 78M and Stalite 5/16" aggregates were used for the bottom, middle, and the top layers, respectively. The aggregate application rates for the triple seal are 16 lb/yd^2, 12 lb/yd^2 and 9 lb/yd^2 for the bottom (granite 78M), the middle (granite 78M) and the top (Stalite 5/16") layers, respectively. The emulsion (CRS-2) application rates are 0.30 gal/yd^2, 0.25 gal/yd^2, and 0.20 gal/yd^2 from the bottom layer to the top layer of the triple seal, respectively. A pneumatic tire roller was used to roll the aggregate.

6.3.2 Sample Weight Variations

A t-test was conducted to test various statistical hypotheses regarding the mean of the distributions from two sets of samples. Two-tailed t-tests with significance levels of 0.05 were performed to evaluate whether there are differences in variances of mean weights between zero and two coverages in the coverage distributions at the bottom of the triple seals. Table 6-3 summarizes the statistical results for the different coverage distributions of the triple seals. As seen in Table 6-3, no significant differences in the means are evident between zero and two coverage distributions of the bottom layer of the triple seal, as the p-values are greater than 0.05, except in the FOT sample groups. In the case of the FOT sample groups, the Stalite 5/16" shows a difference in weights. Figure 6-7 plots the distribution of the triple seal sample weights for this study and shows a narrow sample-to-sample variable. The Stalite 5/16" aggregate of the top layer, obtained from the Vialit test, and the FOT samples were manually torn off and weighed.

Table 6-3 Results of t-tests for Sample Weights

Test Method	Types	Coverage	Mean	Variance	Std. Dev.	t-Test	p-Value	Conclusion
Vialit	Mixture	Zero	682.8	833.6	28.9	-0.09	0.93	Accept H_0
		Two	684.1	418.4	20.5			
	Stalite	Zero	135.0	33.5	5.8	0.66	0.53	Accept H_0
		Two	132.9	29.2	5.4			
FOT	Mixture	Zero	1192.1	926.7	30.4	-1.49	0.17	Accept H_0
		Two	1232.1	2886.2	53.7			
	Stalite	Zero	226.8	16.7	4.1	-2.33	0.04	Reject H_0
		Two	243.3	149.8	12.2			
MMLS 3	Mixture	Zero	1185.6	2590.0	50.9	-0.13	0.90	Accept H_0
		Two	1188.2	941.5	30.7			
	Stalite	Zero	230.4	99.7	10.0	-0.13	0.90	Accept H_0
		Two	230.9	36.2	6.0			

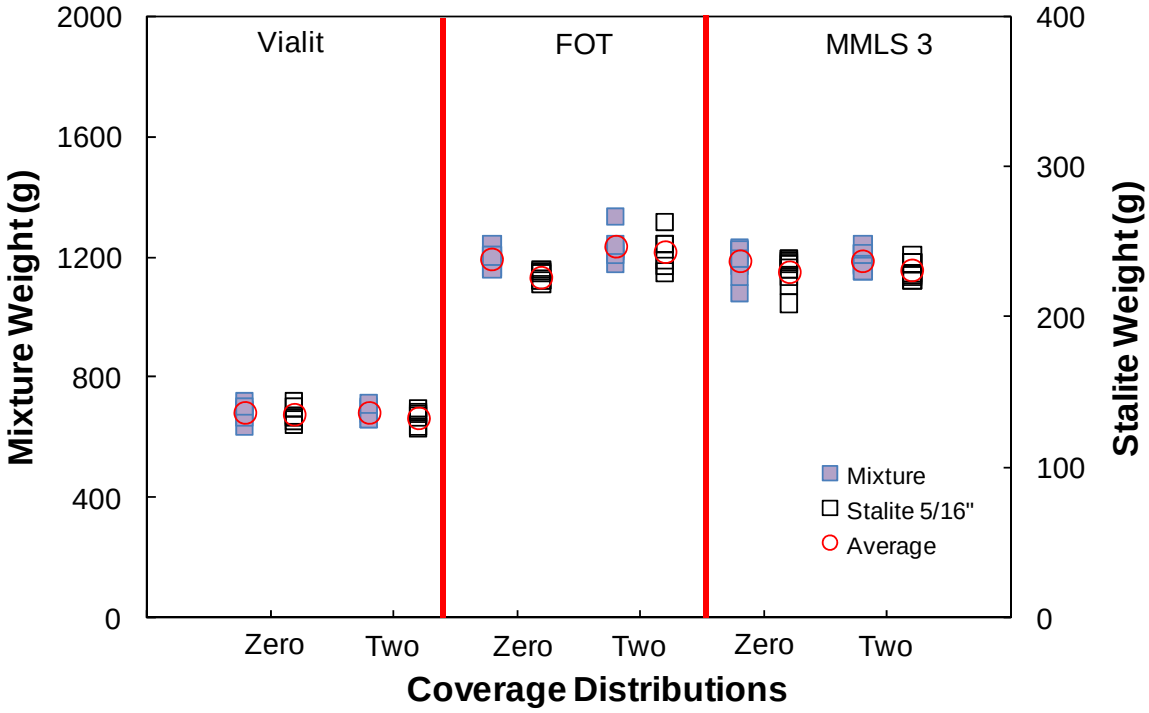

Figure 6-7 Distribution of the triple seal sample weights

However, it is difficult to tear off Stalite 5/16"aggregate from the MMLS3 after traffic loading because some aggregate in the top layer is embedded into the previous layer. Thus, Equation (5) was used to calculate the mixture weight without Stalite 5/16". The Stalite 5/16" weight was calculated by subtracting the mixture weight without Stalite 5/16" from the original mixture weight. Therefore, the Stalite 5/16" weight was plotted, as shown in Figure 6-7.

6.3.3 Test Results

6.3.3.1 Vialit test

As explained and found in the previous case of the split seal, the values of the percentage of aggregate loss based on the mixture weight are significantly different from those based on the aggregate weight. The triple seals have a heavier mixture weight of samples than the split seals because the triple seals are composed of two layers of the

granite 78M and one layer of Stalite 5/16", as shown in Table 6-3. The heavier mixture weight creates a large denominator in the percentage of aggregate loss calculation. Therefore, the Stalite layer was manually torn off the from the triple seal specimen to calculate the percentage of aggregate loss using aggregate weight. Figure 6-8 shows the percentage of aggregate loss performance from the Vialit test using three symbols: a filled symbol, an empty symbol and a large empty circle symbol.

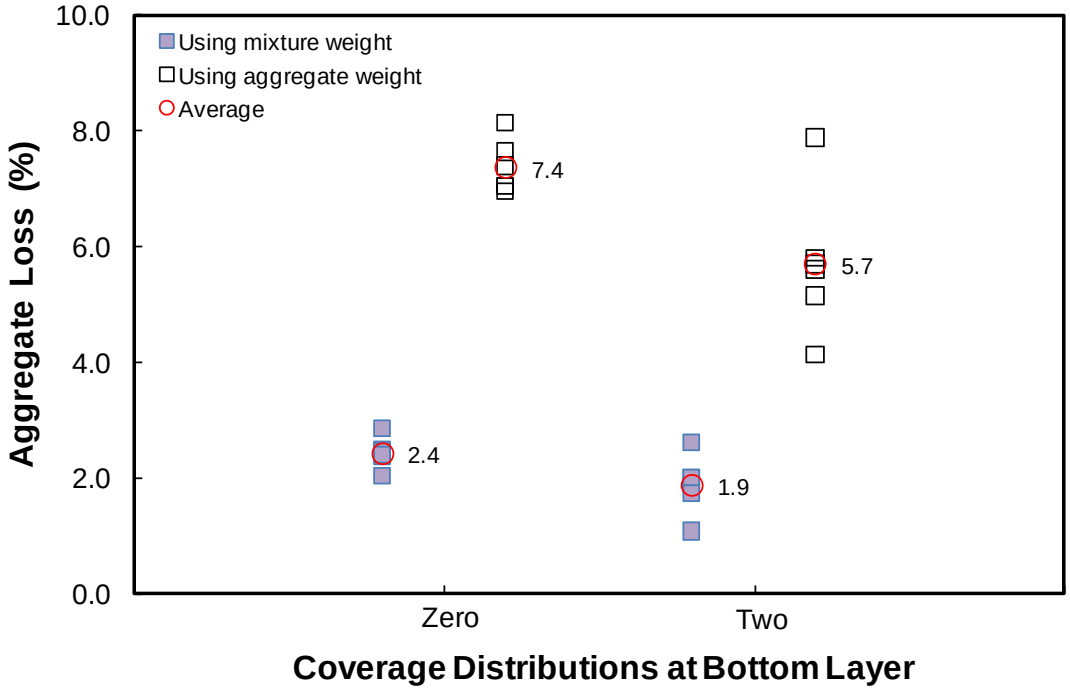

Figure 6-8 Aggregate loss performance from the Vialit test

The large empty circle symbol indicates the averages of the data for each section. The percentage of aggregate loss represented by the filled symbols is determined using the total mixture weight, whereas that represented by the empty symbols is calculated using the weight of the aggregate in the denominator. The percentage of aggregate loss that is calculated using the aggregate weight is higher than the percentage of aggregate loss determined using the mixture weight, because the aggregate weight is smaller than the mixture weight. As demonstrated in Figure 6-8, the aggregate loss performance is slightly

changed due to the rolling operation at the bottom layer of the triple seal. When rolling the aggregate on the bottom layer of the triple seal, the aggregate loss decreases from 7.4 % to 5.7 %.

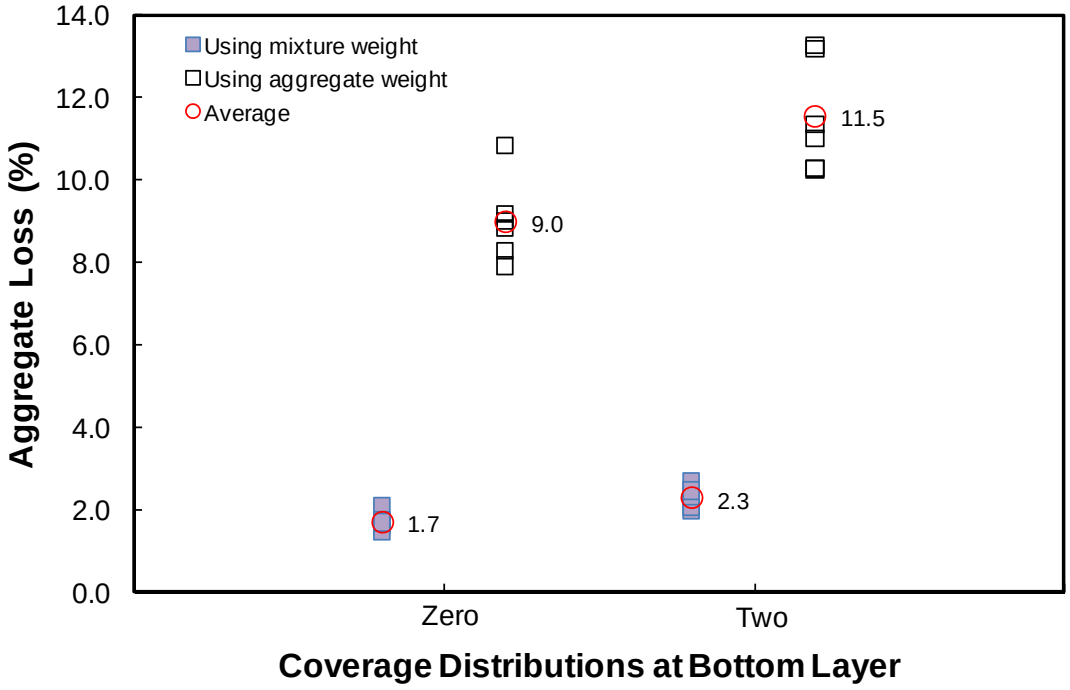

Figure 6-9 Aggregate loss from the FOT

6.3.3.2 Flip-over test

In order to investigate the effects of different coverages at the bottom layer of the triple seal, the FOT was used to determine the amount of excess aggregate on the triple seal versus the coverage distribution of the triple seal. The weight of the aggregate in the top layer only (i.e., Stalite 5/16") was determined using the method presented in the previous section. Figure 6-9 shows the aggregate loss performance obtained from the FOT using the same three symbols as used in Figure 6-8. The empty symbols (i.e., the aggregate weights) in Figure 6-9 show a significant difference between the two different coverage distributions.

The average percentage of aggregate loss with two coverages at the bottom layer of the triple seal is slightly higher than that of the aggregate loss with no coverage at the bottom layer of the triple seal. The percentage of aggregate loss with two coverages at the bottom layer is 11.5%. This percentage is slightly higher than that of the extra aggregate used by the Alaska DOT (Mchattie 2001).

6.3.3.3 Determination of Stalite 5/16" weight

The triple seal for this study is composed of two layers of granite 78M and one layer of Stalite 5/16". In order to measure the Stalite 5/16" weight of the triple seal, the following method was developed to estimate the weight of the aggregate in the top layer of the triple seal, because it is difficult to manually tear off Stalite 5/16" from the triple seal samples after trafficked loading. It was found from FOT experiments with the triple seal that a strong correlation exists between the total mixture weight and the mixture weight without the top layer of aggregate. This relationship is depicted in Figure 6-10 and presented as follows based on regression analysis:

$$W_B = 0.804 \times W_T + 1.960 \quad (5)$$

where

W_B = the mixture weight of the triple seal without Stalite 5/16" and

W_T = the total mixture weight of the triple seal.

Once the total mixture weight is determined, this weight is used in Equation (5) to determine the mixture weight without Stalite 5/16". Because the granite 78M is used in both the bottom and the middle layers, it is reasonable to assume that no loss of this aggregate occurs during testing on the surface. Finally, the calculated mixture weight without the Stalite 5/16" (W_B) and the weight of the felt disk are subtracted from the weight of the chip seal specimen before testing to determine the weight of the Stalite 5/16" in the original specimen before testing.

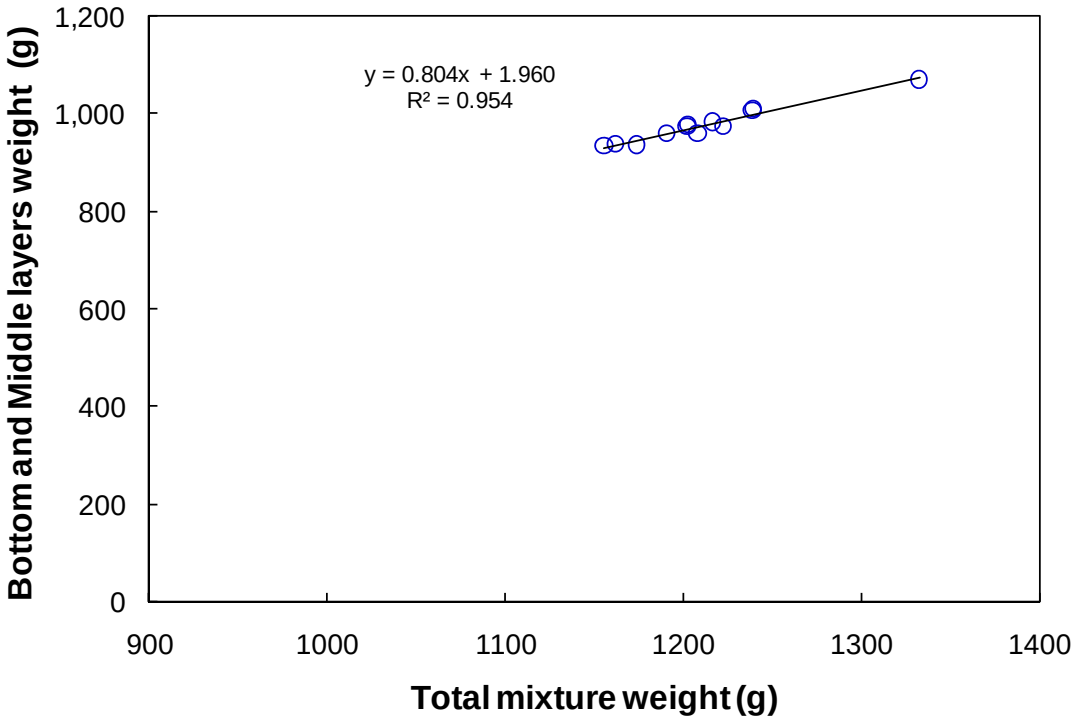

Figure 6-10 Correlation between total mixture weight and mixture weight without top layer aggregate

6.3.3.4 MMLS3 test

It is observed that the determination of the weight of the aggregate in the top layer only (i.e., Stalite 5/16") is important in estimating the percentage of aggregate loss performance as a function of the different coverages at the bottom layer of the triple seal. To determine the Stalite 5/16" weight at the top layer, the correlation described in Figure 6-10 was used. Figure 6-11 shows the percentage of aggregate loss during the 2 hr. 10 min. (12,940 wheel passes) aggregate retention test on the triple seals. The percentage of aggregate loss represented by the empty symbols was calculated using the weight of the Stalite 5/16" in the denominator in Equation (2). In comparison to the split seal, the average percentage of aggregate loss using aggregate weight increases slightly from 10.1% to 12.1%, due to the application of the rolling process at the bottom layer of the triple seal. The percentage of aggregate loss with zero coverage at the bottom layer is

10.1%. This percentage is similar to that of the extra aggregate used by the Alaska DOT (Mchattie 2001). However, the variance of the aggregate loss results shows similar ranges, which implies that no significant improvement of aggregate loss performance occurs as a function of the rolling operation at the bottom layer of the triple seal.

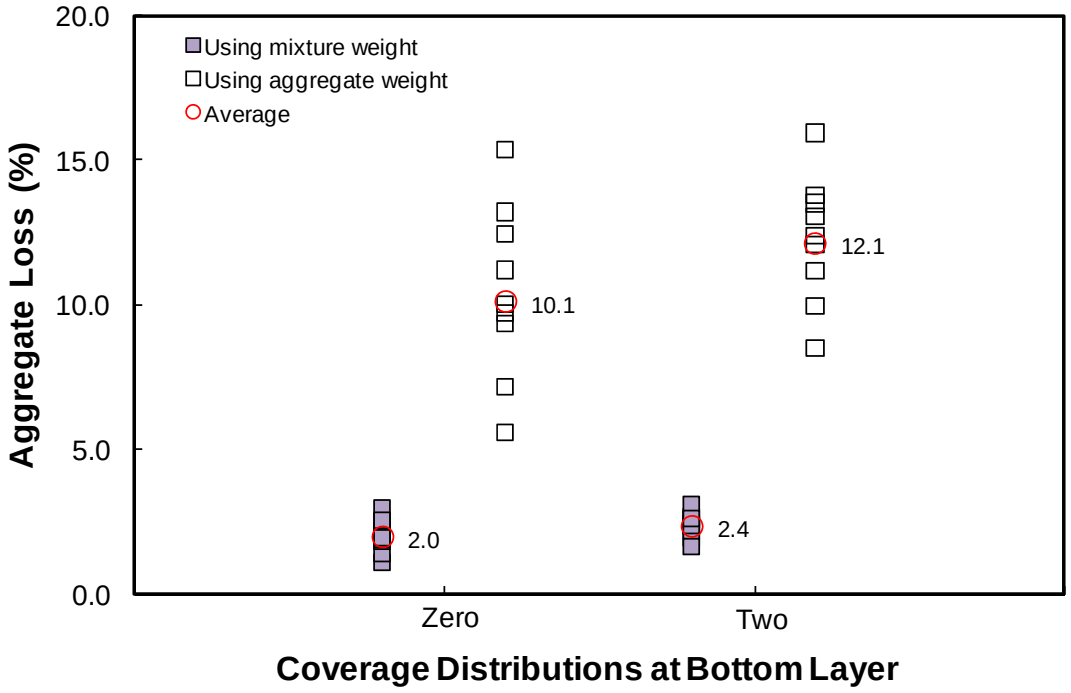

Figure 6-11 Aggregate loss performance from MMLS 3 test

6.3.3.5 Comprehensive analysis of triple seal study

The t-test was conducted to evaluate whether the aggregate retention performances of two groups, i.e., the different coverage distributions of the triple seal, are statistically different from each other. Two-tailed t-tests using the general alpha value of 0.05 were used. Table 6-4 summarizes the results of the t-tests for different coverage distributions at the bottom layers of the triple seal. The p-values from both the Vialit test and FOT are less than the alpha value, 0.05, thus indicating that the percentage of aggregate loss performance per each test is significantly different between zero and two coverages at the bottom layer of the triple seals. However, the results from MMLS 3 testing reach a

different conclusion from the t-test. These results indicate no significant difference of aggregate retention performance between zero and two coverages at the bottom layer of the triple seal, as the p-value is greater than 0.05.

Table 6-4 Results of t-tests for Coverage Distributions of the Triple Seal

Statistic	Vialit		FOT		MMLS 3	
	Mixture	Aggregate	Mixture	Aggregate	Mixture	Aggregate
Standard error	0.28	0.72	0.21	1.00	0.25	1.28
t-test	-2.03	-2.32	2.62	2.52	1.42	1.41
p-value	**0.07**	0.04	0.03	0.03	**0.18**	**0.18**
Conclusion	**Accept H_0**	Reject H_0	Reject H_0	Reject H_0	**Accept H_0**	**Accept H_0**

6.3.4 Results from the Digital Image Process

Interesting results from the study of coverage distributions at the bottom layer were found, as explained in Table 6-5. Table 6-5 shows a remarkable difference between the split seal and the triple seal in a comparison of the rolling effect in terms of aggregate retention performance. The single coverage at the bottom layer of the split seal is critical to improving the chip seal performance. However, the rolling operation at the bottom layer of the triple seal may be eliminated because its effects on aggregate retention results are not clear in Table 6-5. In order to investigate this difference between split and triple seals, the digital image processing (DIP) technique was adopted to investigate the aggregate structure of the multilayer seal. To assess the structure of the multilayer seals, profiles were created. Then, the relationship between the profiles and the aggregate retention performance was investigated based on the finding from Ball et al. (2005) that because the aggregate in the multiple layers has a theoretical optimal packing arrangement.

Table 6-5 Comparison of Aggregate Retention Test Results

Test Methods	Split seal			Triple seal		
	Zero	One	Difference	Zero	Two	Difference
Vialit	**14.4**	7.8	**6.6**	**7.4**	5.3	**2.1**
FOT	**32.0**	22.6	**9.4**	9.0	**11.5**	**2.6**
MMLS 3	**27.1**	19.7	**7.4**	10.1	**12.1**	**2.0**

Figure 6-12 Digital image of triple seal cut surface

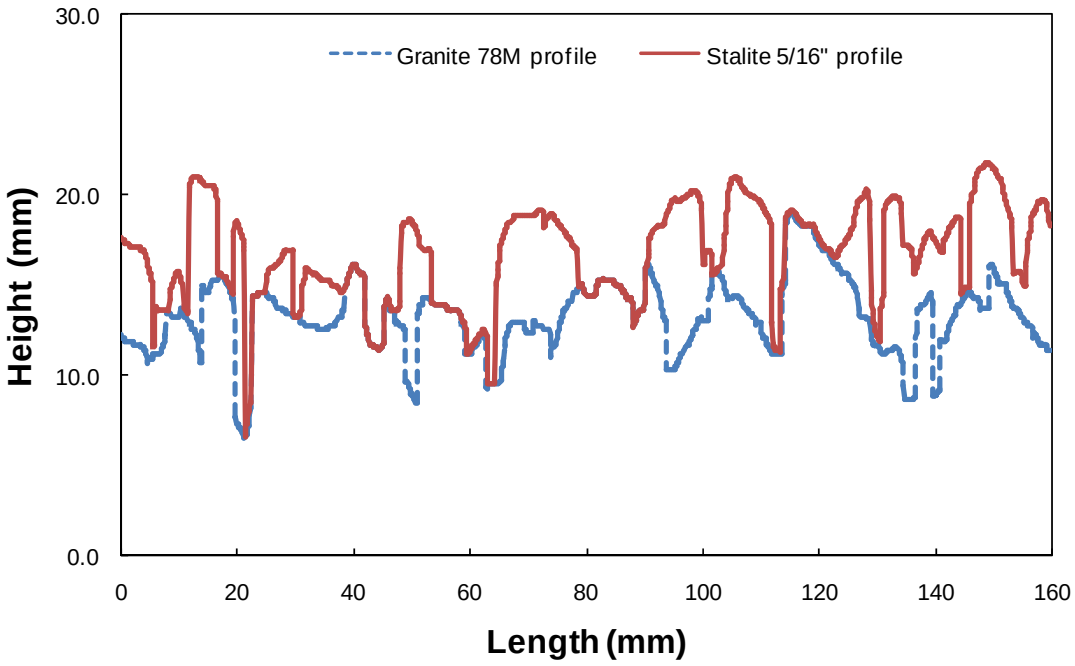

Figure 6-13 Profile of cutting surface of the triple seal

In order to create a profile of the multilayer seal, a specimen prepared for DIP was sliced using an electrical saw into 15 pieces, each 2 cm wide. The surface of the cut specimen was placed on the HP scanner that captured the digital image of a cross-section of the triple seal, as shown in Figure 6-12. Some aggregate particles appear to be floating in the air, as indicated by an arrow. This appearance is due to the fact that the digital image shown in Figure 6-12 is a two-dimensional, cross-sectional view of the chip seal sample. These aggregate particles are attached to the emulsion at different locations on the particles, which cannot be shown in the cross-sectional view.

The profile, as shown in Figure 6-13, was created using a code based on MATLAB® R2007a. Figure 6-13 shows two profiles of the triple seal specimen: the red one is the Stalite 5/16" aggregate profile that indicates the original top surface profile; the blue profile is the second layer profile created after the Stalite 5/16" aggregate profile was deleted manually using Photoshop.

Based on the profile developed for each image, R_q (the root mean square roughness) of the profile deviations was calculated within the evaluation length and measured from the mean line. R_q is given by Equation (6) (ASME 2002).

$$R_q = [(1/L)\int_0^L Z(x)^2 dx]^{1/2} \qquad (6)$$

As shown in Figure 6-14, the profile height $Z(x)$ presented the point-by-point deviations between the measured profile and the mean or reference line (ASME 2002, Lemaster 2004).

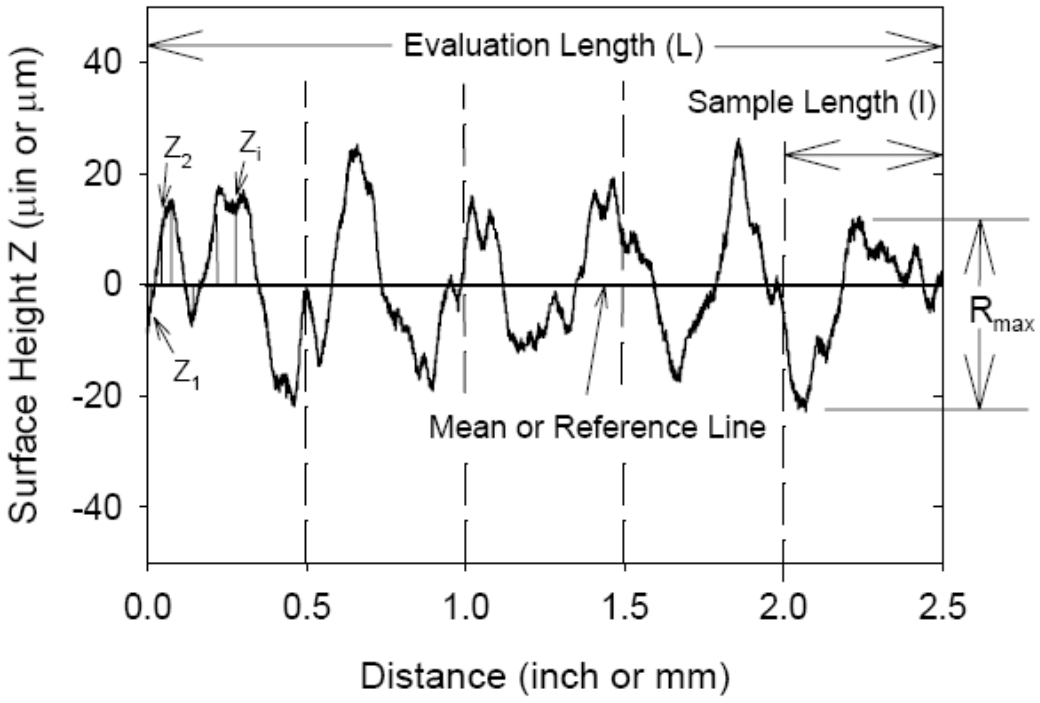

Figure 6-14 Illustration for the calculation of root mean square roughness R_q (Lemaster 2004)

Figure 6-15 shows the average roughness of the top layer in terms of the state of rolling operation at the bottom layer of the multilayer seal. Figure 6-16 shows the plot of the average roughness of the previous layer, that is, a layer without Stalite 5/16". A significant difference in roughness among the chip seal types appears between Figure 6-15 and Figure 6-16.

Three clear observations can be made from these figures. First, the reduction of the average roughness due to rolling is definitely recovered in the time between before and after applying traffic loading using the MMLS 3. Specifically, the split seal without the rolling operation at the bottom layer shows a huge reduction in average roughness from 8.5 to 3.4. This reduction affects aggregate reorientation and embedment into the underlying layer of the multilayer seal (Ball et al. 2005). It is possible that the split seal without rolling at the bottom layer has more voids than with rolling at the bottom layer,

because the rough surface texture can create voids. As traffic loading is applied, the voids of the split seal without rolling at the bottom layer clearly decrease according to aggregate reorientation and compaction. In the case of the split seal with rolling at the bottom layer, closely similar roughness values, 1.8 and 1.7, are seen in terms of traffic loading.

The second observation from Figure 6-16 is that there are clearly different roughness values for the bottom layer of the split seal as a function of the rolling operation. Figure 6-16 shows the different average roughness values based on the profile of the bottom layer according to the application of the rolling operation at the bottom layer. Figure 6-16 thus implies the higher the roughness, the higher the surface texture. Thus, a higher surface texture can be built from the excess volumes in the split seal. More emulsion is required to fill the excess in the higher surface texture; this larger amount of emulsion is based on the standard sprayer rate algorithm (Ball et al. 2005).

The third observation from Figure 6-15 and Figure 6-16 is that there is no significant decrease in the average roughness of the triple seal compared to that of the split seal. The average roughness values, measured as a function of the different rolling operation at the bottom layer, are closely similar to the average roughness values from the middle layer of the triple seal. As shown in Figure 6-16, the average of the roughness values between *No Rolling* and *Rolling* is the same, which implies that the two sections (i.e. the zero and the two coverages sections) have a surface texture similar to the middle layer of the triple seal, because the aggregate becomes reoriented and embedded in both the bottom and the middle layers. Thus, the roughness is similar between the two different conditions, which indicates a similar aggregate retention performance in the triple seals.

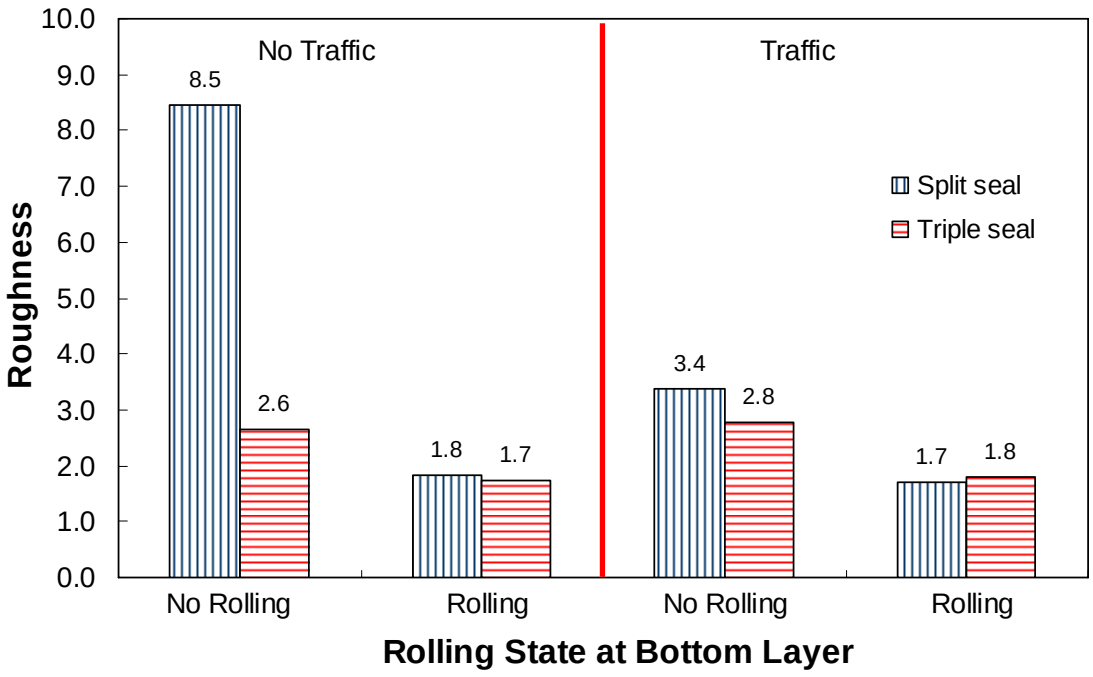

Figure 6-15 Roughness of original multilayer seals

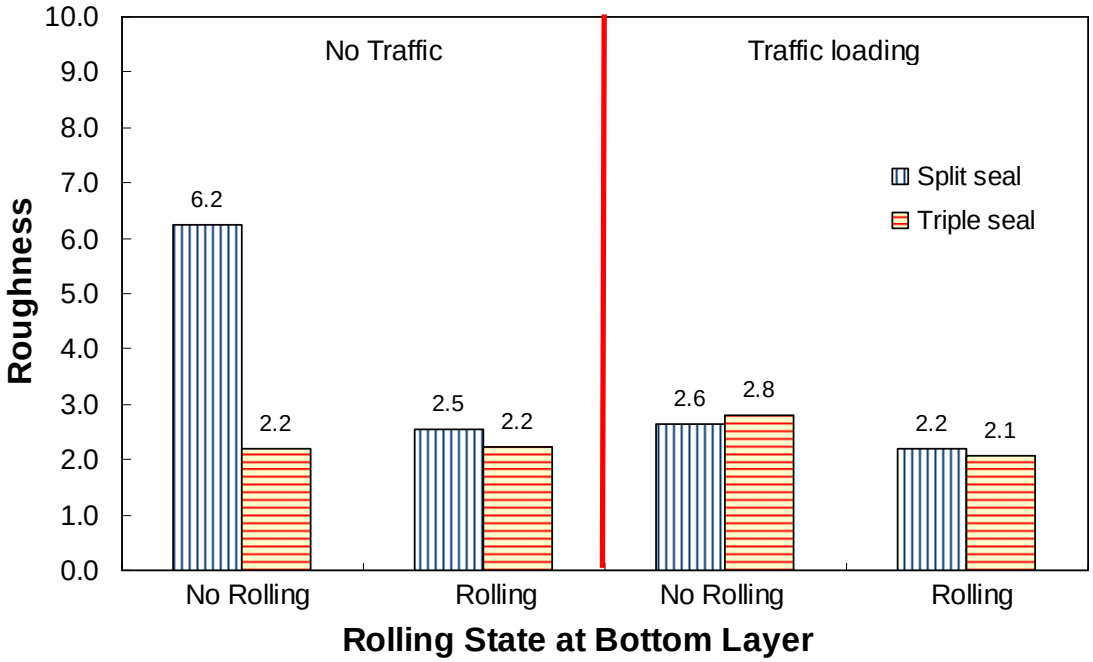

Figure 6-16 Roughness of multilayer seals without Stalite 5/16"

7. ROLLING PATTERNS

7.1 Experimental Program

One of the important variables in chip seal construction is the rolling pattern. The rolling pattern must completely cover both edges and the center of the lane to achieve proper aggregate embedment before the breaking of the emulsion. The rolling pattern is designed according to the number of rollers and the type of roller used. Various rolling patterns are currently used by each Division of the NCDOT as well as by other state DOTs. The California DOT (Caltrans 2003) requires a rolling pattern that uses a minimum of two rollers to cover the entire width of the lane. The Texas DOT (2004) has developed the most efficient rolling system, which uses three or four pneumatic tire rollers. Each Division of the NCDOT uses a different number of rollers and a different type of roller. Thus, the rolling pattern is determined as a function of the number of rollers and the type of roller. In order to determine an optimal rolling pattern in this study, a total of five rolling patterns are designed as a function of the number of rollers and type of roller based on current NCDOT patterns.

The rolling patterns were constructed on the same road, New Sandy Hill Church Road (SR 1131) near Bailey in Wilson County, NC. Case I and Case II were constructed June 12, 2007. The other three cases were constructed October 9, 2007. The application rates for the aggregate and emulsion are 17 lb/yd^2 and 0.35 gal/yd^2, respectively. Division 4 provided an aggregate spreader for the granite 78M and an emulsion sprayer. Division 5 provided both the combination roller and pneumatic tire roller and division 8 was provided a combination roller.

Schematic diagrams of rolling pattern designs as a function of both number of rollers and roller type are illustrated in Figure 7-1. The rolling patterns shown in Figure 7-1 (a) and Figure 7-1 (b) illustrate the possible rolling patterns using two rollers. The

pattern shown in Figure 7-1 (a), Case I, is currently used by the NCDOT. Each roller applies one coverage to the entire rolling area with three passes. The first roller follows the aggregate spreader to apply the initial rolling before the breaking of the emulsion. The second roller begins when the first roller moves into its third pass. The target number of coverages in this pattern is two, because it is difficult to achieve the optimal coverage of three coverages under this scenario. That is, it is impossible to use one roller to produce two coverages because the roller must move forward during the last pass in actual construction.

Another pattern, as shown in Figure 7-1 (b), Case II, is of two rollers moving parallel. This pattern covers the entire width of the aggregate spreader and provides three coverages with three passes at the same time. This pattern is the same as that described in the California chip seals manual (Caltrans 2003).

Figure 7-1 (c), Case III, shows the same pattern and coverages as Case I, but two different roller types are used. Based on the findings from Chapter 4, pneumatic tire and combination rollers are used in this case. The first roller in Case III is a pneumatic tire roller that follows the aggregate spreader to cover the entire aggregate spread area with three passes. The second is a combination roller that starts once the pneumatic tire roller moves into its third pass. Figure 7-1 (d) and (e), Cases IV and V, depict rolling patterns using three rollers. The pattern shown in Figure 7-1 (d) is recommended by the Asphalt Emulsion Manufacturers Association (AEMA). Two rollers are kept close to the aggregate spreader to conduct the initial rolling over the aggregate before the emulsion breaks; the third roller applies target coverage for back rolling. The target number of coverages in this pattern is the optimal three coverages that was determined by the number of coverages study.

As for the roller type, Case IV employs two pneumatic tire rollers to apply one coverage to the entire lane width, and then use a third roller (the combination roller) to apply two additional coverages, as shown in Figure 7-1 (d). Figure 7-1 (e), Case V, is designed based on current NCDOT practice and illustrates the use of three rollers, one pneumatic tire roller and two combination rollers. A visual observation of the chip seal surface rolled only by the pneumatic tire roller during the Phase I study reveals that the

surface is much rougher than the surfaces rolled by the other rollers. Therefore, the pneumatic tire roller is used first behind the aggregate spreader, and the two combination rollers are used as the secondary roller, as seen in Case V in Figure 7-1. The pneumatic tire roller applies one coverage with three passes. The two combination rollers begin when the pneumatic tire roller moves into its third pass; they give three coverages with three passes. The target number of coverages for Case V is therefore four coverages.

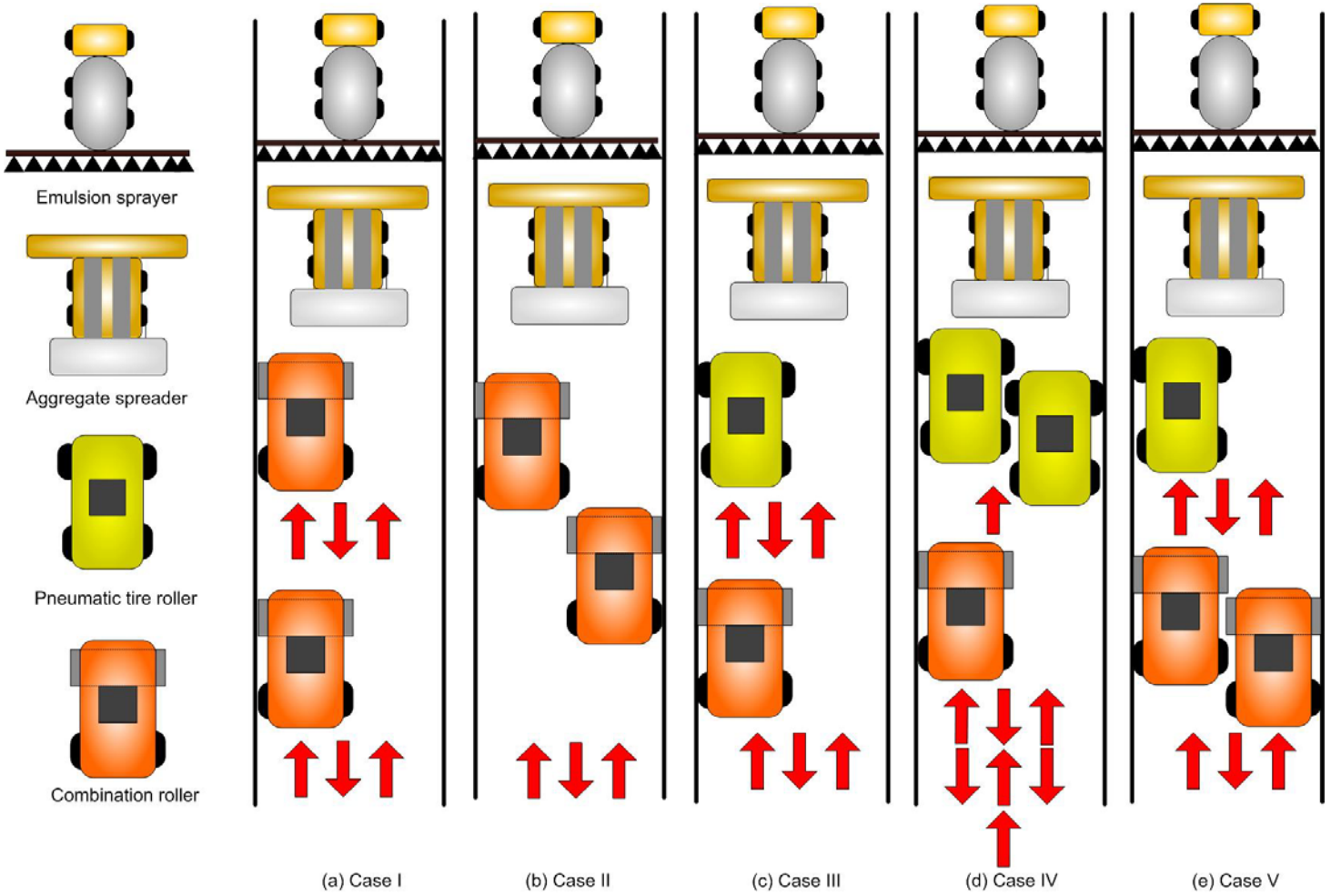

Figure 7-1 Schematic diagram of rolling patterns

7.2 Rolling Patterns Using Two Combination Rollers

The two rolling patterns were designed for this study based on their practical use in field construction and because the Divisions of the NCDOT currently use two rollers to roll aggregate in chip seal construction. For cases of rolling patterns using two rollers, three cases are evaluated in this study and described as Case I, Case II, and Case III in Figure 7-1. Case I uses a typical zig-zag pattern used by the NCDOT Divisions, whereas Case II provides an opportunity to evaluate the staggered rolling pattern recommended by the Arizona DOT and Texas DOT. Because Case III uses two different roller types, this case will be presented in the next section.

7.2.1 Sample Weight Variations: One Roller Type

Table 7-1 shows both the basic statistical analysis and a comparison with the t-test results for the mixture and aggregate weights obtained from different rolling patterns using two combination rollers. A significance level of 0.05 was used for the t-test. From the t-test results, as shown in Table 7-1, all the p-values are larger than 0.05, except the Vialit test results. The distribution of both the mixture and aggregate weights is examined and plotted, as shown in Figure 7-2. The aggregate weight from the straight seal samples is calculated by the Ignition Oven method, as explained in Chapter 3. Because the weights of the Vialit test samples are statistically different between Case I and Case II, the percentage of aggregate loss calculated from these weights may not accurately represent the aggregate retention performance of these two cases.

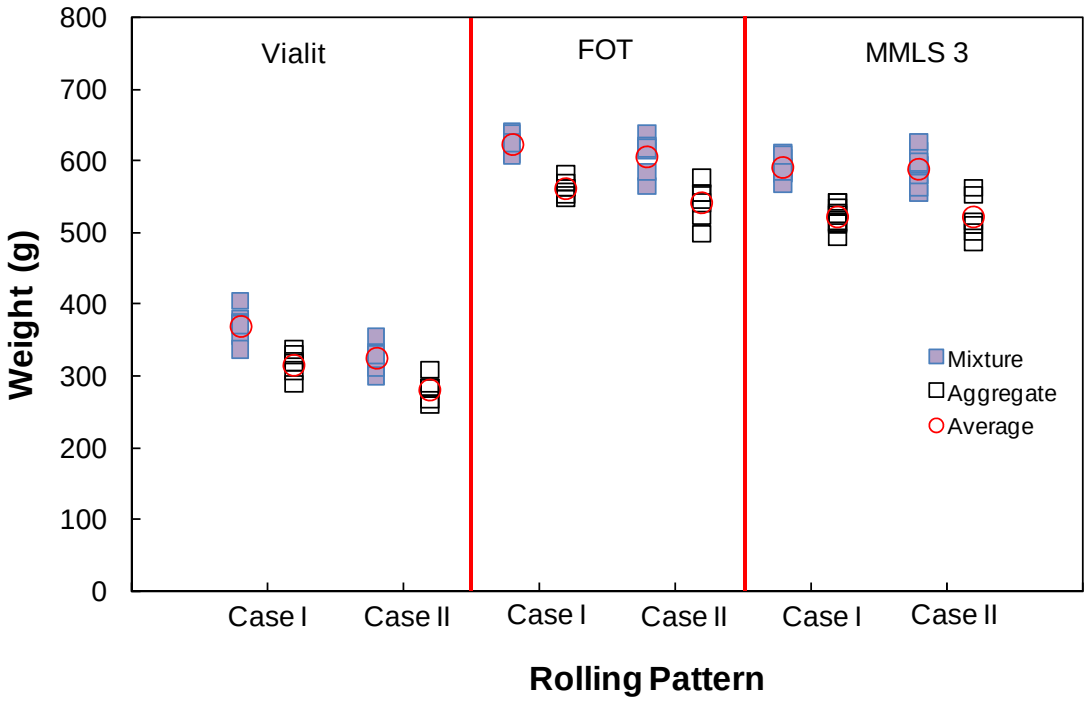

Figure 7-2 Distribution of sample weights

Table 7-1 Results of t-tests for Sample Weights

Test Method	Type of Weight	Pattern	Mean	Variance	Std. Dev.	t-test	p-value	Conclusion
Vialit	Mixture	Case I	369.2	524.2	22.9	-2.52	0.03	Reject H_o
		Case II	324.0	364.8	19.1			
	Aggregate	Case I	315.4	291.7	17.1	3.63	0.005	Reject H_o
		Case II	279.8	285.3	16.9			
FOT	Mixture	Case I	622.6	190.8	13.8	-1.32	0.22	**Accept H_o**
		Case II	605.5	736.5	27.1			
	Aggregate	Case I	561.4	138.4	11.8	1.76	0.11	**Accept H_o**
		Case II	540.0	750.7	27.4			
MMLS3	Mixture	Case I	590.0	193.7	13.9	-0.26	0.80	**Accept H_o**
		Case II	587.8	523.8	22.9			
	Aggregate	Case I	521.5	259.0	16.1	0.09	0.93	**Accept H_o**
		Case II	520.4	879.1	29.6			

7.2.2 Test Results

7.2.2.1 Flip-over test

In order to determine the effects of the rolling pattern that uses two combination rollers in terms of excess aggregate, the flip over test (FOT) was conducted. Figure 7-3 and Table 7-3 show the percentage of aggregate loss from the FOT of the straight seal in terms of the two different rolling patterns. The percentage of aggregate loss represented in Table 7-3 is determined using the weight of the aggregate using Equation (2). An empty circle symbol in Figure 7-3 indicates the average of the data for each rolling pattern. The average percentages of aggregate loss for Case I and Case II are about 6.5% and 8.7%, respectively. The range of the percentage of aggregate loss seen in Figure 7-3 is below the maximum allowable aggregate loss specified, 10%, in the Alaska chip seal guide (Mchattie 2001). Case II shows slightly higher aggregate loss performance, as shown in Figure 7-3, although the mixture weights of Case II are slightly less than the weights of Case I.

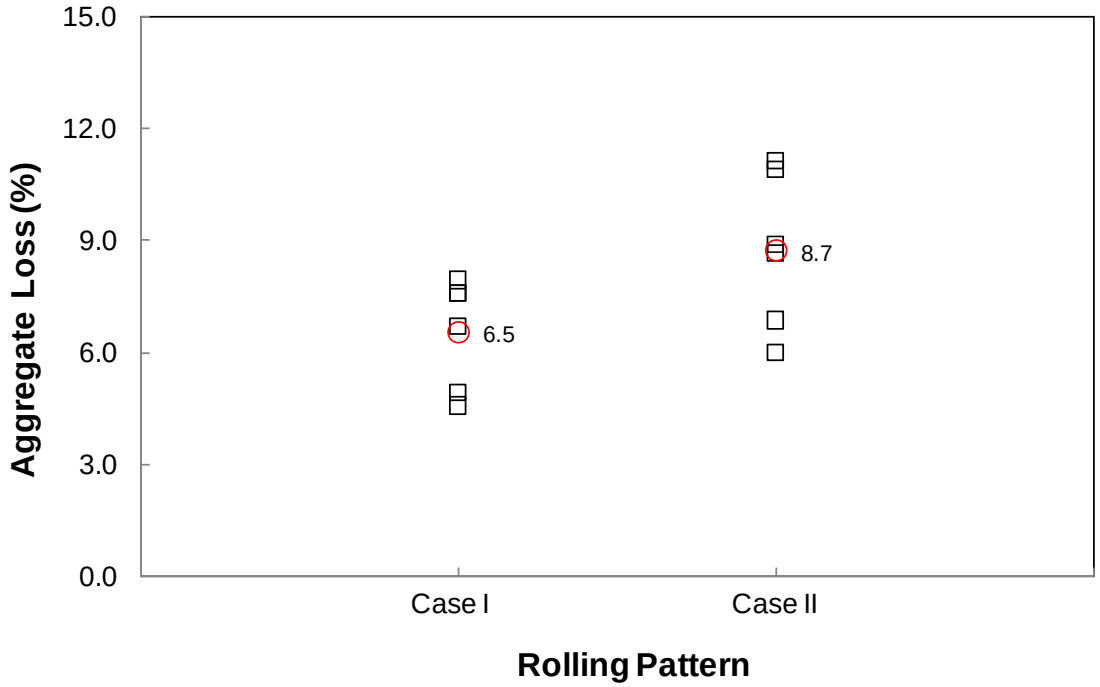

Figure 7-3 Aggregate loss performance from the FOT

7.2.2.2 Vialit test

The details of the Vialit test procedure and the Ignition Oven method to determine the emulsion weight in the chip seal mixture are described in previous chapters and, therefore, are not provided here.

Figure 7-2 shows the aggregate weight distributions of the Vialit samples after burning. As explained in the previous statistical analysis, significant differences were found in the sample weights from the Vialit test. It is possible that the aggregate weight affects the percentage of the aggregate loss performance. The aggregate loss performance was calculated using Equation (2) and is presented in Figure 7-4 in terms of the different rolling patterns. The largest variation in aggregate loss occurred in the Case I pattern, which is contrary to the FOT results. It is clearly seen in Figure 7-4 that the aggregate loss performance indicates a slight difference in aggregate loss, although those values are below the maximum allowable aggregate loss specified, 10%, in the Alaska chip seal guide (Mchattie 2001).

7.2.2.3 MMLS3 test

Figure 7-5 shows the percentage of aggregate loss during the 2-hr 10-min. (12,940 wheel passes) aggregate retention test of the straight seal. Equation (2) was used to calculate the aggregate loss performance. A trend similar to that found from the FOT aggregate retention tests (Figure 7-3) is observed in Figure 7-5. Comparing Case I with Case II, the lower aggregate loss percentage is observed in Case I. There is an approximately 2% difference of the average of aggregate loss between the two rolling patterns. The range of aggregate loss from the MMLS3 test is smaller than that of the other tests because some extra aggregate particles can be seated into the emulsion by the MMLS3 wheel loading.

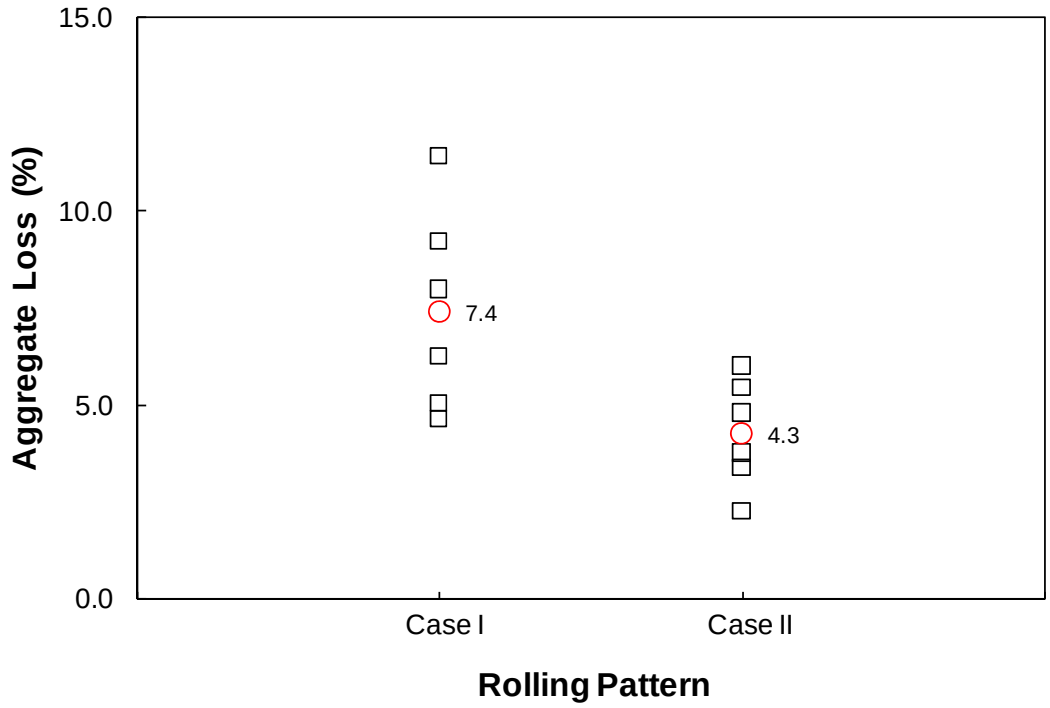

Figure 7-4 Aggregate loss performance from the Vialit test

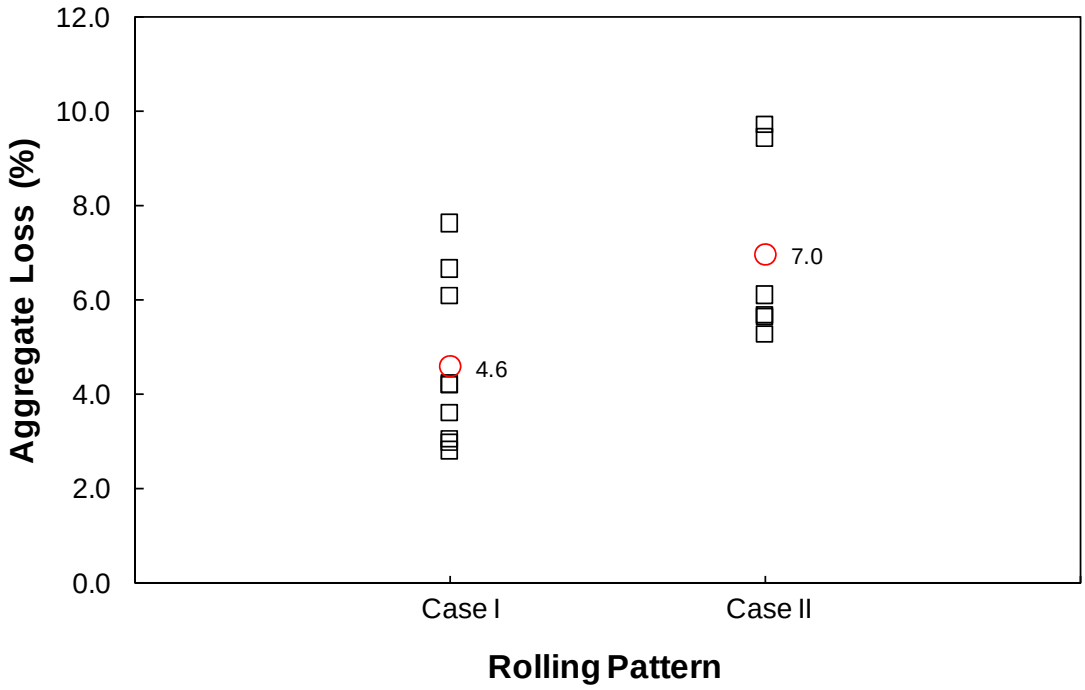

Figure 7-5 Aggregate loss performance from MMLS3 testing

7.2.2.4 Comprehensive analysis: using an one roller type

Table 7-2 shows the t-test results for the percentage of aggregate loss. Most of the p-values for the t-tests are less than 0.05, which indicates that a significant difference exists between Case I and Case II in terms of the aggregate loss performance. Table 7-3 summarizes the percentage of aggregate loss using aggregate weight as a function of rolling pattern. The average of aggregate loss from the MMLS3 test is slightly less than that of the other tests shown in Table 7-3. Case II, the parallel pattern, provides higher values of aggregate loss, although all the percentages of aggregate loss shown in Table 7-3 are less than the maximum allowable aggregate loss, 10%, specified by the NCDOT. In conclusion, Case I indicates a better performance of aggregate retention using two rollers of a single type. However, it is difficult to attribute this trend solely to the rolling pattern difference because of other factors that were not controlled in this experiment, such as the delay in initial rolling time. In the next section, the effects of delayed rolling time will be explained.

Table 7-2 t-Test Results for Aggregate Retention Tests: Using One Roller Type

Statistic	Test Methods		
	Vialit	FOT	MMLS3
Sample Mean	3.16	-2.19	-2.38
Std. Err.	1.21	1.03	0.99
t-test	2.60	-2.11	-2.41
p-value	0.03	0.06	0.03
Conclusion	Reject H_o	**Accept H_o**	Reject H_o

Table 7-3 Summary of Average Percentage of Aggregate Loss

Test Methods	Rolling Patterns	
	Case I	Case II
FOT	6.5	8.7
Vialit	7.4	4.3
MMLS3	4.6	7.0

7.3 Rolling Patterns Using Two Types of Roller

Both the pneumatic tire roller and the combination roller were recommended in Chapter 4 to roll aggregate for field construction. Thus, rolling patterns that use these two types of rollers are designed and evaluated for aggregate retention performance. The three rolling patterns are shown in Figure 7-1: Case III, Case IV, and Case V. Case III uses two rollers, and Case IV and Case V use three rollers.

7.3.1 Sample Weight Variations: Two Roller Types

The application rates of both the aggregate and emulsion were fixed during construction. Thus, theoretically, those samples should have approximately the same weight. However, variations from sample to sample were observed, as plotted in Figure 7-6. The aggregate weights in Figure 7-6 were measured after burning the mixtures in the ignition oven. Table 7-4 shows the results of statistical analysis and of analysis of variance (ANOVA) for all the sample weights. A significant difference in the weights of the FOT samples for the three patterns was observed from the ANOVA results shown in Table 7-4.

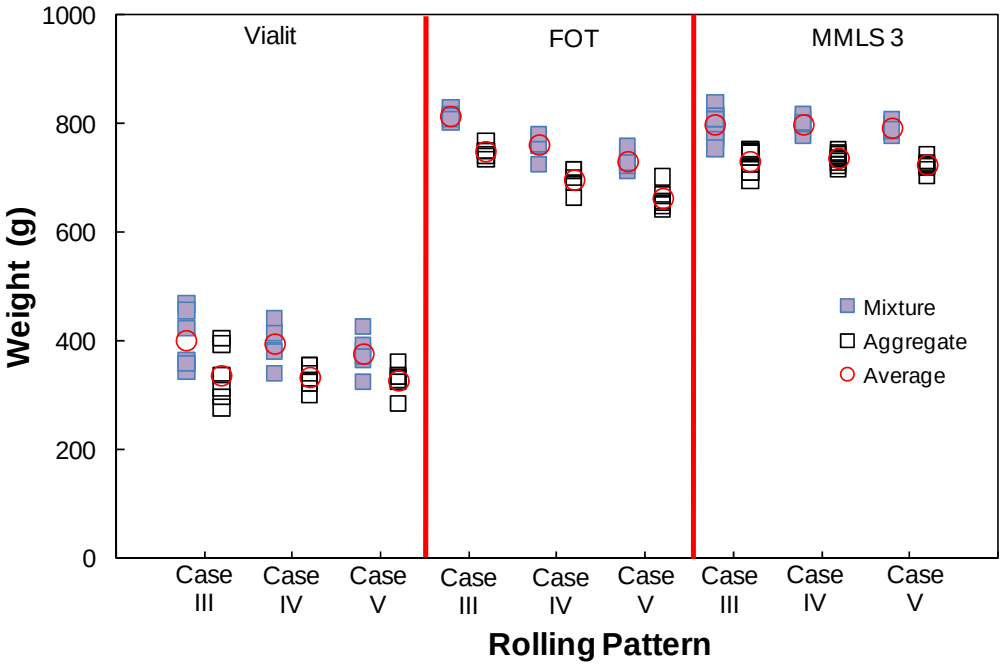

Figure 7-6 Distribution of mixture and aggregate weights

Table 7-4 Statistical Analysis of Sample Weights

Test Methods	Patterns	Mean	Variance	Std. Dev.	F-test	P-value	Conclusion
Vialit	Case III	335.9	2743.3	52.4	0.11	0.90	Accept H_o
	Case IV	331.9	456.6	21.4			
	Case V	375.2	1094.5	33.1			
FOT	Case III	747.7	129.2	11.4	33.63	<0.0001	Reject H_o
	Case IV	696.1	473.3	21.8			
	Case V	661.2	437.4	20.9			
MMLS 3	Case III	729.8	468.8	21.7	1.43	0.26	Accept H_o
	Case IV	734.1	125.6	11.2			
	Case V	722.1	102.1	10.1			

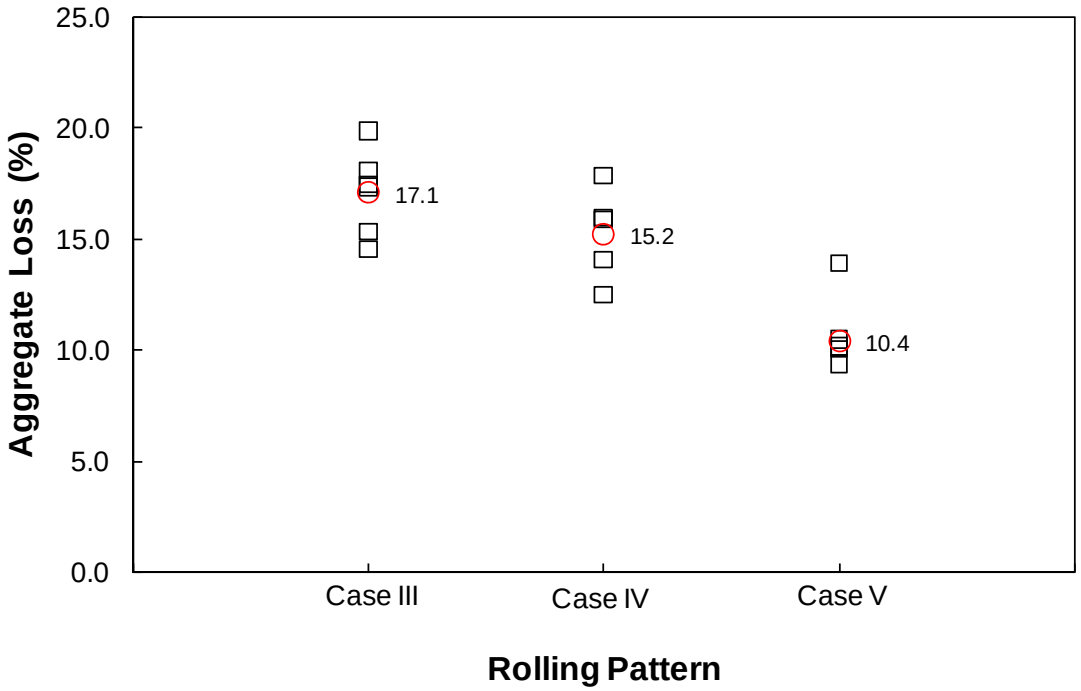

Figure 7-7 FOT aggregate loss performance

7.3.2 Test Results

7.3.2.1 Flip-over test

The FOT was conducted to measure the amount of excess aggregate. Figure 7-7 shows the percentage of aggregate loss from the FOT with the straight seal in terms of the three different rolling patterns. The percentage of aggregate loss represented in Figure 7-7 is determined using the weight of the aggregate using Equation (2). The Case V rolling pattern shows the least aggregate loss performance among the three rolling patterns. The percentage of aggregate loss shown in Case V is 10.4%. This percentage is similar to that of the extra aggregate used by the Alaska DOT (Mchattie 2001).

7.3.2.2 Vialit test

The Vialit sample weights are plotted in Figure 7-6 against the three different rolling patterns. As described in the ANOVA test results (seen in Table 7-4), the p-value

is greater than 0.05, which indicates that there is no statistical difference among the weights of the samples produced by the three rolling patterns.

The percentage of aggregate loss is determined using the aggregate weight and is plotted in Figure 7-8. Figure 7-8 indicates that a significant decrease in aggregate loss is evident from Case III to Case V. For example, the range of the percentage of aggregate loss for the rolling patterns is about 23.3% and 9.9%, respectively. The same trend as found from the FOT test (seen in Figure 7-7) is observed in Figure 7-8. Case V shows the best aggregate loss performance. Also, it is noted that the NCDOT specifications recommend a 10% aggregate loss as the maximum allowable aggregate loss for chip seals. According to this criterion, only Case V meets the specification.

7.3.2.3 MMLS3 test

Figure 7-9 shows the percentage of aggregate loss during the 2-hr. 10-min. (12,940 wheel passes) aggregate retention test on a straight seal. Equation (2) is used to calculate the percentage of retention. A trend similar to that found from other aggregate retention tests (Figure 7-7 and Figure 7-8) is observed in Figure 7-9. The best aggregate loss performance appears with Case V. Case III and Case IV show a similar range of aggregate loss, and the average value of the aggregate, represented by the empty circle symbol, is two times larger than that of Case V. These two values do not satisfy the NCDOT specification of the maximum allowable aggregate loss for chip seals. Only Case V is under the maximum allowable aggregate loss, 10%. The range of aggregate loss from the MMLS3 test is smaller than that of the other tests because some extra aggregate particles can be seated into the emulsion by the MMLS3 wheel loading.

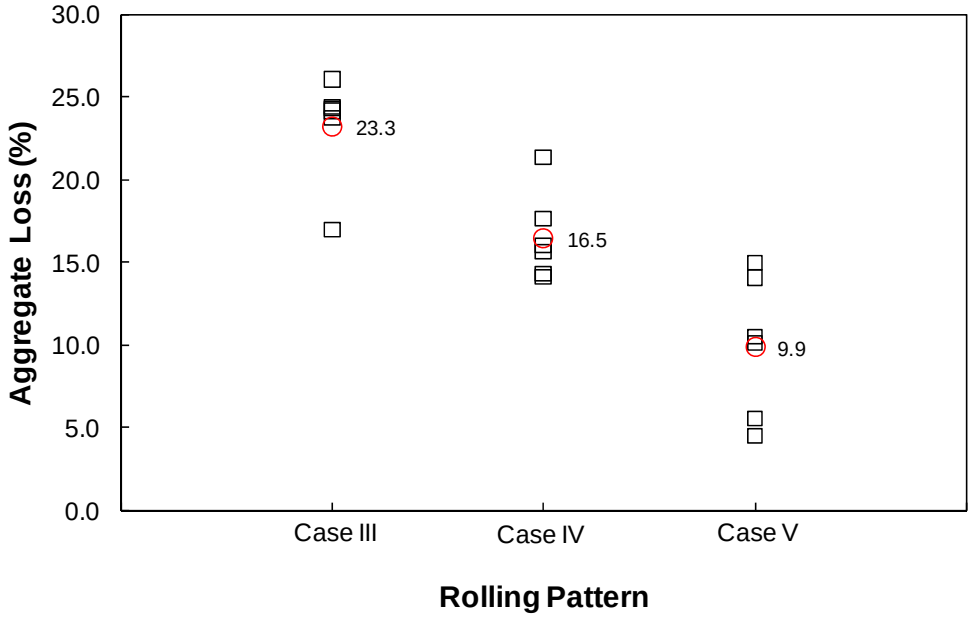

Figure 7-8 Aggregate loss of a straight seal from Vialit test

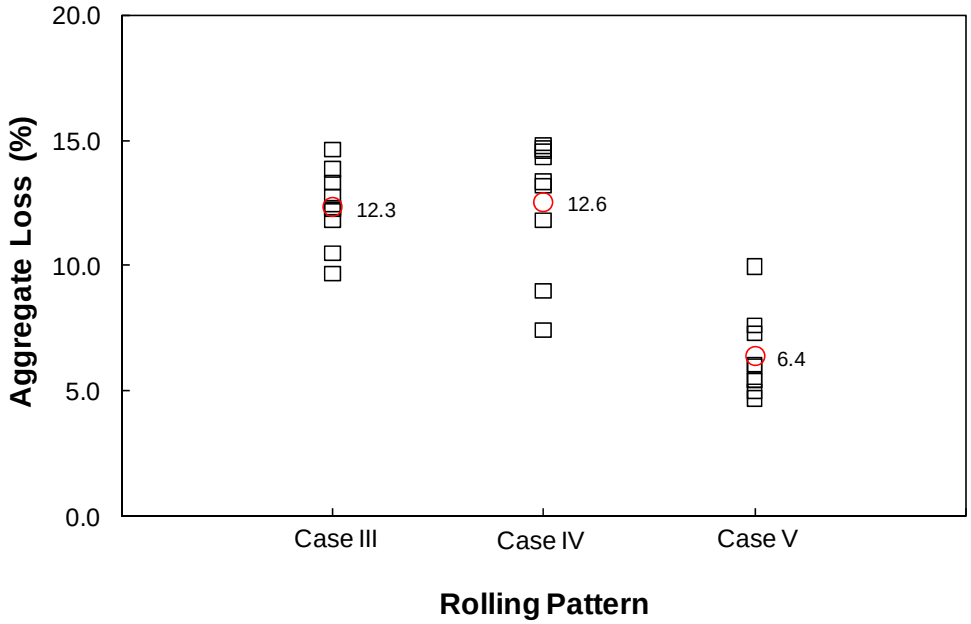

Figure 7-9 MMLS3 aggregate loss performance

7.3.2.4 Comprehensive analysis: using two roller types

The objective of this study is to assess the three rolling patterns using two types of roller and two and three numbers of roller. The rolling pattern is associated with both the number of rollers and type of roller that are used. In this study, the designed rolling patterns are based on two types of rollers, the pneumatic tire roller and the combination roller. These three patterns are used to evaluate the performance of the straight seal using granite 78M. Table 7-5 shows the ANOVA test results for the percentage of aggregate loss for the three rolling patterns. Table 7-5 indicates that there is a significant difference among the three patterns for the aggregate retention tests.

Table 7-6 summarizes the percentage of aggregate loss using the aggregate weight according to each of the three rolling patterns. Case V is clearly the best rolling pattern among the three.

Table 7-5 Results of ANOVA: Percentage of Aggregate Loss

Test Method	F-Test	P-value	Conclusion
Vialit	6.37	0.01	Reject H_o
FOT	18.98	0.0001	Reject H_o
MMLS 3	9.01	0.0012	Reject H_o

Table 7-6 Summary of Average Percentage of Aggregate Loss

Test method	Rolling patterns		
	Case III	Case IV	Case V
Vialit	23.3	16.5	9.9
FOT	17.1	15.2	10.4
MMLS 3	12.3	12.6	6.4

In order to explain the best performance demonstrated by Case V, the time delay between the aggregate spreader and the initial rolling was investigated. Time delays between the time the aggregate is placed on the samples and the time that the different rollers pass over the samples were measured and are summarized in Table 7-7. As can be seen in this table, the samples in Case V were rolled between 109 seconds and 345 seconds, whereas this range is much wider in Case IV (between 20 seconds and 500 seconds). This difference can be explained by the different speeds of the different rollers. Speeds of various equipment items used in chip seal construction are summarized in Table 7-8. It is noted that these speeds are not typical speeds of the equipment items, but actual speeds used in the rolling pattern study. It can be seen that the pneumatic tire roller is 1.4 times faster than the combination roller.

Table 7-7 Delay Time between Aggregate Spreader and Rolling Time

Coverage	Roller Type	Patterns		
		Case III	Case IV	Case V
One	Pneumatic tire roller	126 sec	25 sec	109 sec
Two	Combination roller	303 sec	197 sec	168 sec
Three	Combination roller	-	247 sec	213 sec
Four	Combination roller	-	500 sec	345 sec

Table 7-8 Equipment Speed during Construction

Equipment	Patterns			Average
	Case III	Case IV	Case V	
Emulsion sprayer	6.0 mph	6.2 mph	6.0 mph	6.1 mph
Aggregate spreader	3.8 mph	3.5 mph	3.8 mph	3.7 mph
Pneumatic tire roller	4.4 mph	4.1 mph	4.3 mph	4.3 mph
Combination roller	2.8 mph	2.6 mph	2.4 mph	2.6 mph

In Table 7-7, Case IV shows that the first coverage using the pneumatic tire roller finishes 25 seconds after it passes the aggregate spreader. This observation suggests that almost no delay occurs between the aggregate spreader and the roller because the roller can closely follow the chip spreader. However, Case III and Case V show a delayed time, approximately 2 minutes, between the aggregate spreader and the initial rolling due to the use of one roller. A question arises from this observation: How much delay between the aggregate spreading and initial rolling is best for the chip seal performance? To answer this question, a literature review was conducted with regard to delayed rolling time.

It is well known that rolling must be completed more quickly during cool weather than in warm weather. *Sprayed Sealing* (AAPA) emphasizes that aggregate that is rolled before the emulsion sets properly becomes too viscous to achieve wetting and adhesion. South Africa (1986) delays the initial rolling until the aggregate is almost dry. Based on this knowledge, a delayed rolling time possibly affects the aggregate loss performance. Therefore, the delayed rolling time parameter was studied under improved, controlled laboratory conditions, and the results are discussed in the next section.

7.4 Delayed Rolling Time

In order to study delayed rolling time, a small-scale aggregate retention performance test was designed using the MMLS3. Figure 7-10 describes the sample fabrication procedure for the delayed rolling time study using the MMLS3 in the laboratory. Five different delayed rolling times are used in the MMLS3 test: 2.0, 3.5, 5.0, 7.5, and 10 minutes. The aggregate for this study, granite 78M, is a one-size aggregate retained on a 1/4" sieve to avoid the effects of gradation or fine content. The aggregate and the emulsion application rates in this study are 17 lb/yd^2 and 0.25 gal/yd^2, respectively.

The chip seal specimen used for the MMLS3 testing has a rectangular shape 7 in. wide and 12 in. long. The width is designed to cover the entire wheel path under wandering MMLS3 loading. The felt disk is placed on a scale, and the template is placed and centered over the felt disk. The emulsion, heated to 158°F, is sprayed with a portable

sprayer onto the felt desk resting on the scale so that the emulsion is sprayed at a specified rate in the laboratory, as seen in Figure 7-10 (a) and Figure 7-10 (b). Then, the aggregate is immediately spread by ChipSS, shown in Figure 7-10 (c). This device simulates the aggregate spreader currently used in the field construction. ChipSS was designed to be a scaled-down version of the actual field spreader, and the intent of this device is to mimic the aggregate application in the field as closely as possible. Once the aggregate is spread on the emulsion, the specimen is placed immediately into the MMLS3 environmental chamber that maintains a target temperature of 86°F (Figure 7-10 (d)). The specimen is kept at rest for the duration of a specific delayed rolling time and then compacted using the half-circle hand kneading compactor for three half-cycles along the wheel pass direction of the specimen (Figure 7-10 (e)). The compacted specimen is then cured in a forced mechanical convection oven at 95°F and 30 ± 3% relative humidity (RH) for 24 hours for the aggregate retention test using the MMLS3. Therefore, all the specimens are tested after 24 hours of curing, but with different delayed rolling times.

7.4.1 MMLS 3 Test Results

In this section, the results of the MMLS3 test are presented to evaluate the effects of the delayed initial rolling times between the aggregate spreader and the initial rolling on aggregate retention. The aggregate used in this study has two different water contents. One aggregate is completely dry (0% water content) and is ideal aggregate for chip seal construction; the other is wet (2% water content) and is included here because the aggregate used in chip seal construction is commonly stockpiled in an open yard and is often wet when used. The aggregate loss performance under MMLS3 traffic loading for 2 hrs 10 minutes is shown in Figure 7-11 and Figure 7-12 as a function of the delayed initial rolling times and the two different water contents of the aggregate.

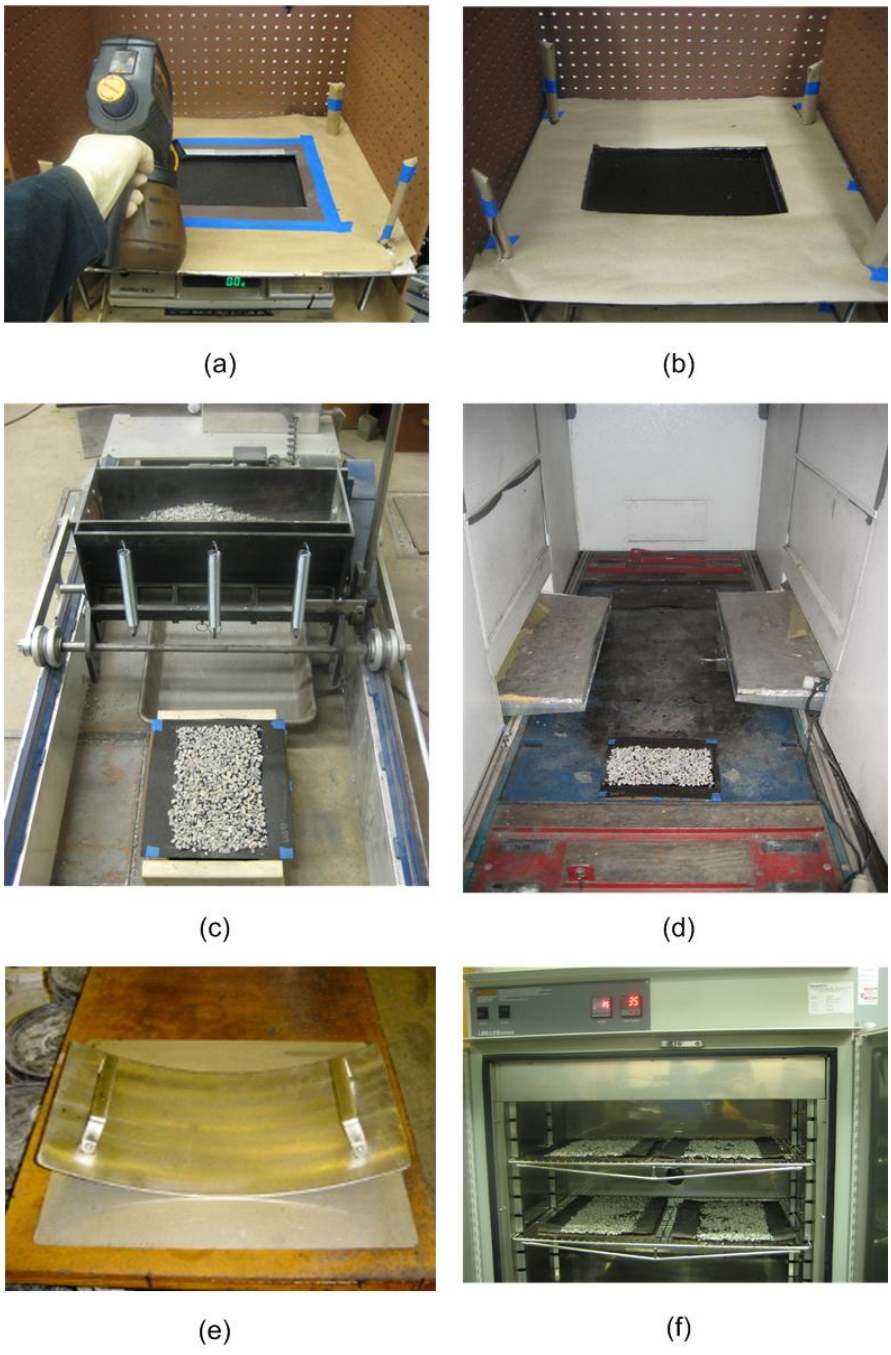

Figure 7-10 Chip seal specimen fabrication procedure: (a) emulsion application gun; (b) applied CRS-2 on the felt disk; (c) applied aggregate on the emulsion by CHIPSS; (d) sample in the environmental chamber for the delayed rolling times; (e) hand steel compactor; (f) curing sample in the oven.

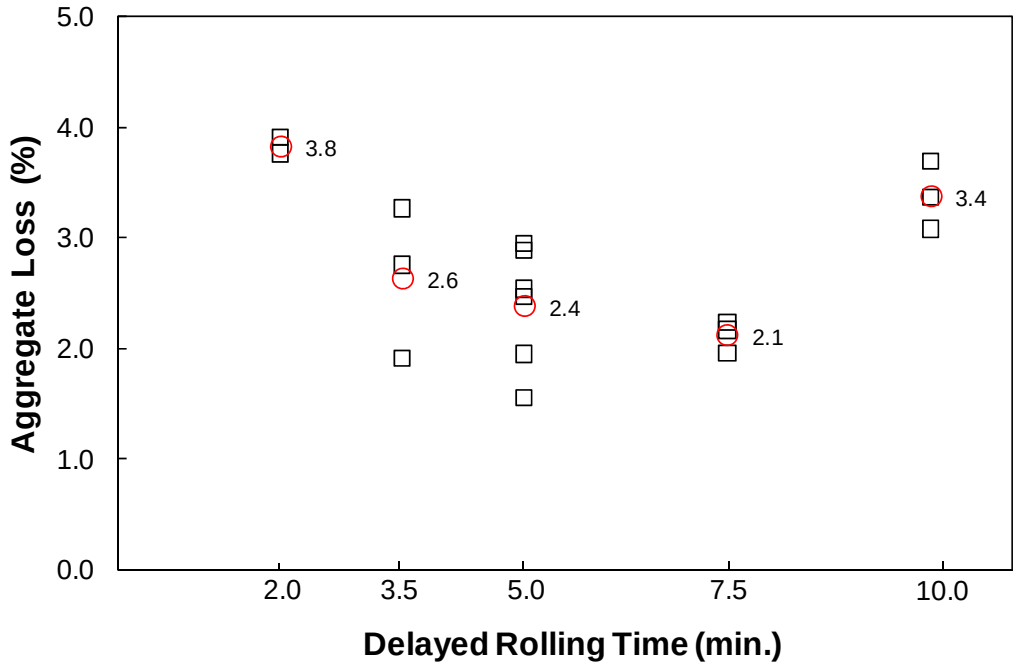

Figure 7-11 Aggregate loss results as a function of delayed rolling time using dry aggregate (0% water content)

The percentage of aggregate loss using unwashed dry aggregate represented in Figure 7-11 is calculated using the weight of the aggregate and using Equation (2). The large empty circle symbols indicate the average aggregate loss of the three replicates for each delayed rolling time. The MMLS3 test results in Figure 7-11 show a significant trend in the amount of aggregate loss according to the five delayed rolling times (2.0, 3.5, 5.0, 7.5, and 10 min.). Contrary to normal expectations, the worst aggregate retention performance among the various delayed rolling times occurred when the compaction was conducted with a 2 min. delayed rolling time after the aggregate was spread. This result may be due to the water in the emulsion that is comprised of binder and water. The aggregate in the emulsion is wet with water from the emulsion because water is more forcefully attracted to aggregate when the aggregate is spread on the emulsion film. This water between the aggregate and binder eventually evaporates, but nonetheless leaves a weaker zone at the interface. If the newly constructed chip seal pavement is subjected to

rolling too early, a greater surface area of aggregate is exposed to water and, therefore, the chip seal contains a greater area of weak interface due to poor adhesion between aggregate and binder. On the other hand, if the initial rolling is delayed too much, the emulsion viscosity becomes too high for the aggregate particles to be seated properly. Both of these conditions result in a greater aggregate loss. If the delayed rolling time is optimal, i.e., not too early to cause a weak interface and not too late to seat the aggregate properly, the aggregate loss is expected to be the lowest.

This hypothesis is well supported by the trend shown in Figure 7-11. As the delayed rolling time increases from 2 minutes to 3 minutes, the percentage of aggregate loss decreases due to the decrease in the weak interface area. As the delayed rolling time increases from 7.5 minutes to 10 minutes, the aggregate loss increases due to the increase in the emulsion viscosity.

The percentages of aggregate loss do not change significantly between 3.5 minutes and 7 minutes from the statistical analysis (t-test) results. This time window seems to be the optimal period in which to roll the aggregate.

Figure 7-12 shows the aggregate retention test results of the straight seal with the wet aggregate that has a 2% water content. Equation (2) was used to calculate the aggregate loss performance. A trend similar to that found using the dry aggregate (seen in Figure 7-11) is observed in Figure 7-12. However, a slightly different pattern can be found from Figure 7-12. That is, a significant decrease in aggregate loss is evident up to a 5-minute delayed rolling time. Also, the optimal rolling time window in the wet aggregate case is between 5 minutes and about 8 to 9 minutes. This shift in the optimal rolling time to a longer time for wet aggregate can be explained by a greater amount of water, which takes a longer time to evaporate, on the aggregate surface. This shift in the optimal rolling time is better depicted in Figure 7-13 with averages.

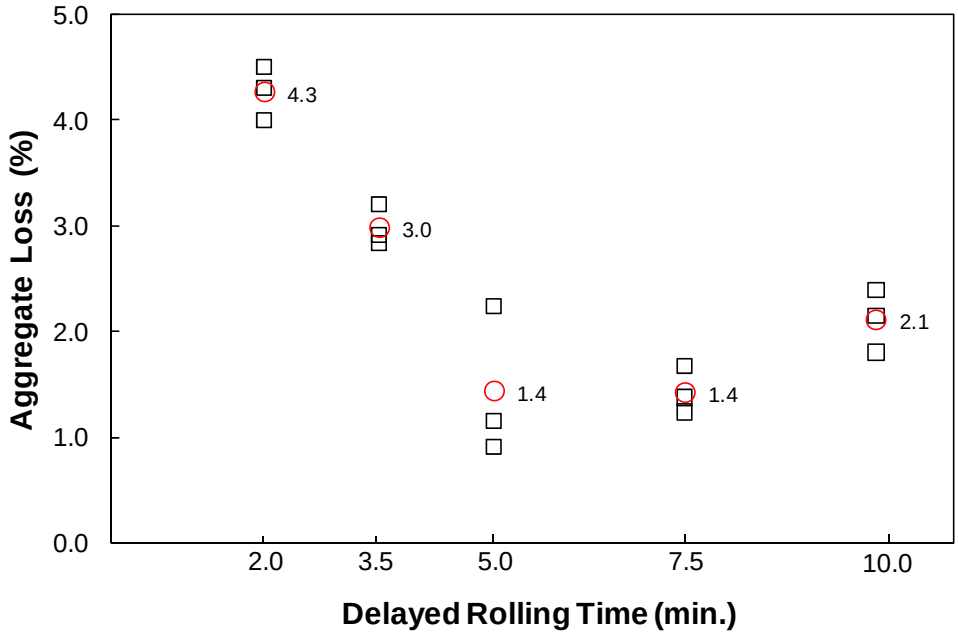

Figure 7-12 Aggregate loss results as a function of delayed rolling time using wet aggregate (2% water content).

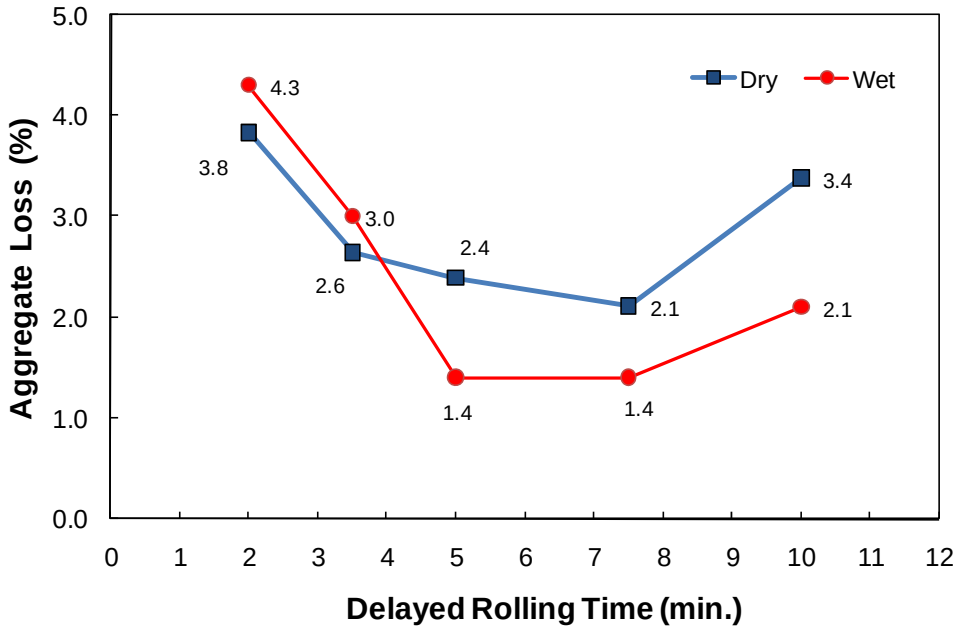

Figure 7-13 Average of aggregate loss results plotted against the condition of the aggregate.

This study finds that a delayed rolling time between the aggregate spreader and the first rolling operation may improve the aggregate retention performance. The optimal rolling time is between 3.5 minutes and 7.5 minutes for dry aggregate, whereas this window shifts to 5 minutes to 9 minutes for wet aggregate with a 2% water content. It is noted that these optimal rolling times are determined from laboratory conditions. It is expected that the optimal rolling time in the field would vary as a function of various environmental conditions, such as wind, humidity, and temperature. Generally, the time range between the aggregate spreader and the initial rolling obtained from survey results in the United States is from immediate rolling to 5 minutes. (Gransberg et al. 2005). The initial rolling is generally conducted within 5 minutes after spreading the aggregate in all Divisions of the NCDOT. This time span is determined by work experience with chip seals. This time span is also the same as that used in the Gransberg survey.

Because it is expected that normal field conditions accelerate the water evaporation from the emulsion, the commonly accepted 5-minute window seems to be reasonable compared to the 7.5-minute to 9-minute window from the laboratory study. Based on the limited data shown in Figure 7-11 and Figure 7-12 and the experience from the field, the optimal rolling time window of 2 minutes to 5 minutes is recommended for normal field conditions for chip seal construction. It is strongly recommended that this finding be verified and adjusted for various field conditions using additional laboratory and field testing. Another important observation is that this finding is valid only for unmodified emulsion. Polymer-modified emulsion is known to set much more quickly and, therefore, would require a different set of recommendations for the optimal rolling time.

7.5 Comprehensive Analysis

Based on all the results presented so far in Chapter 7, three rolling patterns have been selected for further study. These three patterns are denoted as Case A, Case B, and Case C in Figure 7-14. Case A was selected because this pattern is commonly used by several Divisions of the NCDOT. Case B has an advantage over Case A in that the entire

lane width is subjected to rolling at the same time. Case C combines the strengths found from Cases IV and V, shown in Figure 7-1. These strengths are the two rollers in a staggered pattern in the front (Case IV), which yields more consistent rolling along the lane width, and a smaller rolling time window (Case V), which results in the least aggregate loss, as shown in Figure 7-7 to Figure 7-9 and in Table 7-6.

The chip seal pavement construction schedule is simulated for these three cases to determine if these patterns can roll the aggregate within the time window that produces the most effective rolling. The primary consideration for the optimal rolling time window is that all the sections should be rolled within 5 minutes. Thirty seconds are allocated between the beginning of aggregate spreading and the initiation of rolling. This time delay allows the spreader to travel about 150 feet before the roller starts rolling, which is a necessary distance to move forward safely at full speed.

Four different section lengths were used in the simulations: 1,200, 1,500, 2,000, and 2,500 ft per section. These section lengths cover a range of section lengths that can be constructed by a fully loaded aggregate spreader without stopping. The calculations are done using the typical chip seal construction equipment speeds shown in Table 7-9. The roller speeds shown in this table are faster than those used in the rolling pattern study presented earlier in this chapter. This difference is due to the fact that in the rolling pattern field experiments, the section length was much shorter than a typical section length in normal construction, and therefore, the roller operators did not use the full speeds of the rollers.

The construction sequence and related times are plotted in a bar chart format in Figure 7-15 to Figure 7-17, and the calculated times are summarized in

Table 7-10. Figure 7-15 shows the construction time schedule for Cases A and C. Because the types of rollers involved in Cases A and C are the same and the second roller in the front row of Case C adds minimal additional time to the overall rolling operation, their construction time schedule is considered to be the same. Figure 7-16 and Figure 7-17 display the construction time schedules for Case B with two pneumatic tire rollers and Case B with two combination rollers, respectively.

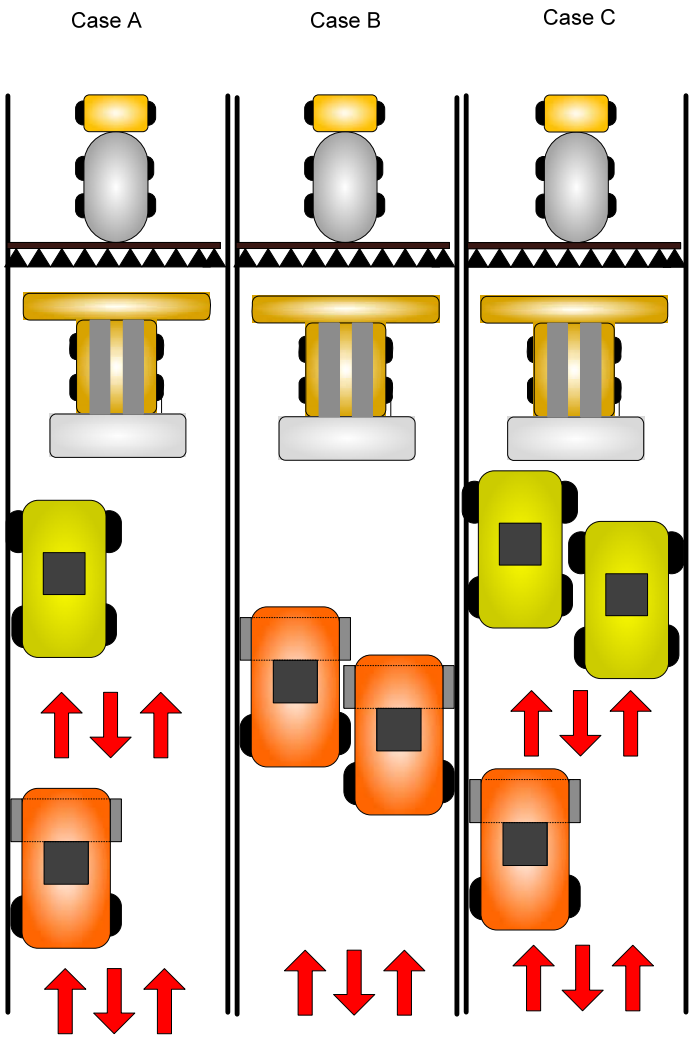

Figure 7-14 Rolling patterns with two and three rollers selected for the final evaluation

Table 7-9 Typical Chip Seal Construction Equipment Speeds

		mph	ft/min.
Emulsion sprayer speed		6.1	536.8
Aggregate spreader speed		3.7	325.6
Roller speed during Rolling Pattern Study	Pneumatic tire roller	4.3	378.4
	Combination roller	2.6	228.8
Normal roller speed	Pneumatic tire roller	8.3	730.4
	Combination roller	6.0	528.0

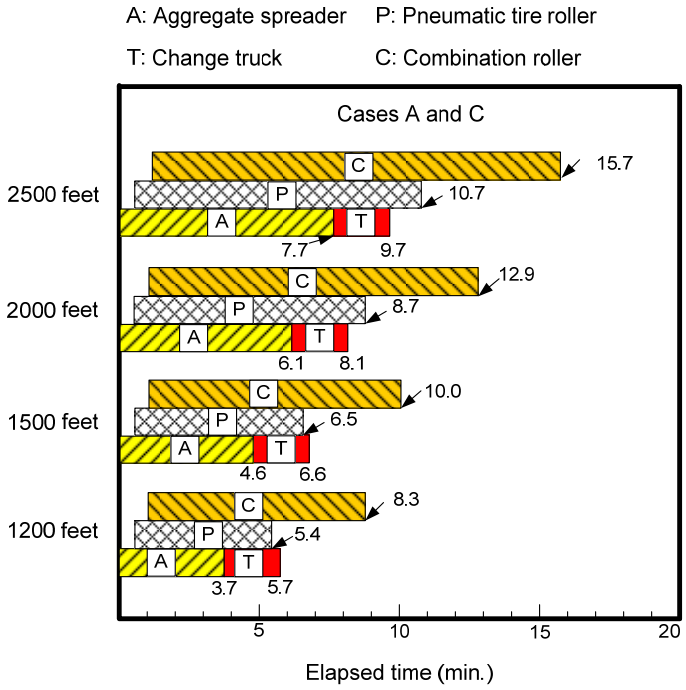

Figure 7-15 Construction time scheduling for Cases A and C

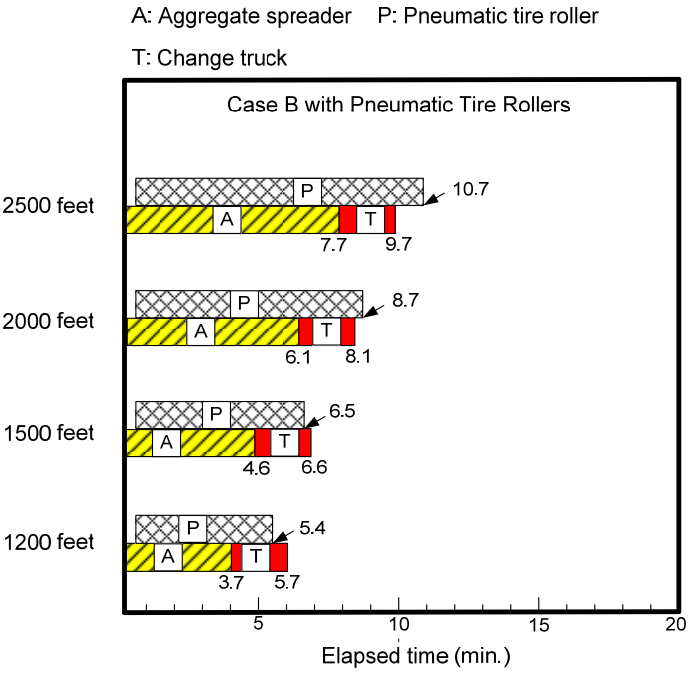

Figure 7-16 Construction time scheduling for Case B with two pneumatic tire rollers

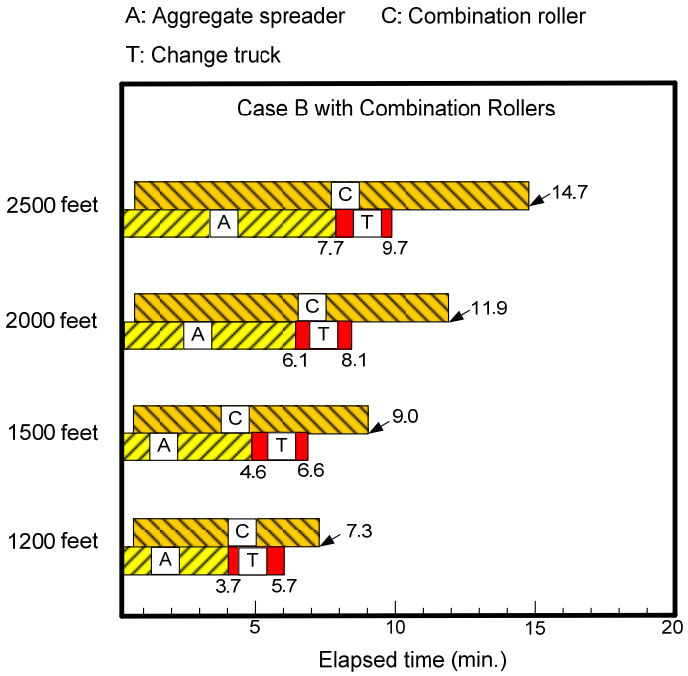

Figure 7-17 Construction time scheduling for Case B with two combination rollers

Table 7-10 Calculated Times for Chip Seal Construction Operation

		Required time to construct the entire section											
Distance		1200 feet			1500 feet			2000 feet			2500 feet		
Case		A	B	C	A	B	C	A	B	C	A	B	C
Emulsion sprayer		2.2	2.2	2.2	2.8	2.8	2.8	3.7	3.7	3.7	4.6	4.6	4.6
Aggregate spreader		3.7	3.7	3.7	4.6	4.6	4.6	6.1	6.1	6.1	7.7	7.7	7.7
Rolling time	Pneumatic tire roller		5.4			6.5			8.7			10.7	
	Combination roller	8.3	7.3	8.3	10.0	9.0	10.0	12.9	11.9	12.9	15.7	14.7	15.7
Delayed rolling time		4.6	3.6	4.6	5.4	4.4	5.4	6.8	5.8	6.8	8.0	7.0	8.0

The primary factor to be used in the evaluation of different rolling patterns with different section lengths is the time difference between the end of the aggregate spreading and the end of rolling. Case C with a 2,000 ft section length illustrates this point, as shown in

Table 7-10. According to the calculation, the aggregate spreader spreads the aggregate for the entire section length of 2,000 feet within 6.1 minutes. With the 30-

second delay between the aggregate spreader and the first roller, the rolling by the second roller (i.e., the combination roller) is completed within 12.9 minutes. Therefore, in this case the time delay between the aggregate spreading and the rolling at the last portion of the section is 6.8 minutes (i.e., 12.9 minus 6.1 minutes). This delay is greater than 5 minutes and, therefore, this scenario is not an acceptable one for effective rolling. The approach described above was applied to all the cases, and the delayed rolling times are tabulated at the bottom of

Table 7-10. The cases that do not meet the maximum delayed rolling time of 5 minutes are shaded in the bottom row.

Based on the results shown in Figure 7-15 to Figure 7-17 and

Table 7-10, the following observations can be made.

Two roller cases (i.e., Case A versus Case B)

- Case B, regardless of the roller type used, results in a shorter rolling duration than Case A. The shorter rolling duration allows more flexibility for field engineers within the 5-minute criterion.
- This reduction in the rolling duration is accomplished even though the number of coverages in Case B is more than that of Case A (three in Case B versus two in Case A).
- Case B rolls the entire lane width at the same time, whereas in Case A the delayed rolling time varies significantly among different locations in the section.
- The maximum section length to be spread by the aggregate spreader at once is about 1,400 feet for Case A and 1,700 feet for Case B. The longer allowable section length in Case B saves time in the chip seal pavement construction because of fewer interruptions.
- Based on the findings described above, the staggered rolling pattern in Case B is recommended for the two roller cases.
- With regard to the roller type for Case B, the pneumatic tire roller can roll the same section length in a shorter time due to its faster speed as compared to the

combination roller. The roller type study presented in Chapter 4 suggests that the aggregate shape and gradation affects the relationship between the aggregate retention performance and the roller type. However, visual observation of the field sections rolled by different roller types indicates that the pneumatic tire roller tends to leave a rougher surface texture than the steel wheel and combination rollers. It is not clear from this research the extent to which this negative effect of a rough surface from the pneumatic tire roller has on the chip seal performance. Based on the literature review and the data generated from this research, both pneumatic tire and combination rollers are recommended to be used with the Case B rolling pattern.

- If the rolling pattern in Case A is to be used, it is recommended to use the pneumatic roller first followed by the combination roller. This arrangement takes advantage of the faster speed of the pneumatic tire roller than that of the combination roller. Also the pneumatic tire roller's ability to roll an uneven existing pavement needs to be taken advantage of earlier than later in the chip seal construction process. The ability of the combination roller to produce a smoother surface than the pneumatic tire roller makes it a better choice as the second roller to finish the rolling.

Three roller case (i.e., Case C)

- In terms of rolling time, Case C is the same as Case A currently used by some Divisions in the NCDOT.
- However, Case C brings in two important advantages over Case A, that is, more consistent rolling along the lane width and more coverages (four coverages in Case C versus two coverages in Case A) within the same amount of rolling time.
- The rolling pattern in Case C fully captures the pneumatic tire roller's ability to roll an uneven surface of existing pavement and the combination roller's ability to produce a smooth surface.

- The maximum section length to be constructed by the Case C pattern is about 1,400 feet.

8. CONCLUSIONS AND FUTURE RESEARCH RECOMMENDATIONS

The following conclusions are drawn based on the results presented in this report:

1. The range of aggregate loss percentages obtained from the MMLS3 test is narrower than that of the other tests because some extra aggregate particles can be seated into the emulsion by the MMLS3 wheel loading. This observation can be extended to claim that the conventional aggregate retention tests, which determine the aggregate loss before significant trafficking, are conservative test methods for determining aggregate retention performance.
2. Based on the results from aggregate retention performance tests and visual observation, both the pneumatic roller and the combination roller are recommended to improve chip seal performance. With regard to order, rolling should start with the pneumatic tire roller and finish with the combination roller to produce a smooth surface, because the combination roller provides a smoother, flatter finished texture than the pneumatic tire roller.
3. The optimal number of coverages for both straight and split seal construction is three, according to aggregate retention test results and measurements of the aggregate embedment depth using the modified sand circle test. Five coverages seem to improve the aggregate retention performance further; however, the extra time needed for the two additional coverages makes rolling patterns with five coverages impractical.
4. The optimal coverage distribution on the underlying layer of a multiple chip seal (split and triple seals) is determined according to the results of the aggregate retention performance tests and digital image analysis. The split seal clearly

requires rolling for the bottom layer; the triple seal does not, and therefore, the rolling operation may be eliminated for the bottom layer.

5. The rolling pattern is closely correlated to the delayed rolling time between the aggregate spreading and the rolling. The effect of the delayed rolling time is shown by the aggregate retention performance using MMLS3 testing. The optimal delayed rolling time changes according to the water content of the aggregate.
6. The optimal rolling pattern is strongly related to the delayed rolling time. Considering the calculated rolling times, consistency of rolling across the lane width, presence of an uneven surface from existing pavements, number of coverages, and roughness of the finished chip seal surface, Case B and Case C are recommended for two rollers and three rollers, respectively.

The following recommendations are made for future research:

1. Effects of delayed rolling time on the aggregate retention performance need to be evaluated over a wider range of conditions that can be encountered in the field.
2. As more Divisions in the NCDOT utilize polymer-modified emulsion, it is important to develop optimal rolling pattern(s) for chip seal pavements using polymer-modified emulsion.

REFERENCES

Asphalt Emulsion Manufacturers Association. (2004) A Basic Asphalt Emulsion Manual.

ASTM, *Standard Test Method for Asphalt Content of Hot-Mix Asphalt by Ignition Method.* American Society for Testing and Materials, D 6307. 2004.

ASTM. *Standard Test Method for Sweep Test of Bituminous Emulsion Surface Treatment Specimens*. American Society for Testing and Materials, D 7000. 2005.

Arizona Department of Transportation. (2003) Chip Seal Guide Application and Construction.

Austroads Inc. (2004) Sprayed Sealing Guide Austroads Pavement Technology Series.

Australian Asphalt Pavement Association. (AAPA) (2000) Sprayed Sealing-Rolling of Cover Aggregate. Pavement work tips-no.24. http://www.aapa.asn.an/au/content/aapa/download/worktips24.pdf. Accessed March 2008.

American Society of Mechanical Engineers. (ASME) (2002) An American National Standard Surface Texture (Surface Roughness, Waviness, and Lay).

Ball, G. F. A., J. E. Patrick, and P. R. Herrington. (2005) Factors Affecting Multiple Chipseal Layer Instability. Land Transport New Zealand Research Report, No. 278.

Benson, F. J. and B. M. Galloway. (1953) Retention of Cover Stone by Asphalt Surface Treatments. Bulletin 133, Texas Engineering Experiment Station, Texas A&M University System.

Bullard, D. J., R. E. Smith, and T. J. Freeman. (1992) Development of a Procedure to Rate the Application of Pavement Maintenance Treatments, Strategic Highway Research Program.

Caltrans Division of Maintenance. (2003) Chip seals. http://www.dot.ca.gov/hq/maint/ mtag/ch5_chip_seals.pdf. Accessed March 2008.

Croteau, J., P. Linton, J. K. Davidson, and G. Houston. (2005) Seal Coat Systems in Canada: Performances and Practice. 2005 Annual Conference of the Transportation Association of Canada, Calgary, Alberta. http://www.tac-atc.ca/english.pdf/conf2005/s15 croteau.pdf. Accessed March 2008.

Davis, D., M. Stroup-Gardiner, J. A. Epps and K. Davis. (1991) Correlation of Laboratory Tests of Field Performance for Chip Seals. Transportation Research Record 1300, TRB, National Research Council, Washington, D.C., pp. 98~107.

Elmore, W. E., M. Solaimanian, R. B. McGennis, C. Phromsorn, and T. W. Kennedy. (1995) Performance–Based Seal Coat Asphalt Specifications. Center of Transportation Research-the University of Texas at Austin.

Emmanuel, C. (1999) Esso Abrasion Cohesion Test A Description of the Cohesive Breaking of Emulsions for Chip Seals. ISAET'99 International symposium on Asphalt Emulsion Technology: Manufacturing, Application, and Performance.

Estakhri, C. K. and M. A. Gonzalez. (1998) Design and Construction of Multiple Seal Coats. Texas Transportation Institute.

Gransberg, D. D., I. Karaca, and S. Senadheera. (2004) Calculating Roller Requirements for Chip Seal Projects. Journal of Construction Engineering and Management, Vol. 130, No. 3, pp. 378~384.

Gransberg, D. D. and D. M. B. James. (2005) Chip Seal Best Practices. NCHRP Synthesis 342, Transportation Research Board, Washington, D. C..

Hudson, K .C., L. R. Saunders, K. F. Nicholls, and P. H. Hambleton. (1986) Rolling of Chip Seals. 13th ARRB-5th REAAA Combined Conference, Vol. 13, pp. 173~186.

Jackson, D. C., N. C. Jackson, and J. P. Mahoney. (1989) 1989 West side chip seal study. Washington State Department of Transportation.

Janisch, D. W. and F. S. Gaillard. (1998) Minnesota Seal Coat Handbook. Minnesota Department of Transportation.

John, R. and D. Whiteoak. (2003) The Shell Bitumen Handbook. Fifth Edition, American Society of Civil Engineers.

LaCroix, A., Y. R. Kim, and C. Arellano. (2008) Comparison of Dynamic Moduli Determined from Different Geometries and Compactions. In Transportation Research Board: 87th Annual Meeting Compendium of Papers, National Research Council, Washington, D.C..

Lee, J. (2007) Performance Based Evaluation of Asphalt Surface Treatments Using Third Scale Model Mobile Loading Simulator. *Ph.D. Dissertation*, North Carolina State University.

Lee, S. (2004) Long-Term Performance Assessment of Asphalt Concrete Pavements Using the Third Scale Model Mobile Loading Simulator and Fiber Reinforced Asphalt Concrete. *Ph.D. Dissertation*, North Carolina State University.

Lemaster, R. L. (2004) Development of an Optical Profilometer and the Related Advanced Signal Methods for Monitoring Surface Quality of Wood Machining Applications. *Ph.D. Dissertation*, North Carolina State University.

Kim, Y. R. and J. Lee. (2005) Optimizing Gradations for Surface Treatments. North Carolina Department of Transporation Report.

Khalid, H. A. (2000) Correlation the Rheological Properties of Binders with the Mechanical Properties of their Surface Dressing Systems. International Journal Pavement Engineering, Vol. 1, pp. 193~201.

Ksaibati, K. (2000) Field Evaluation of Pavement Surface Treatment. International Journal of Pavement Engineering, Vol. 1, pp. 87~95.

Mathews, D. H. (1958) Adhesion in Bituminous Road Materials: A Survey of Present Knowledge. Journal of the Institute of Petrolem, Vol. 44, No. 420, pp. 423~432.

Mchattie, R. L. (2001) Asphalt Surface Treatment Guide. Alaska Department of Transportation.

Miller, J. E. (1987) Chip Sealing in New Brunswick. Transportation Research Record 1115, TRB, National Research Council, Washington, D.C., pp. 226~229.

Milne, T. and K. Jenkins. (2005) Towards Modeling Road Surface Seal Performance: Performance Testing and Mechanistic Behavioural Model. Journal of the South African Institution of Civil Engineering, Vol. 47, No. 3, pp. 2~13.

Mouaket, I. M., K. C. Sinha and T. M. White. (1992) Guidelines for Management of Chip and Sand Seal Coating Activities in Indiana. Transportation Research Record 1344, TRB, National Research Council, Washington, D.C., pp. 81~90.

North Carolina Division of Highway State Road Maintenance. (2000) Asphalt Surface Treatment Procedural Training Manual.

Petrie, D. D., W. J. Sheppard, and L. R. Saunders. (1990) Towards More Efficient Rolling of Chipseals. Proceedings IPENZ Annual Conference, Feb. 12~17, Vol. 1, pp. 291~300.

Roque, R., M. Thompson, and D. Anderson. (1991) Bituminous Seal Coats: Design, Performance Measurements, and Performance Prediction. Transportation Research Road 1300, TRB, National Research Council, Washington, D.C., pp. 90~97.

Roads and Traffic Authority Test Method T 119. (2001) Determination of Density of Road Materials in Situ using the Sand Replacement Methods.

Senadheera, S., R. W. Tock, S. Hossain, and B. Yazgan. (2006) A Testing Evaluation Protocol to Assess Seal Coat Binder-Aggregate Compatibility. Texas DOT(TX-06/0-4362-1).

Shuler, S. (1991) High-Traffic Chip Seal Construction: the Tulsa Teat Road. Transportation Research Road 1300, TRB, National Research Council, Washington, D.C., pp. 116~124.

Shuler, S. (1998) Design and Construction of Chip Seals for High Traffic Volume. Flexible Pavement Rehabilitation and Maintenance, ASTM STP 1348, pp. 96~114.

South Africa (1986) Surfacing Seals for Rural and Urban Roads. Technical Recommendations for Highways.

Stevenson, J. and D. Williams. (2000) Chip seal Manual. Maintenance Review Section in Montana Department of Transportation.

State of California Department of Transportation. (2003) Maintenance Technical Advisory Guide.

Stroup-Gardiner, M., D. E. Newcomb, J. A. Epps and G. L. Paulsen. (1990) Laboratory Test Methods and Field Correlation for Predicting the Performance of Chip Seals. Asphalt Emulsion, ASTM STP 1079, pp. 2~19.

Texas Department of Transportation. (2004) Seal Coat and Surface Treatment Manual.

Transit New Zealand. (1993) Bituminous Sealing Manual, 2nd Edition. Transit New Zealand Manual.

Transit New Zealand. (2005) Chipsealing in New Zealand.

Yazgan, B. and S. Senadheera. (2004) A New Testing Protocol for Sal Coat (Chip Seal) Material Selection. Transportation Research Board, TRB 2004 Annual Meeting CD-Rom.